POST-INSPECTION EVALUATION: THERMAL MODELING OF HI-STORM 100S-218 VERSION B STORAGE MODULES AT HOPE CREEK NUCLEAR POWER STATION ISFSI

Fuel Cycle Research & Development

Prepared for
U.S. Department of Energy
Used Fuel Disposition Campaign

JM Cuta
HE Adkins

September 21, 2015
FCRD-UFD-2015-000491
PNNL-24542

Reviewed by:

PNNL Project Manager

_____

Brady Hanson

SUMMARY

This report fulfills the M3 milestone M3FT-15PN08100412, "Hope Creek Post-Inspection Report", under Work Package FT-15PN081004.

Thermal analysis is being undertaken at Pacific Northwest National Laboratory in support of inspections of selected storage modules at various locations around the United States, as part of the Used Fuel Disposition Campaign of the U.S. Department of Energy, Office of Nuclear Energy Fuel Cycle Research and Development. This report documents pre-inspection predictions of canister surface temperatures and post-inspection comparisons to measured data obtained during the inspection of two modules at the Hope Creek Nuclear Generating Station Independent Spent Fuel Storage Installation (ISFSI). Pre-inspection thermal modeling calculations were performed for four modules that were identified as candidates for inspection in late summer or early fall/winter of 2013. These predictions were documented in an earlier report, (Cuta and Adkins 2013), publication date August 30, 2013. The actual inspection was performed November 19-22, 2013, and measurements were obtained on two of the four candidate modules, containing multi-purpose canisters (MPC)-144 and MPC-145. The modules inspected at Hope Creek are HI-STORM 100S-218 Version B vertical storage modules, storing BWR 8x8 fuel in MPC-68 canisters.

The temperature predictions reported in this document were obtained with detailed COBRA-SFS models of these storage systems, with the following boundary conditions and assumptions.

- Individual assembly and total decay heat loadings for each canister, based on ORIGEN modeling and a parallel set of values obtained using the methodology endorsed by Regulatory Guide 3.54[1]. This information was provided by PSEG Nuclear Fuels, from their on-site fuel tracking database.
- Axial decay heat distributions based on a typical generic profile for BWR fuel. Realistic profiles for the actual on-site fuel were not available.
- Ambient conditions assumed still air at 80°F (27°C), based on an initial planned inspection date in August 2013. Additional evaluations were also performed, for the modules containing MPC-144 and MPC-145, at 90°F (32°C), 70°F (21°C), and 50°F (10°C), to cover a range of possible conditions at the time of the inspection. The actual inspection occurred in November, with a nominal ambient temperature of 45-55°F at the time measurements were taken.

All calculations are for steady-state conditions, on the assumption that the surfaces of the module that are accessible for temperature measurements during the inspection will tend to follow ambient temperature changes relatively closely, with minimal delay due to thermal inertia.

[1] Regulatory Guide 3.54 endorses methodology documented in NUREG/CR-5625, **Technical Support for a Proposed Decay Heat Guide Using SAS2H/ORIGEN-S Data**, OW Hermann, CV Parks, and JP Renier, Oak Ridge National Laboratory, Oak Ridge, Tennessee. July 1994.

The site inspection of MPC-144 and MPC-145 at the Hope Creek ISFSI was carried out over a 4-day period, November 19-22, 2013. The inspection activities were conducted by PSEG and Holtec personnel, following inspection procedures developed by Holtec and PSEG, per the HI-STORM 100 Certificate of Compliance Amendment 2 Design Bases, which is the governing licensing document for operations at the Hope Creek ISFSI. The purpose of the inspections was to collect site data to assess the effect of environmental factors (specifically, a marine air environment) on the potential for stress corrosion cracking of stainless steel spent fuel canisters. The site data collected consisted of surface sampling of salt concentration in material adhering to the canister sides and accumulated on the top lid, using a sampling tool developed by Holtec. Samples were collected by inserting the inspection tool into the storage module through one of the outlet vents, from which the bird screen and gamma shield structure had been removed.

Temperature measurements on the canister side and top lid surfaces were also obtained, in conjunction with the surface sampling. Comparison of these measured temperatures with pre-inspection model predictions is the focus of this report. It is important to understand the difficulties in making these measurements, as reported from the perspective of the observer team. There were significant obstacles in terms of the ambient weather conditions.

As is discussed in some detail in this report, the wind speed was high and fluctuated significantly during the initial part of this test period, and in the latter half, wind was at all times significantly variable, although at generally lower speeds. In addition, the ambient temperature had unusual and greater than normal variation during the entire inspection period. As would be expected for such ambient conditions, the thermal plume from the cask outlet vent could be clearly seen to fluctuate significantly with varying wind speed and changing wind direction, while measurements were being taken. Uncalibrated local wind meter readings in the range of 35 mph at the site were witnessed by the observer team members during periods of data collection. These conditions were approaching the wind speed limit mandated for operation of the Genie lift being used to support equipment and personnel carrying out the test measurements.

The physical structure of the HI-STORM 100 storage module presented considerable difficulties in inserting the instrumentation probe to the desired measurement point and holding it in place for sufficient time and with adequate pressure to obtain reliable local measurements. The magnitude of the difficulty can be appreciated by examining the required pathway (shown by the dashed arrows) in the generic module section view in Figure S-1.

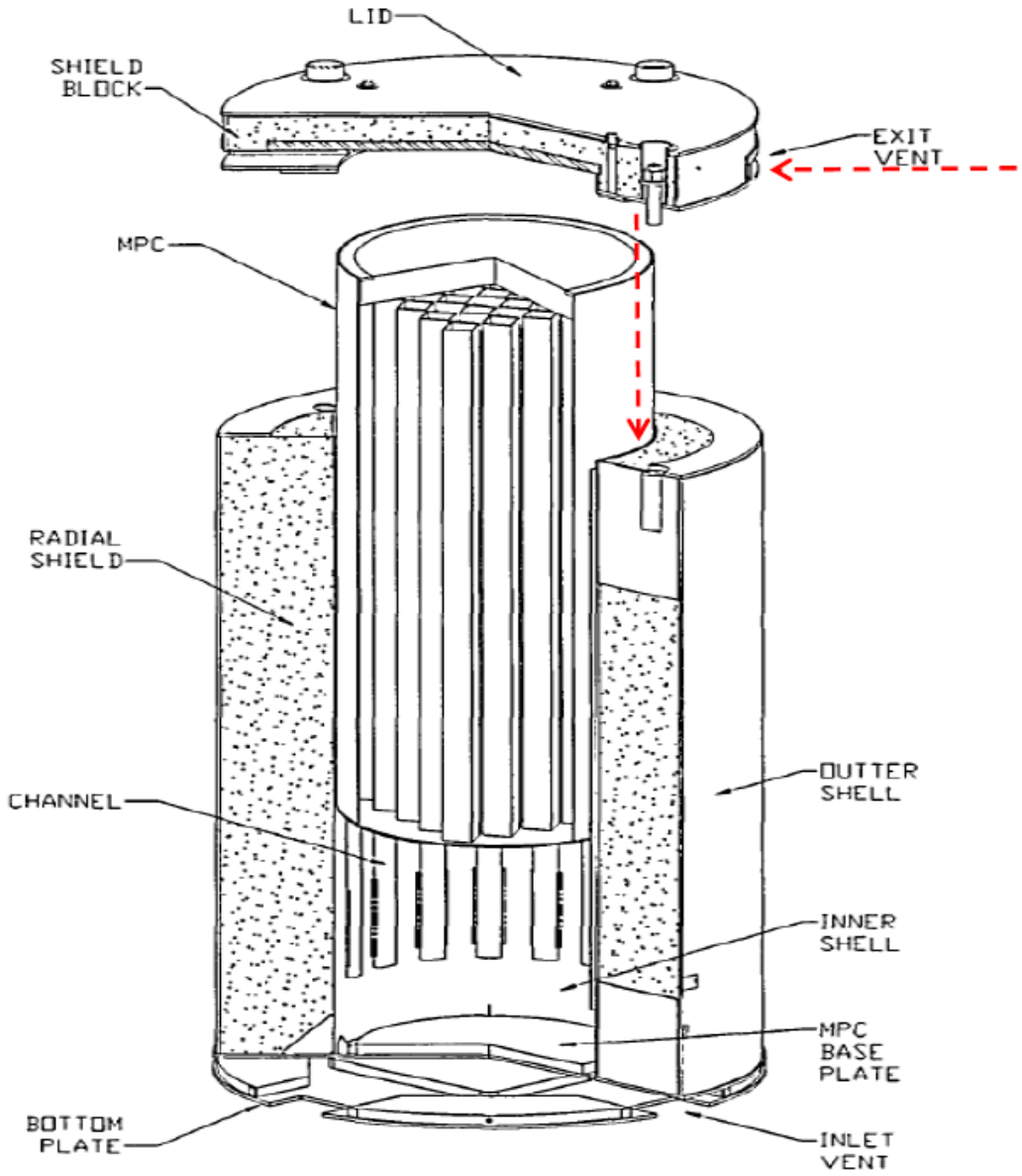

Figure S-1. Illustration of Instrument Access Path for Canister Surface Measurements (Image courtesy of Holtec International; reprinted with permission)

Although ambient air temperatures were recorded for some measurements, the times, method, and location of such measurements were not documented as part of the test procedure. This presents some difficulties in interpreting the measured data for comparison to thermal modeling predictions.

Information on site weather at the time of the inspection has been supplied by PSEG, from an on-site meteorological tower recording wind speed, direction, and local ambient temperature. This tower is located approximately one mile south-east of the ISFSI, and the reported data is from

instrumentation at an elevation of 33 ft above local ground level. The height of the storage modules is approximately 18 ft, so the meteorological data is from a height approximately twice as far above the ground, and a mile away.

Based on the meteorological data from the tower, the ambient temperature followed an unusual diurnal cycle over the week of the inspection, and the wind speed varied over a large range. Figure S-2 shows a plot of the ambient temperature recorded at the tower, and also notes the number and type of inspection measurements taken on each day. The wind conditions that accompanied this temperature trace are plotted in Figure S-3. This plot shows high and gusty winds on the day before the inspection and throughout the daytime hours of Day 1 of the inspection. There was significantly less wind on Days 2, 3, and 4 of the inspection, but wind was at all times present, and showed significant variation over time. At no time during the 4-day inspection did the condition of "still air" assumed in the thermal modeling prevail at the ISFSI. Wind effects, the unusual diurnal swings over the inspection week, and the lack of a time-stamp on the data collected introduce some uncertainty in the evaluation of temperature measurements obtained during the inspection, when compared to steady-state temperature predictions.

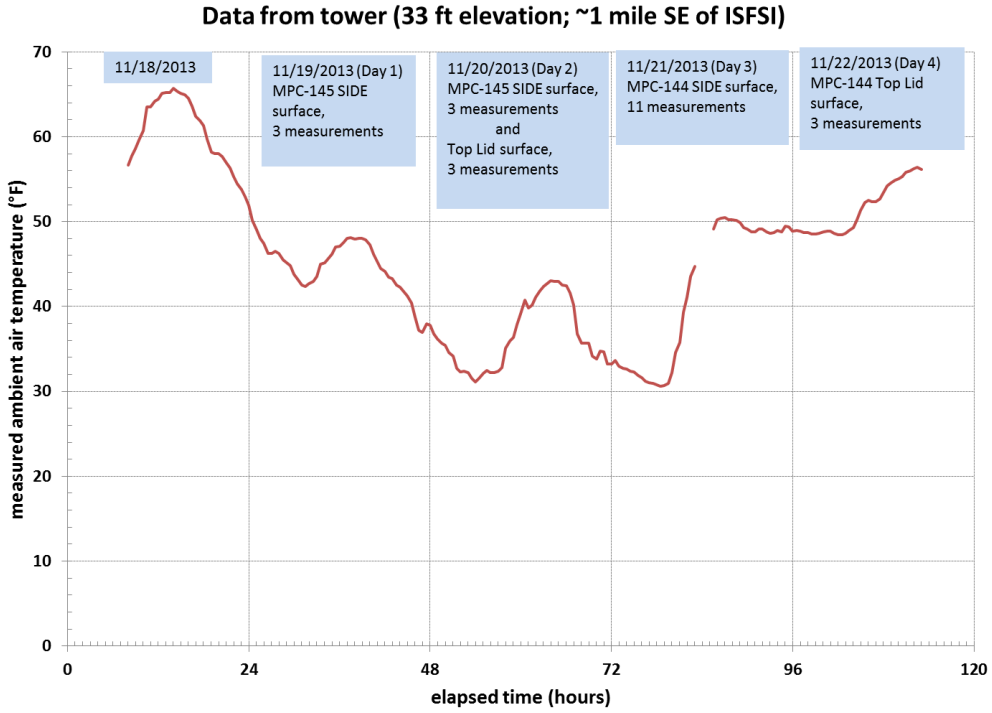

Figure S-2. Ambient Air Temperature Recorded on Meteorological Tower during Inspection Week

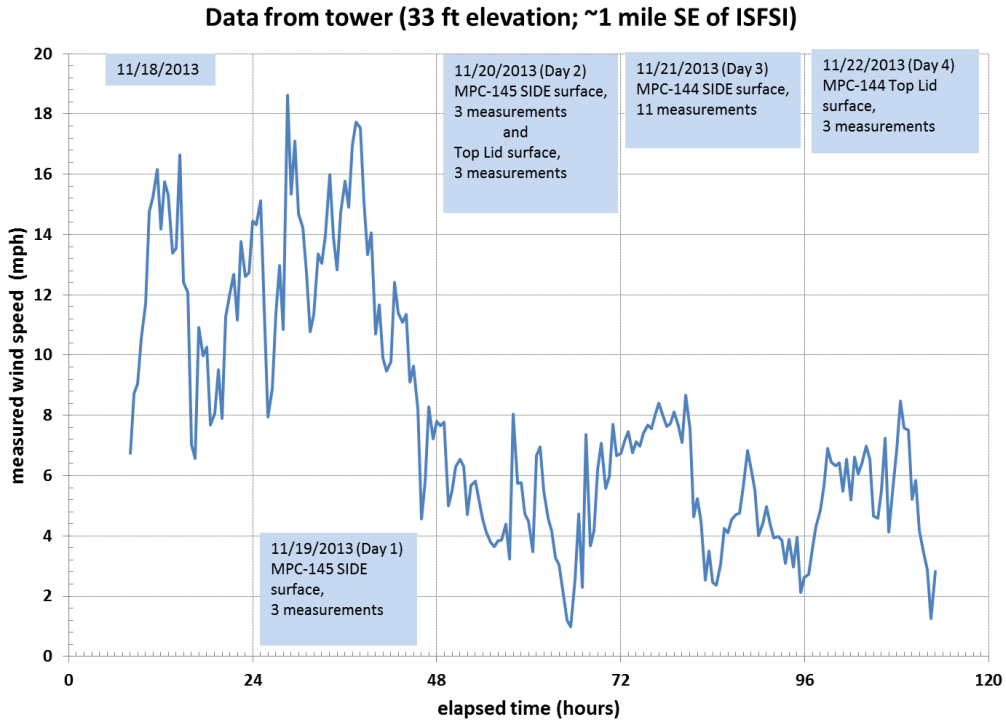

Figure S-3. Wind Speed Recorded on Meteorological Tower during Inspection Week

Tables S-1 through S-5 summarize the measured temperatures obtained on the side and top lid surfaces of the two canisters during the four days of the inspection. These tables also include the ambient air temperature measurements recorded in conjunction with the surface temperature measurements. The "insertion depth" shown in these tables for the side surface measurements is the distance down the annulus between the canister and overpack shell, relative to the base of the outlet vent through which the inspection tool was inserted. The "insertion depth" for the top lid surface measurements is the radial distance across the top of the canister, relative to the inner edge of the outlet vent.

Table S-1. Site Inspection Results: Temperature Measurements on MPC-145 Side (11/19/2013)

Date	Insertion depth (ft)	Measured side surface temperature (°F)	Measured ambient air temperature (°F)
11/19/2013	13.5	70.9	51.4
	8.5	93.3	51.8
	1.5	122.5	50.1

Table S-2. Site Inspection Results: Temperature Measurements on MPC-145 Side (11/20/2013)

Date	Insertion depth (ft)	Measured side surface temperature (°F)	Measured ambient air temperature (°F)
11/20/2013	13	70.6	38.8
	7.5	100.8	49.1
	1	130.3	46.2

Table S-3. Site Inspection Results: Temperature Measurements on MPC-145 Top Lid (11/20/2013)

Date	Insertion depth (inches)	Measured top lid surface temperature (°F)	Measured ambient air temperature (°F)
11/20/2013	64.5	172.1	51.1
	58.5	174.1	52.9
	41.75	129	48

Table S-4. Site Inspection Results: Temperature Measurements on MPC-144 Side (11/21/2013)

Date	Insertion depth (ft)	Measured side surface temperature (°F)	Measured ambient air temperature (°F)
11/21/2013	13.5	84.1	46.2
	10	85.6	48.4
	8.5	89.6	50.1
	5	104.4	49.3
	12	110.7	49.3
	5	105	50.5
	2.5	118	55
	1	126.4	53
	13	93.2	53
	7.5	116.5	52.7
	1	133.9	54

Table S-5. Site Inspection Results: Temperature Measurements on MPC-144 Top Lid (11/22/2013)

Date	Insertion depth (inches)	Measured top lid surface temperature (°F)	Measured ambient air temperature (°F)
11/22/2013	40.5	141.2	52.7
	58.5	138	52.1
	64.5	132.6	52

Results of the pre-inspection thermal modeling with COBRA-SFS for an assumed ambient temperature of 50°F are compared to the measured data obtained during the inspection of MPC-144 and MPC-145. No new information on fuel loading, axial decay heat profiles, or system geometry was provided for the modules inspected. Therefore there is no justification for making any modifications to the thermal model for post-inspection evaluations. The pre-inspection calculations assume steady-state conditions, at the specified ambient air temperature, for still air.

It is unlikely that the modules were at steady-state at the time of the inspection, due to the large changes in ambient conditions over the 4-day span, including significant and varying wind during the entire inspection. It is expected that ambient conditions would have affected the canister surface temperatures, and in general would tend to drive them to values lower than corresponding “still air” temperatures. However, evaluation of the effect of wind conditions on the thermal performance of the storage modules is beyond the scope of this analysis.

The temperatures measured on the side surface of MPC-145 were obtained on the first two days of the inspection; three measurements on 11/19/2013, and three measurements on 11/20/2013, as shown in Figure S-4. Measured ambient air temperatures were approximately the same each day, with the exception of the one ambient air temperature measurement on Day 2 (recorded when the side surface measurement was taken at an insertion depth of 13 ft). This measured temperature was the lowest (38.8°F) air temperature recorded as part of the inspection process during the entire 4-day time span. Wind conditions were quite different on these two days, however, with the measurements on Day 1 taken with wind speed in the range 13-18 mph. On Day 2, the wind speed was in the range of 3 to 6 mph, during the time interval of inspection activities, reported by site observers as between about 9:00AM and 5:00PM each day.

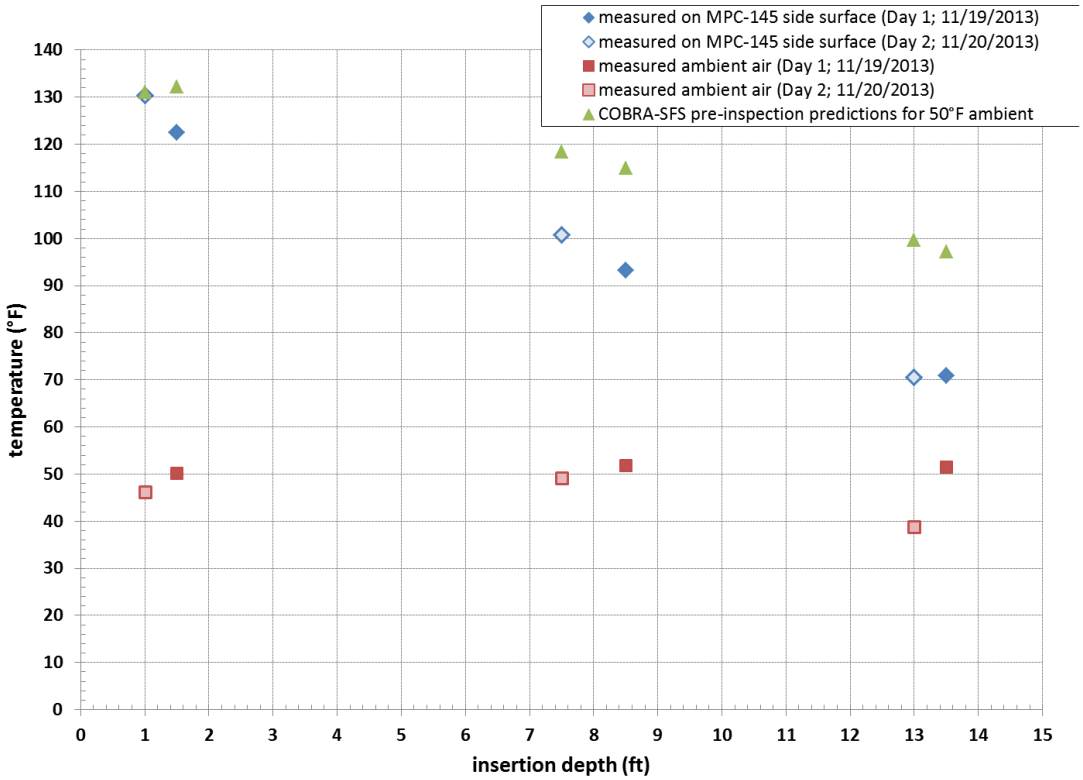

Figure S-4. Point-by-Point Comparison of COBRA-SFS Pre-Inspection Temperature Predictions to Measured Temperatures on MPC-145 Side Surface

The comparison in Figure S-4 shows that the thermal modeling predictions, assuming still air, yield temperatures that are somewhat higher than the measured values for the MPC side surface. Figure S-5 shows the same measured data compared to the axial temperature profile on the MPC side surface predicted with the COBRA-SFS model, assuming still air. Both plots show the expected relationship, when comparing predictions obtained assuming still air temperatures to surface temperatures that would be achieved with additional forced convection cooling due to wind. That is, the temperatures with wind would be expected to be somewhat below temperatures for equivalent conditions with still air.

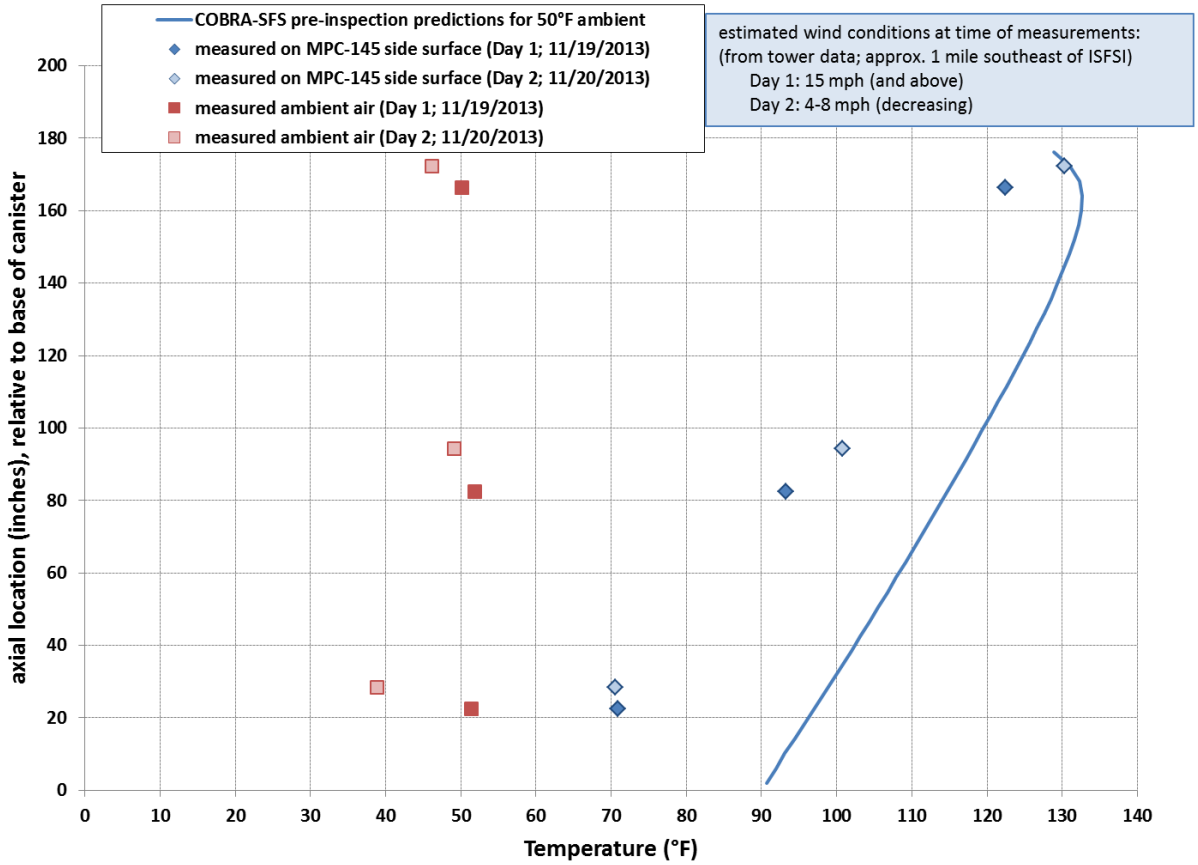

Figure S-5. Axial Profile Comparison of COBRA-SFS Pre-Inspection Temperature Predictions to Measured Temperatures on MPC-145 Side Surface

The three temperatures measured on the top lid of MPC-145 were all obtained on the second day of the inspection (11/20/2013). The COBRA-SFS model of the lid is essentially 1-D, with only axial resolution of the temperature gradient and an average value approximating any radial gradients. Therefore, the top lid temperature predicted with the model is in effect an average surface temperature for the lid. Figure S-6 compares this average lid temperature with the local point measurements obtained on the top lid surface of MPC-145.

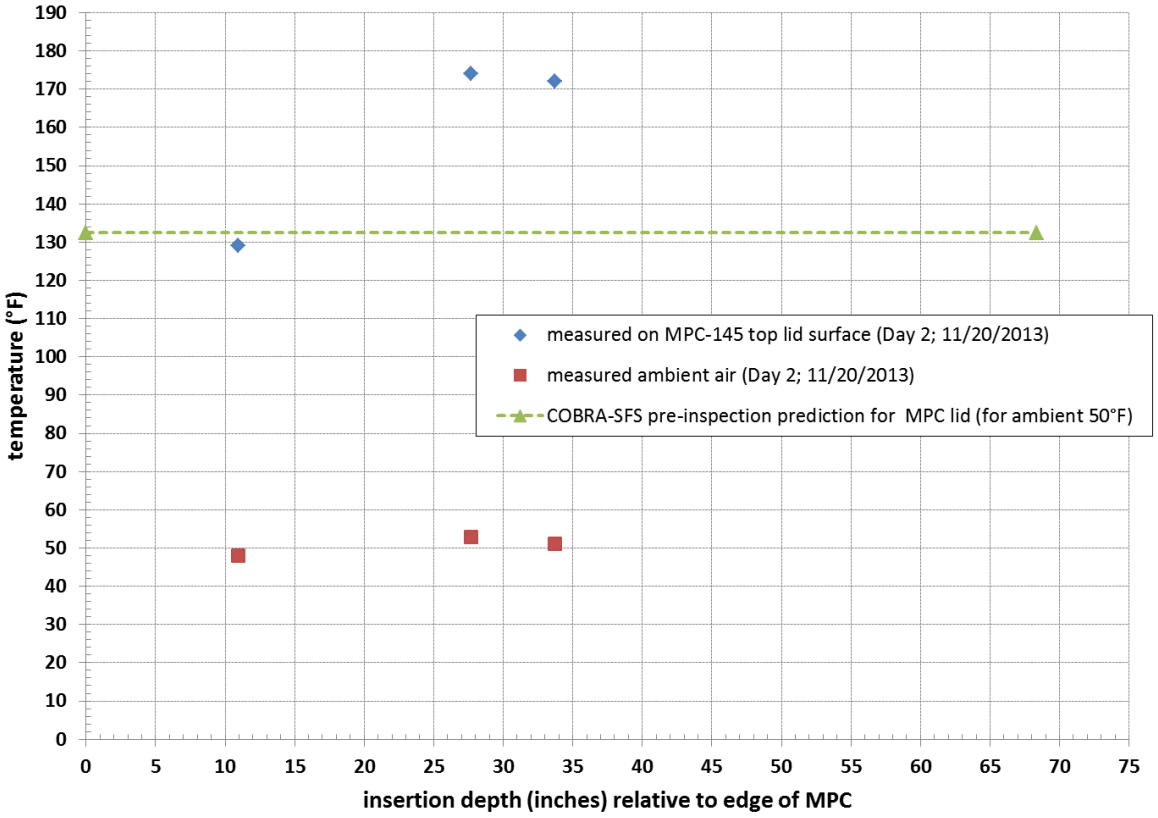

Figure S-6. Comparison of COBRA-SFS Pre-Inspection Temperature Predictions to Measured Temperatures on MPC-145 Top Lid Surface

Meaningful comparison between model predictions and measured temperatures for the top lid surface is not possible, due to wind effects at the time of measurement. The measurement insertion depths do not adequately span the diameter of the lid, with only three measurements on one side of the centerline. This is a particularly significant shortcoming of these measurements, since the radial temperature distribution on the lid is no likely to have been symmetrical for the conditions at the time the measurements were obtained. Therefore, MPC-145 top lid temperatures measured on Day 2 cannot be used to infer an average lid temperature that could be compared to the COBRA-SFS model predictions. The only useful observation that can be derived from this comparison is that differences between measured and predicted temperatures can be reasonably attributed to wind effects resulting in non-equilibrium temperatures on the canister lid surface.

The eleven temperatures measured on the side surface of MPC-144 were all obtained on Day 3 of the inspection, on 11/21/2013. Measured ambient air temperatures recorded at the meteorological tower increased steadily throughout the day, with wind speeds in the range 2-5 mph. The comparison with COBRA-SFS predictions presented in Figure S-7 and Figure S-8 show that the model predictions are in reasonable agreement with the measured data, within the limitations of the boundary conditions and modeling assumptions.

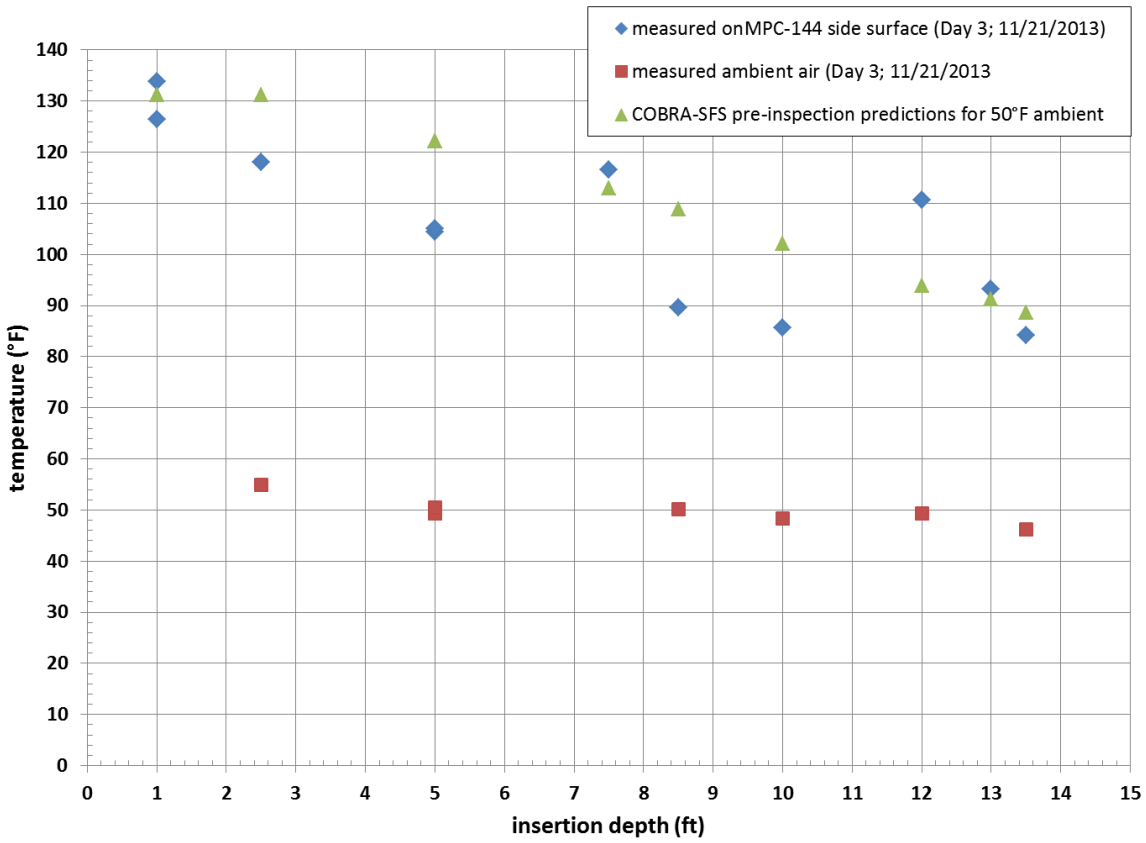

Figure S-7. Point-by-Point Comparison of COBRA-SFS Pre-Inspection Temperature Predictions to Measured Temperatures on MPC-144 Side Surface

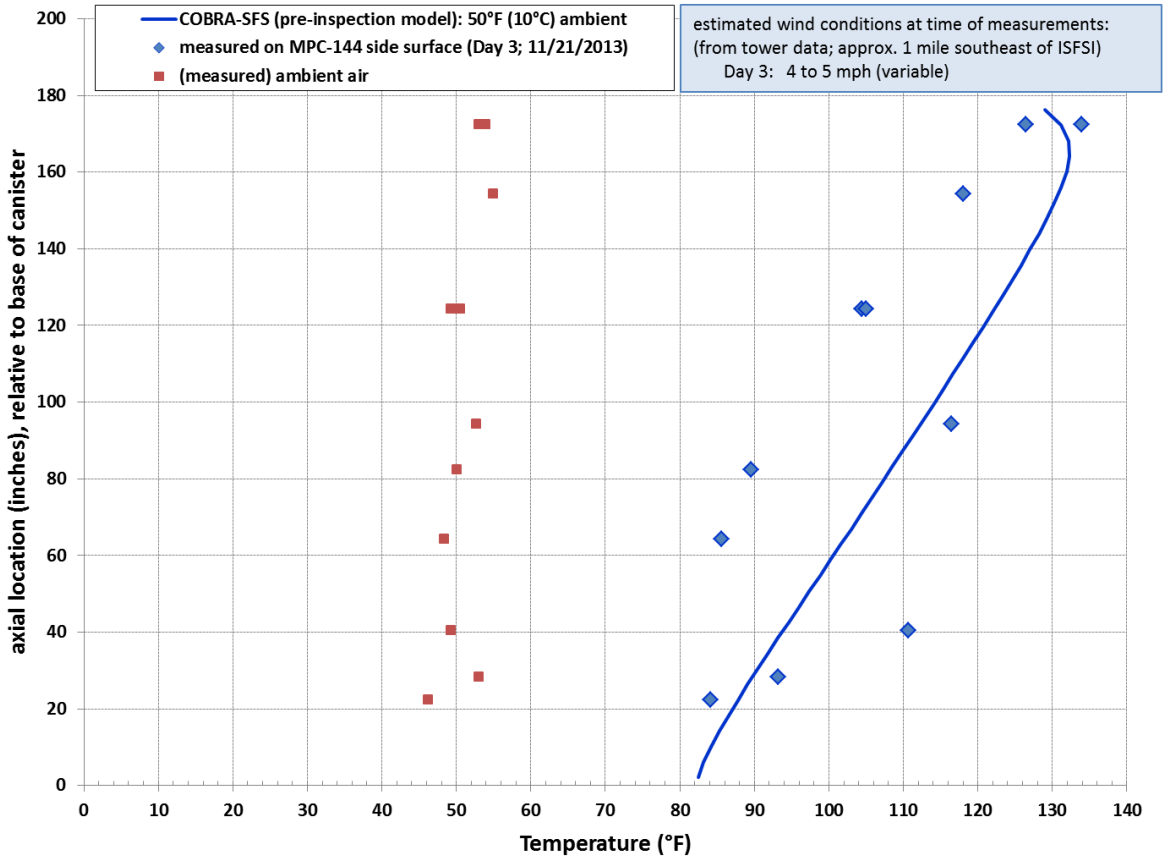

Figure S-8. Axial Profile Comparison of COBRA-SFS Pre-Inspection Temperature Predictions to Measured Temperatures on MPC-144 Side Surface

The measured temperatures on the plots in Figure S-7 and Figure S-8 show large and somewhat erratic axial variation that may simply be the effect of the "light and variable" winds experienced on site during the 6-7 hours over which the measurements were obtained. In addition to wind effects, there may also be contributions due to measurement uncertainty and thermal non-equilibrium due to the unusual diurnal variation in ambient air temperatures over the week of the inspection. However, there is no means of evaluating this, due to lack of information that could be used to assess the uncertainty in the data.

The three temperatures measured on the top lid of MPC-144 were obtained on the fourth day of the inspection (11/22/2013). This was the last day of the inspection, and these three measurements were the only temperature measurements obtained on MPC-144 on this day. Figure S-9 compares the measured temperatures to the top lid average surface temperature predicted in the thermal modeling with COBRA-SFS. This average temperature is a reasonable, although slightly low, estimate of the measured values, and is well within the uncertainty of the measurements. The trend of lower temperatures near the center of the lid, compared to the outer edge, may reflect measurement uncertainty. It is unlikely that they represent the actual temperature distribution on the lid top surface, except possibly as a transient response to changing ambient conditions.

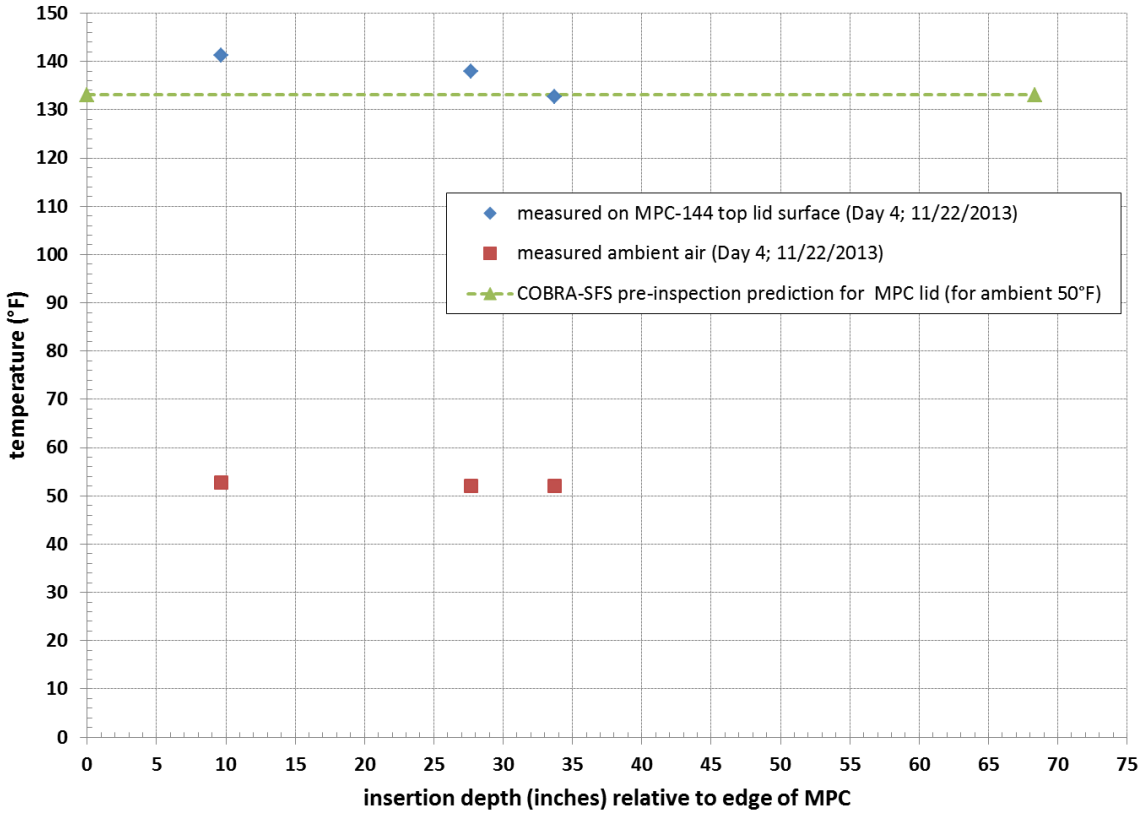

Figure S-9. Comparison of COBRA-SFS Pre-Inspection Temperature Predictions to Measured Temperatures on MPC-144 Top Lid Surface

The most significant thing about the comparison in Figure S-9 is that it shows the expected relatively flat temperature distribution across the MPC lid for conditions of the least wind during the inspection days. This is as close as actual conditions came to the thermal modeling assumption of still air, and gives the best agreement between measured and predicted temperatures obtained for the MPC lid temperatures. This tends to confirm the appropriateness of the usual COBRA-SFS modeling assumption that axial gradients are more significant than radial gradients in the lid structures of the MPC and overpack in ventilated vertical storage modules such as the HI-STORM100.

The post-inspection comparison of modeling results to measured temperature data from the Hope Creek site inspection shows that thermal modeling with the COBRA-SFS code can yield reasonable estimates of temperatures and temperature distributions in an actual storage module within an operating ISFSI. The assumption of steady-state conditions with still air provides reasonable bounding results as a function of canister decay heat load and loading pattern. The demonstrably non-equilibrium conditions that prevailed at the Hope Creek ISFSI during the site inspection limit the usefulness of the temperature measurements obtained in this inspection. This suggests certain recommendations relative to inspection procedures for obtaining thermal modeling data in future inspections. Specifically, if a major goal of a site inspection is to obtain temperatures for evaluation of thermal conditions and thermal modeling, the following should be considered.

- There is a significantly reduced benefit in gathering temperature data at a site in the presence of strong and fluctuating wind. If possible, inspection dates should be chosen based on expected typical conditions for the time of year, and alternative dates planned, on a contingency basis, so that the inspection can be postponed if conditions are likely to yield temperature data of reduced benefit. The effects of wind on storage module thermal performance may be a topic of some interest, but in practical terms, its effect on one-time data gathering efforts is to introduce an unquantifiable and non-uniform uncertainty in the measured temperatures obtained. In this instance of data gathering in highly variable ambient conditions, there is insufficient information to quantify the uncertainty in the measured data.
  - For an actual study of wind effects, measurements would have to be obtained over a large range of conditions, with and without wind, with consistent and repeatable measurement methodologies. (This may be a useful thing to do, but is beyond the current scope of the site inspections, which are aimed primarily at investigations of the potential for conditions that could result in accelerated stress corrosion cracking of the storage canister.)
- On-site data gathering procedures should include time-and-date stamps for every measurement recorded. Ambient conditions should be continuously monitored, using calibrated on-site instrumentation. If such is not available, the Test Plan should include setting up a portable monitoring station at the location of the module being inspected, to create a continuous record of ambient temperature and wind conditions throughout the inspection. This data can then later be reconciled with the date-and-time stamps of measured data, to obtain accurate boundary conditions for thermal modeling of the system at the time the measurements were taken.
- Documentation of on-site inspection measurements and procedures should be complete and specifically circumstantial, and should include an uncertainty analysis that includes the instrumentation uncertainty and the experimental uncertainty.

For the modeling effort, the usefulness of the thermal evaluations for a specific site depends on the accuracy of the model that can be constructed for the site being inspected. This means having timely access to information on the storage module configuration, the configuration and condition of the fuel stored within the canisters to be inspected, and some reasonable estimate of the expected ambient boundary conditions for the time of the inspection.

- Accurate information on assembly axial decay heat profiles (in general corresponding to axial burnup profiles) is needed to fully characterize the axial distribution of temperature on the storage canister outer shell.
  - This information seems generally unavailable at operating ISFSIs, so an alternative approach could be to perform modeling studies to quantify the uncertainty in surface temperatures (and internal component temperatures) due to variation in assumed axial decay heat profiles, relative to realistic profiles, for a range of fuel types.
- Accurate information on site-specific variations from the nominal design basis of the storage module or canister is needed to be able to predict accurate detailed temperature distributions,

particularly on surfaces that might potentially be accessible for on-site inspection and measurement.

ACKNOWLEDGMENTS

Holtec International generously allowed access to the Final Safety Analysis Report for the HI-STORM 100 System, making possible construction of accurate and complete models of the system in place at the Hope Creek plant Independent Spent Fuel Storage Installation. Special thanks are owed to Keith Waldrop, Electric Power Research Institute, who provided detailed information on the conditions at the site during the inspection, and supplemental information on the inspection procedures.

ACRONYMS AND ABBREVIATIONS

BWR	boiling water reactor
ISFSI	Independent Spent Fuel Storage Installation
MPC	multi-purpose canister
NOAA	National Oceanic and Atmospheric Administration
ORNL	Oak Ridge National Laboratory
PNNL	Pacific Northwest National Laboratory
PSEG	Public Service Electric and Gas [Nuclear, LLC (operator of Hope Creek Nuclear Generating Station)]

CONTENTS

FIGURES

TABLES

POST-INSPECTION EVALUATION: THERMAL MODELING OF HI-STORM 100S-218 VERSION B STORAGE MODULES AT HOPE CREEK NUCLEAR POWER STATION ISFSI

1.0 INTRODUCTION

As part of the Used Fuel Disposition Campaign of the U.S. Department of Energy, Office of Nuclear Energy Fuel Cycle Research and Development, a consortium of national laboratories[2] and industry[3] are performing site inspections of selected storage modules at various locations around the United States. In June 2012, inspections were performed on two horizontal storage modules in the Calvert Cliffs Nuclear Power Station's Independent Spent Fuel Storage Installation (ISFSI). Inspections originally scheduled for late summer 2013 at the Hope Creek Nuclear Generating Station ISFSI, and for later in 2013 at the Diablo Canyon Power Plant ISFSI, were performed in November 2013 at Hope Creek, and in January 2014 at Diablo Canyon. Thermal analyses in support of these inspections were undertaken at Pacific Northwest National Laboratory (PNNL). Similar to pre-inspection and post-inspection evaluations for the modules inspected at Calvert Cliffs in June 2012 (Suffield et al. 2012), this report documents pre-inspection and post-inspection evaluations of the inspected modules at the Hope Creek Nuclear Generating Station ISFSI.

The Hope Creek site utilizes the HI-STORM 100 vertical storage system developed by Holtec International. In this design, the spent fuel is sealed within a helium-pressurized stainless steel canister that is loaded into a vertical steel-lined concrete overpack. The specific module design at Hope Creek is the HI-STORM 100S-218 Version B, containing multi-purpose canister (MPC)-68 canisters (for boiling water reactor [BWR] fuel). The thermal models were developed using COBRA-SFS (Michener et al. 1995), a code developed by PNNL for thermal-hydraulic analysis of multi-assembly spent fuel storage and transportation systems. The COBRA-SFS code uses a finite-difference subchannel analysis approach for predicting flow and temperature distributions in spent fuel storage systems and fuel assemblies under forced and natural circulation flow conditions. It is applicable to both steady-state and transient conditions in single-phase gas-cooled spent fuel packages with radiation, convection, and conduction heat transfer. The code has been validated in blind pretest calculations using test data from spent fuel packages loaded with actual spent fuel assemblies, as well as electrically heated single-assembly tests (Creer et al. 1987, Rector et al. 1986, Lombardo et al. 1986).

[2] Pacific Northwest National Laboratory, Oak Ridge National Laboratory, Sandia National Laboratories, and Idaho National Laboratory.

[3] Electric Power Research Institute, TN/AREVA, Holtec International, PSEG Nuclear LLC (owner of Hope Creek Nuclear Generating Station), Constellation Energy (Owner of Calvert Cliffs Nuclear Power Station), and Pacific Gas and Electric Corporation (owner of Diablo Canyon Power Plant).

The data obtained in these on-site inspections provide an opportunity to develop structural and thermal models that can yield realistic predictions for actual storage systems, in contrast to conservative and bounding design-basis calculations. The analytical approach used in this study does not include many of the conservatisms and bounding assumptions normally used in design-basis and safety-basis calculations for spent fuel storage systems.

The primary storage modules considered in this study consist of four modules in the Hope Creek Nuclear Generating Station's ISFSI, designated as MPC-143, MPC-144, MPC-145, and MPC-146. Figure 1-1 shows an aerial view of the ISFSI, illustrating the layout of the double rows (2xN) of storage units. A typical HI-STORM100 module is illustrated in Figure 1-2. Planning and procedures development for the inspection was a long process, and the decision on which specific modules to inspect was not finalized until sometime after the pre-inspection modeling evaluations were scheduled for completion. As a result, pre-inspection evaluations were performed for all four candidate modules. The final decision, made in late summer 2014, was to inspect the two modules containing MPC-144 and MPC-145. Therefore, the post-inspection evaluations presented in this report are only for these two modules. However, all four modules are essentially identical, except for the contents of the MPC, which vary somewhat in total decay heat load and loading pattern. Thermal evaluation models were developed for all four modules, and pre-inspection calculated results are presented (in this report and in the pre-inspection report [Cuta and Adkins 2013]) for all four modules.

Figure 1-1. Aerial View of Hope Creek Nuclear Generating Station ISFSI, Showing Arrays of Vertical Storage Modules (Google Earth 2011)

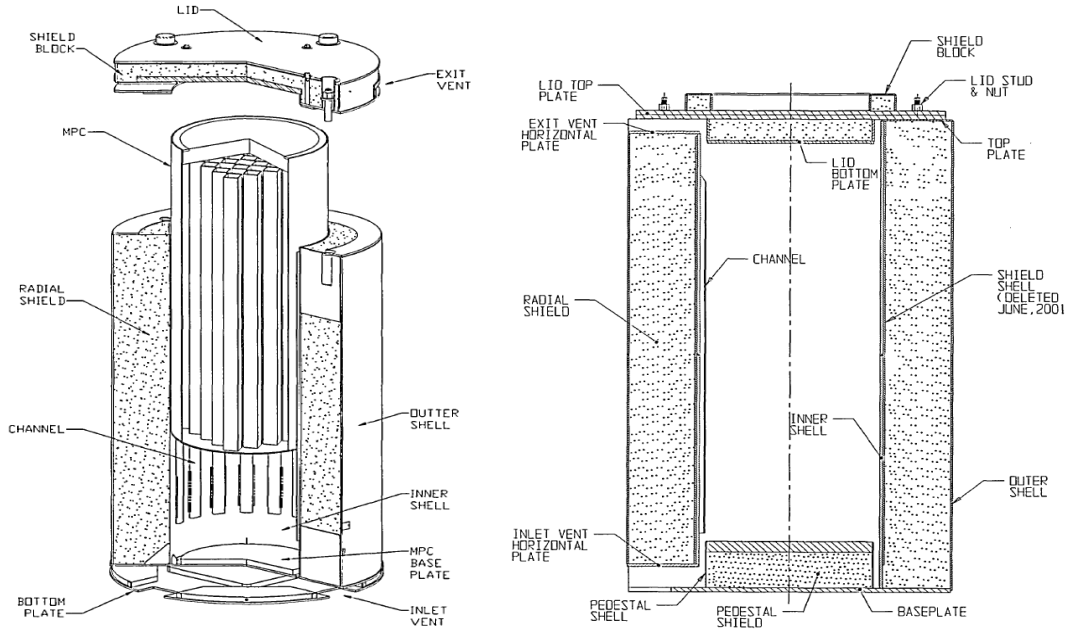

Figure 1-2. Typical HI-STORM 100 Vertical Storage Module (Image courtesy of Holtec International; reprinted with permission) NOTE: the 100S-218 Version B design used at Hope Creek differs in some details from this image.

The COBRA-SFS model geometry for the HI-STORM 100S-218 Version B with MPC-68 canister is described in detail in Section 2.0, along with the boundary conditions and modeling assumptions. This section is unchanged from the original "pre-inspection" report (Cuta and Adkins 2013). No new or additional data was provided on the system design, and therefore no changes were made in the COBRA-SFS model for the system. Section 3.0 presents pre-inspection predictions of component temperatures and temperature distributions within the module, based on the estimated decay heat loads in the MPCs as of the planned inspection timeframe of August 2013. This section also includes pre-inspection predictions for a range of assumed ambient temperatures, to span the possible range of conditions that might prevail during the inspection.

The site inspection was performed November 19-22, 2013, and the measured temperature data obtained is summarized in Section 4.0. Temperature measurements were obtained at an estimated nominal ambient temperature of 50°F (10°C). The "pre-inspection" predictions for this assumed ambient condition are shown in Section 5.0. Comparisons between these pre-inspection predictions and measured temperature data obtained during the inspection are presented in Section 6.0.

2.0 COBRA-SFS MODEL DESCRIPTION

This section is identical to the model description section in the pre-inspection report (Cuta and Adkins 2013). No changes were made to the system model, as no additional or revised information on the system configuration was supplied from Public Service Electric and Gas (PSEG) or from Holtec. The information in this section of the pre-inspection report is reproduced here in this post-inspection report as a convenience to the reader.

The HI-STORM 100 system is a vertical storage module design developed by Holtec International, and consists of an MPC inserted into a steel-lined concrete overpack (Holtec 2010). The general design of the overpack is similar for all configurations of the system, such that the main site-specific character of a particular installation is the design of the canister stored within the overpack. At the Hope Creek ISFSI, the canister design is the MPC-68, which is for BWR fuel, and stores up to 68 BWR fuel assemblies. The storage modules to be inspected in the Hope Creek ISFSI are designated MPC-143, MPC-144, MPC-145, and MPC-146. Each of these modules contains an MPC-68 canister. To avoid potential confusion with the MPC design designation used by Holtec and the module designation used at the Hope Creek ISFSI, the specific storage modules to be modeled in this evaluation are referred to as Module 143, Module 144, Module 145, and Module 146. When referring specifically to post-inspection information on the canisters within the storage modules that were actually inspected, the designation MPC-144 and MPC-145 is used.

A COBRA-SFS model for a vertical storage system consists of three major pieces; the canister, the air flow channel that allows external ambient air to circulate through the module, and the external overpack surrounding the canister. The general structure of the model of the HI-STORM 100S-218 Version B storage system is illustrated in Figure 2-1. The detailed three-dimensional nodalization of the fuel assemblies, basket, canister, and overpack walls extends only over the axial length of the basket within the MPC. This highly detailed portion of the model represents the region of radial heat transfer from the fuel rods to the ambient environment. The axial length of this region is defined by the length of the basket, which in this case is only 5.24 cm (2.06 inches) short of the total axial length of the canister internal cavity. Axial heat transfer out the top and bottom of the system is represented with a simpler, one-dimensional thermal resistance network, consisting of the upper and lower plenum regions.

Diagrams illustrating the model representation of the entire system of Module 143 are shown in Figures 2-2 and 2-3. For clarity, the canister and overpack portions of the model are shown separately. Figure 2-2 shows a 3-D diagram of the canister portion of the model, including the fuel rods, fuel channel, basket plates (with neutron poison plates), basket support structure, and canister shell. Different colors are used for different components, for clarity in the complex mesh. This diagram is not to scale, since in a scaled diagram of the mesh, fine details such as the neutron poison plates and fuel channel are difficult to discern. In addition, the detailed rod-and-subchannel arrays within the fuel channel are shown with the rod spacing greatly exaggerated, so that the subchannels are visible.

Figure 2-3 shows a cross-section diagram of the portion of the model representing the overpack. The geometry of the other three modules is essentially identical to that of Module 143, and

therefore the images in Figures 2-2 and 2-3 are applicable to the models for all four modules. The only significant difference in the models for the four modules is in the assembly loading pattern, which is unique for each module. The representation of the decay heat in the fuel assemblies in the COBRA-SFS model is discussed in detail in Section 2.1.

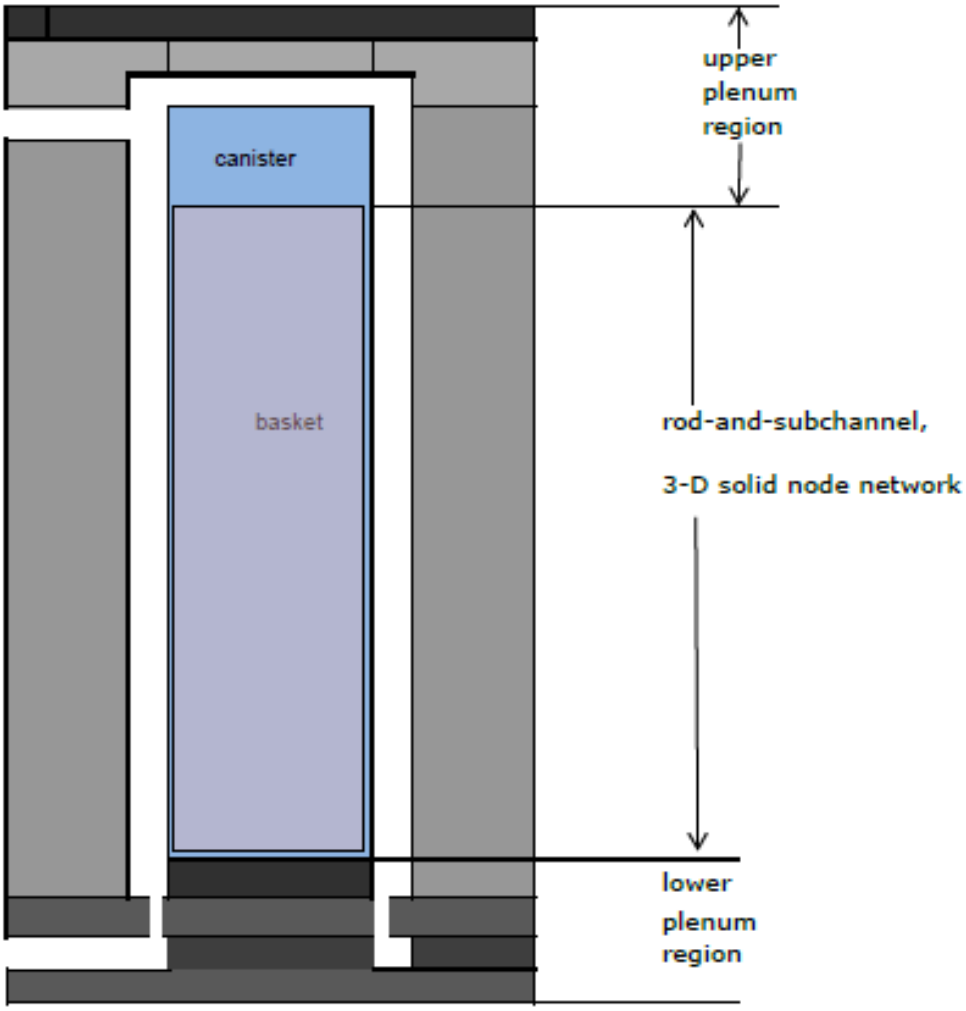

Figure 2-1. Diagram of Modeling Regions in COBRA-SFS Model of HI-STORM 100S-218 Version B Vertical Storage System (NOTE: diagram is not to scale)

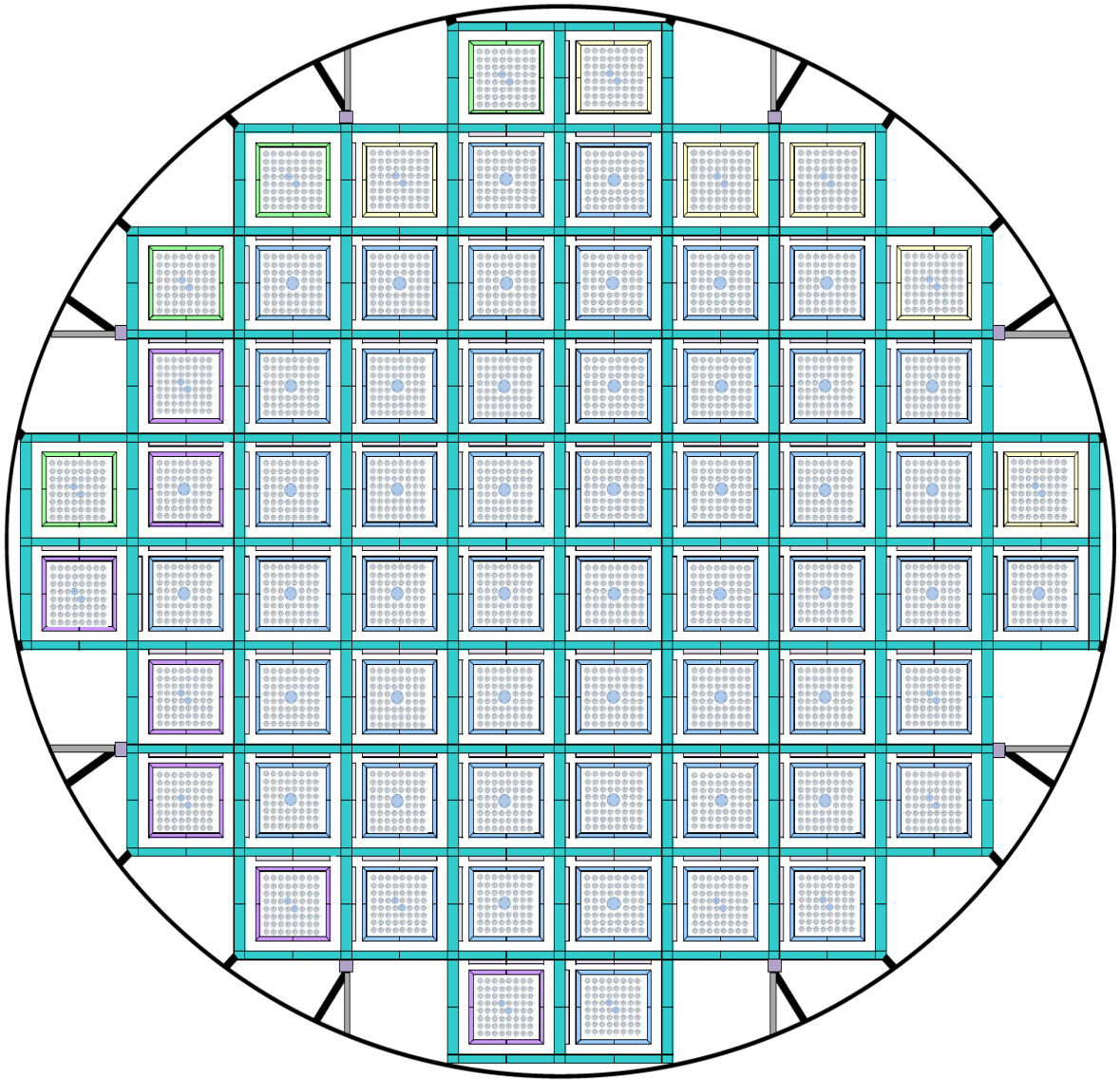

Figure 2-2. Diagram of 3-D COBRA-SFS Model of Canister for Module 143 (NOTE: diagram not to scale; node thicknesses greatly exaggerated for clarity)

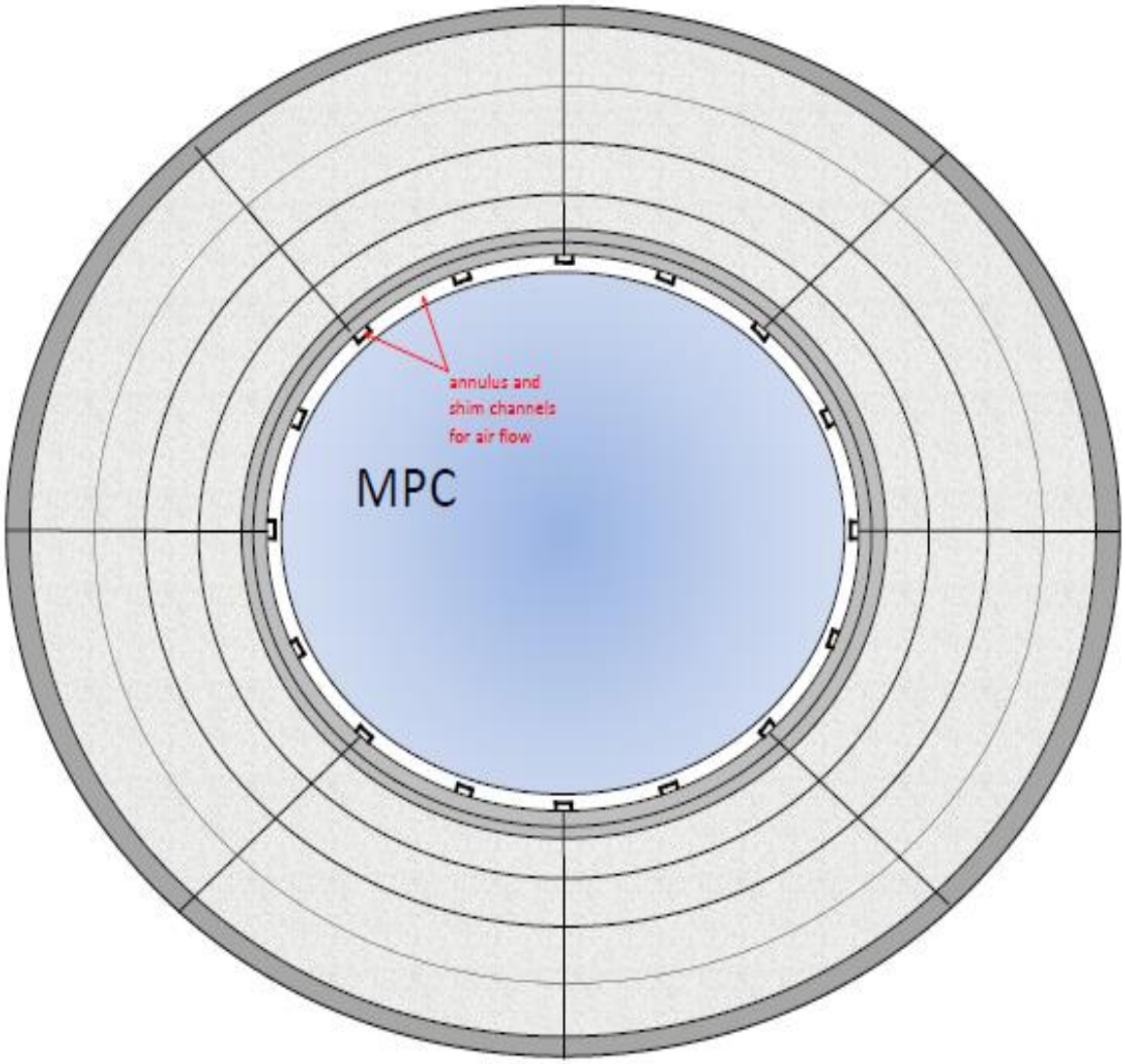

Figure 2-3. Cross-section of COBRA-SFS Model of Overpack for Module 143 (diagram is not to scale. Air annulus width and steel thicknesses are greatly exaggerated for clarity.)

The detailed model of the canister and internals (including the fuel assemblies) shown in Figure 2-2 has the typical mesh resolution generally used for the basket structure in COBRA-SFS models of spent fuel storage systems. Finer mesh resolution can be specified, if needed, but comparison with temperature measurements from single assembly and multi-assembly experiments, including testing of storage systems with spent fuel loaded in the basket (Lombardo et al. 1986; Rector et al. 1986; Creer et al. 1987) has shown that this meshing is sufficient for resolution of temperature gradients typical of spent fuel storage systems. The mesh includes the basket plates, poison plates, and basket support structures, including the shims on these structures that are used to ensure firm contact between the basket frame and canister inner shell.

The solid structure network also includes the thin plates of the zircaloy fuel channels containing the BWR fuel assemblies. The thermal network approach used in COBRA-SFS allows direct representation of thin plates and the contact resistance due to small gaps between adjacent components. In typical models for computational fluid dynamics and finite element analysis codes, structures consisting of adjacent thin plates (such as the basket plates, poison plates, and poison plate sheathing) are modeled as a single material with homogenized properties that may include contact resistances. The approach used in COBRA-SFS modeling allows more detailed resolution of temperature distributions in such structures, using a comparatively smaller mesh.

As shown in Figure 2-2, the main feature of the COBRA-SFS model of the canister is the representation of the flow field within the fuel assemblies in the basket, and the flow paths external to the basket that allow recirculation due to natural convection within the canister. Within the individual basket cells, the fuel assembly and flow field are represented with a detailed subchannel model. This is illustrated in Figure 2-4 for a single assembly of each of the two different fuel configurations stored in the canisters at Hope Creek. This representation of the fuel assembly allows for much more accurate resolution of the local rod temperatures, compared to the typical approach used in computational fluid dynamics and finite element analysis models, in which the fuel assembly region is represented as a homogeneous block with internal heat generation, or as a porous medium. The detailed rod and subchannel model allows the code to calculate individual fuel rod cladding temperatures, accounting for heat transfer by conduction, convection, and thermal radiation, and permits detailed modeling of material parameters, such as fuel cladding emissivity and surface conditions.

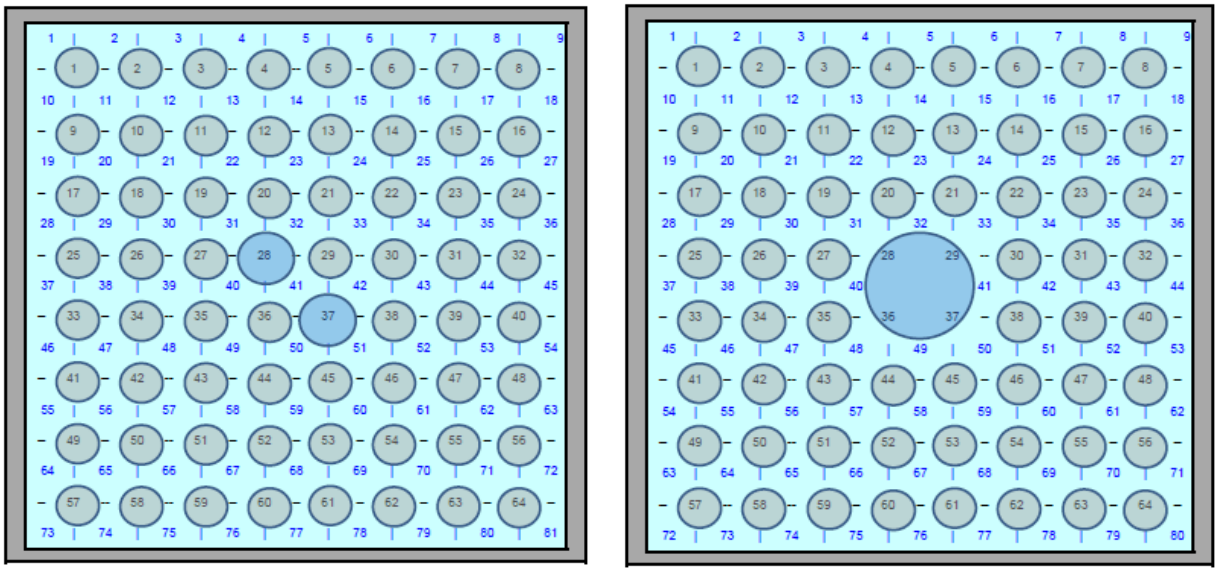

Figure 2-4. Rod-and-subchannel Array Diagram for COBRA-SFS Model of GE 8x8 Fuel Assemblies–GE7 and GE9 Configurations (Note: diagrams are not to scale; rod spacing is greatly exaggerated for clarity. Larger dark blue circles represent water rods.)

For convection heat transfer, the fluid channels within the canister are thermally connected to the fuel rods and to the surrounding solid conduction nodes representing the basket by means of a user-specified heat transfer correlation. Based on validation of the COBRA-SFS code with experimental data from vertical test systems and canisters loaded with actual spent fuel, convection heat transfer in the fuel rod array is represented with the venerable Dittus-Boelter heat transfer correlation for turbulent flow,

$$Nu = 0.023(Re^{0.8})(Pr^{0.4})$$

where Nu = Nusselt number
Re = Reynolds number, based on subchannel hydraulic diameter
Pr = Prandtl number for the backfill gas

For laminar flow conditions, a Nusselt number of 3.66 has been verified as applicable to spent fuel rod arrays. The local heat transfer coefficient is defined as the minimum of the values calculated from the laminar and turbulent correlations specified by user input. Figure 2-5 illustrates the convenient mathematical behavior of these correlations as a function of Reynolds number.

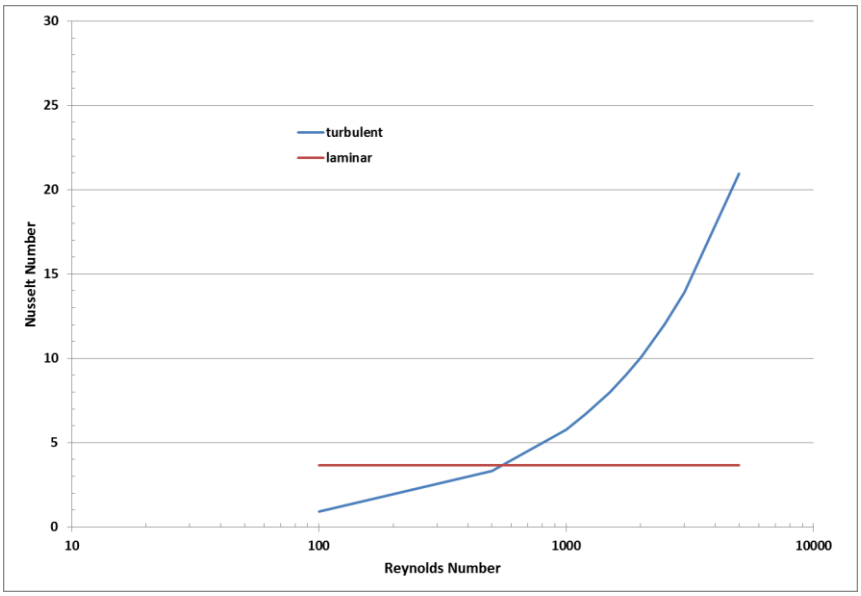

Figure 2-5. Laminar and Turbulent Formulations for Nusselt Number

In addition to convection heat transfer, the fluid energy equation includes conduction through the fluid (helium gas) in the subchannels, and the gas is assumed transparent to thermal radiation. Thermal radiation within the basket is calculated using 2-dimensional (planar cross-section) grey-body view factors for the rod array and surrounding solid conduction nodes of the basket wall. The view factors are calculated for the specific assembly and basket cell geometry using the auxiliary code RADGEN, which is part of the COBRA-SFS package. Thermal radiation across the geometrically simpler flow channels between the basket and the canister shell is determined from user-input black body view factors, calculated using the Hottel crossed-string

correlation methodology. Based on the specified surface emissivity of the nodes of the surfaces of a given flow region, the code calculates the grey-body view factors for thermal radiation exchange.

The annulus between the canister and the overpack is represented in the COBRA-SFS model with 20 flow channels to represent the circumferential variation in the annulus region cross-section due to the 16 shim channels spaced around the inner shell of the storage cavity (see Figure 2-3). The shim channels are open at top and bottom, and therefore constitute isolated flow paths for air circulation within the annulus. These flow paths are treated as separate parallel channels in the COBRA-SFS model. Air flow in the fluid channels representing the annulus is calculated using a pressure drop boundary condition based on the height of system and the specified ambient air temperature. Momentum losses are determined using a friction factor correlation and form drag losses due to the orificing effects of the inlet and exit structures above and below the annulus.

Thermal connections between the annulus flow channels and the solid conduction nodes of the MPC shell, shim channel structures, and overpack inner shell are defined in the COBRA-SFS model for conduction and thermal radiation heat transfer. Convection heat transfer in the air annulus is treated as a forced convection flow, driven by the imbalance between the hydrostatic pressure drop within the annulus and that of the ambient air external to the overpack (Sparrow and Azevedo 1985). The Dittus-Boelter correlation has been shown to be an appropriate heat transfer model for prediction of heat transfer in a vertical storage module (Creer et al. 1987), but requires two minor modifications for application to the specific annulus geometry of the HI-STORM 100 system. The definition of the annulus hydraulic diameter used in the heat transfer correlation's database is twice the radial width of the annulus (i.e., 2*W). The channel hydraulic diameter is defined in COBRA-SFS using the more general formula of four times the flow area divided by the wetted perimeter.

These two formulations are exactly equivalent for a simple circular annulus, but the annulus in the HI-STORM 100 system contains 16 channel shims, to center the MPC within the overpack cavity (as illustrated in the diagram in Figure 2-3.) The presence of the shims effectively reduces the hydraulic diameter by approximately 50%, when calculated using the more general formula. However, evaluations by Holtec have validated appropriate agreement with heat transfer data in a vertical storage module (from Creer et al. 1987) using the Dittus-Boelter correlation for heat transfer in the annulus, with the hydraulic diameter defined as 2*W and the Prandtl number coefficient[4] specified as 0.333.

The equivalent formulation of this variation on the Dittus-Boelter correlation for COBRA-SFS is obtained by specifying the Nusselt number for turbulent flow heat transfer in the annulus channels as

[4] The Dittus-Boelter correlation is derived with the general formulation $Nu = C\,Re^{m}Pr^{n}$, where C=0.023, m=0.8, and specifies n=0.4 for heating and n=0.3 for cooling. The original database did not investigate the effects of heating on one wall and cooling on the other, as is the situation in the HI-STORM100 annulus.

$$Nu = 0.046\ Re^{0.8}Pr^{0.33}$$

where Re = Reynolds number, based on flow channel hydraulic diameter
Pr = Prandtl number for air

The air flow in the annulus is expected to be turbulent for normal conditions of storage, but the COBRA-SFS input also includes a lower bound of Nu = 7.44 (derived[5] from Sparrow et al. 1961), which represents laminar flow conditions in a vertical stack. As illustrated in Figure 2-5, the code uses the mathematical behavior of the correlations to automatically select the appropriate flow regime by taking the maximum of the values obtained with the laminar and turbulent formulations for the local flow conditions.

2.1 Fuel Assembly Decay Heat Modeling

The spent fuel stored at Hope Creek consists of GE 8x8 assemblies in two main configurations, designated GE7 and GE9, as noted above in the discussion of fuel assembly geometry modeling with COBRA-SFS. The GE7 configuration has nominally 62 active fuel rods, with two water rods near the center of the array. The GE9 configuration has nominally 60 active fuel rods, with a large central water rod that displaces four rod positions in the array. Information transmitted from PSEG Nuclear Fuels[6] provided the total canister decay heat loads, calculated assembly decay heat loads, and assembly load maps for the canisters in all four of the modules being considered for inspection. The package included individual assembly decay heat values calculated with ORIGEN[7] and with a second methodology[8] based on Regulatory Guide 3.54 (NRC 1999).

The total canister decay heat loadings for the four Modules are summarized in Table 2-1. This table includes the values reported for the time of loading and for the scheduled time of the inspection, as calculated with the two methodologies. The design basis maximum thermal loading for the MPC-68 in above-ground HI-STORM 100 storage systems is 0.5 kW per assembly, for a total decay heat load of 34 kW. The decay heat at the time of loading of these canisters was therefore 37% of design basis, based on the ORIGEN modeling. Based on the more conservative RG 3.54 modeling, the initial decay heat load was 47% of design basis.

---

[5] The mean value in the reference is Nu=7.86. The value of 7.44 represents the lower bound on the ±5% uncertainty in the data.

[6] Provided in **Transmittal of Design Information**, NF ID# NFS 13-060; *Data for Fuel Loaded into Hope Creek MPC143, MPC144, MPC145 and MPC146*, non-safety related, verified information. Approved 6/3/2013.

[7] The specific version of ORIGEN used is identified in an e-mail from Steven P. Baker of PSEG Nuclear Fuels (sent 7/25/2013 7:09am PDT) as ORIGEN-ARP packaged with SCALE 6.1.1. A current reference for ORIGEN-ARP is ORNL/TM-2005/39, *ORIGEN-ARP: Automatic Rapid Processing for Spent Fuel Depletion, Decay, and Source Term Analysis*. Oak Ridge National Laboratory, Oak Ridge, Tennessee, 2009.

[8] Regulatory Guide 3.54 endorses methodology documented in NUREG/CR-5625, **Technical Support for a Proposed Decay Heat Guide Using SAS2H/ORIGEN-S Data**, OW Hermann, CV Parks, and JP Renier, Oak Ridge National Laboratory, Oak Ridge, Tennessee. July 1994.

Table 2-1. Total Decay Heat Loading per Module

	ORIGEN			RG 3.54	
	decay heat (kW)			decay heat (kW)	
	at loading	at inspection		at loading	at inspection
Module	(11/2006)	(8/2013)		(11/2006)	(8/2013)
143	12.69	10.44		16.01	12.78
144	12.02	9.29		16.03	11.40
145	10.71	9.24		12.89	11.13
146	10.84	9.33		13.03	11.25

The RG 3.54 methodology produces decay heat values that are on average 22% higher than the values obtained with the ORIGEN methodology. The total decay heat load among the four Modules varies by about 13% with the ORIGEN results, and by about 15% with the RG 3.54 results. The decay heat values for all assemblies within the individual canisters are listed in Table 2-2. This table includes both the ORIGEN results and the RG 3.54 results for each assembly. The basket location of an assembly is identified by row number and column letter, as illustrated with the diagram in Figure 2-6.

Table 2-2. Projected Assembly Decay Heat Loading as of August 2013 for Each Module

Basket cell location	Assembly decay heat (kW) ORIGEN					Assembly decay heat (kW) RG 3.54			
	Module 143	Module 144	Module 145	Module 146		Module 143	Module 144	Module 145	Module 146
E-1	0.1045	0.0323	0.1012	0.1031		0.1248	0.0357	0.1187	0.1211
F-1	0.1038	0.0328	0.0981	0.1023		0.1227	0.0362	0.1164	0.1200
C-2	0.0978	0.0327	0.1010	0.1022		0.1160	0.0362	0.1185	0.1199
D-2	0.1061	0.1192	0.1010	0.1018		0.1262	0.1425	0.1184	0.1194
E-2	0.1753	0.1608	0.1528	0.1614		0.2151	0.1945	0.1853	0.1954
F-2	0.1713	0.1842	0.1579	0.1548		0.2163	0.2274	0.1915	0.1896
G-2	0.1026	0.1194	0.1010	0.1030		0.1215	0.1426	0.1184	0.1211
H-2	0.1073	0.0330	0.1017	0.1011		0.1284	0.0364	0.1194	0.1185
B-3	0.1030	0.0322	0.1009	0.1021		0.1210	0.0355	0.1184	0.1198
C-3	0.1562	0.1846	0.1564	0.1585		0.1960	0.2281	0.1893	0.1943
D-3	0.1774	0.1581	0.1538	0.1582		0.2226	0.1918	0.1870	0.1917
E-3	0.1735	0.1963	0.1529	0.1630		0.2122	0.2455	0.1854	0.1990
F-3	0.1770	0.1962	0.1565	0.1541		0.2150	0.2456	0.1896	0.1864
G-3	0.1781	0.1417	0.1564	0.1564		0.2193	0.1693	0.1894	0.1894
H-3	0.1771	0.1782	0.1583	0.1590		0.2230	0.2194	0.1923	0.1950
J-3	0.1009	0.0323	0.1009	0.1024		0.1184	0.0357	0.1184	0.1202
B-4	0.1072	0.1192	0.1009	0.1023		0.1283	0.1425	0.1183	0.1201
C-4	0.1782	0.1429	0.1580	0.1584		0.2156	0.1722	0.1909	0.1923
D-4	0.1670	0.1964	0.1547	0.1525		0.2043	0.2464	0.1895	0.1850
E-4	0.1908	0.1965	0.1532	0.1536		0.2350	0.2458	0.1848	0.1867
F-4	0.1743	0.1952	0.1543	0.1552		0.2119	0.2445	0.1866	0.1893

Table 2-2. (continued)

Basket cell location	Assembly decay heat (kW) ORIGEN					Assembly decay heat (kW) RG 3.54			
	Module 143	Module 144	Module 145	Module 146		Module 143	Module 144	Module 145	Module 146
G-4	0.1698	0.1945	0.1516	0.1564		0.2076	0.2450	0.1834	0.1893
H-4	0.1739	0.1352	0.1567	0.1578		0.2127	0.1624	0.1894	0.1930
J-4	0.1030	0.1172	0.1011	0.1025		0.1228	0.1367	0.1185	0.1213
A-5	0.1029	0.0328	0.1014	0.0978		0.1227	0.0362	0.1189	0.1160
B-5	0.1787	0.1461	0.1575	0.1600		0.2179	0.1755	0.1927	0.1959
C-5	0.1892	0.1964	0.1508	0.1544		0.2449	0.2459	0.1817	0.1867
D-5	0.1605	0.1955	0.1577	0.1561		0.1963	0.2465	0.1921	0.1887
E-5	0.1592	0.1962	0.1584	0.1443		0.1952	0.2455	0.1934	0.1778
F-5	0.1676	0.1955	0.1561	0.1565		0.2051	0.2465	0.1886	0.1895
G-5	0.1928	0.1945	0.1443	0.1616		0.2373	0.2450	0.1779	0.1971
H-5	0.1810	0.1956	0.1550	0.1538		0.2271	0.2466	0.1891	0.1871
J-5	0.1928	0.1354	0.1568	0.1614		0.2430	0.1630	0.1894	0.1969
K-5	0.1069	0.0111	0.1011	0.0981		0.1264	0.0120	0.1185	0.1163
A-6	0.0983	0.0328	0.1021	0.1032		0.1166	0.0362	0.1198	0.1212
B-6	0.1957	0.1698	0.1548	0.1529		0.2465	0.2078	0.1896	0.1854
C-6	0.1785	0.1964	0.1574	0.1541		0.2174	0.2466	0.1920	0.1863
D-6	0.1904	0.1966	0.1558	0.1525		0.2344	0.2460	0.1907	0.1851
E-6	0.1922	0.1952	0.1540	0.1563		0.2345	0.2444	0.1905	0.1889
F-6	0.1919	0.1951	0.1508	0.1612		0.2350	0.2444	0.1826	0.1966
G-6	0.1930	0.1946	0.1582	0.1551		0.2374	0.2451	0.1917	0.1892
H-6	0.1757	0.1963	0.1549	0.1541		0.2139	0.2455	0.1896	0.1863
J-6	0.1958	0.1826	0.1506	0.1629		0.2472	0.2253	0.1824	0.1989
K-6	0.1017	0.0328	0.1011	0.1031		0.1194	0.0362	0.1186	0.1211
B-7	0.1077	0.1189	0.1011	0.1032		0.1292	0.1423	0.1186	0.1212
C-7	0.1826	0.1775	0.1553	0.1581		0.2253	0.2183	0.1894	0.1910
D-7	0.1786	0.1952	0.1562	0.1512		0.2178	0.2445	0.1887	0.1830
E-7	0.1864	0.1965	0.1540	0.1616		0.2273	0.2459	0.1906	0.1957
F-7	0.1772	0.1955	0.1565	0.1541		0.2158	0.2466	0.1895	0.1907
G-7	0.1763	0.1946	0.1551	0.1544		0.2148	0.2450	0.1893	0.1867
H-7	0.1845	0.1367	0.1574	0.1631		0.2321	0.1642	0.1918	0.1991
J-7	0.1062	0.1190	0.1012	0.1011		0.1255	0.1424	0.1187	0.1185
B-8	0.1010	0.0306	0.0981	0.1010		0.1185	0.0337	0.1164	0.1185
C-8	0.1699	0.1485	0.1543	0.1557		0.2080	0.1797	0.1866	0.1905
D-8	0.1783	0.1535	0.1509	0.1509		0.2196	0.1852	0.1818	0.1817
E-8	0.1820	0.1964	0.1569	0.1509		0.2302	0.2466	0.1898	0.1817
F-8	0.1824	0.1965	0.1534	0.1601		0.2250	0.2466	0.1852	0.1960
G-8	0.1906	0.1823	0.1582	0.1532		0.2412	0.2251	0.1920	0.1849
H-8	0.1774	0.1543	0.1576	0.1569		0.2182	0.1867	0.1928	0.1898
J-8	0.1083	0.0252	0.1010	0.1030		0.1298	0.0281	0.1184	0.1210
C-9	0.1070	0.0307	0.1011	0.1032		0.1281	0.0338	0.1185	0.1212
D-9	0.1060	0.1190	0.1010	0.1026		0.1261	0.1424	0.1184	0.1215
E-9	0.1976	0.1443	0.1569	0.1583		0.2436	0.1778	0.1899	0.1920

Table 2-2. (continued)

Basket cell location	Assembly decay heat (kW) ORIGEN					Assembly decay heat (kW) RG 3.54			
	Module 143	Module 144	Module 145	Module 146		Module 143	Module 144	Module 145	Module 146
F-9	0.2019	0.1363	0.1538	0.1600		0.2496	0.1638	0.1871	0.1959
G-9	0.1062	0.1194	0.1011	0.1027		0.1255	0.1426	0.1186	0.1215
H-9	0.1021	0.0281	0.0979	0.1023		0.1199	0.0311	0.1161	0.1201
E-10	0.1023	0.0329	0.1009	0.1021		0.1201	0.0363	0.1184	0.1199
F-10	0.1076	0.0322	0.0978	0.1022		0.1291	0.0355	0.1160	0.1199

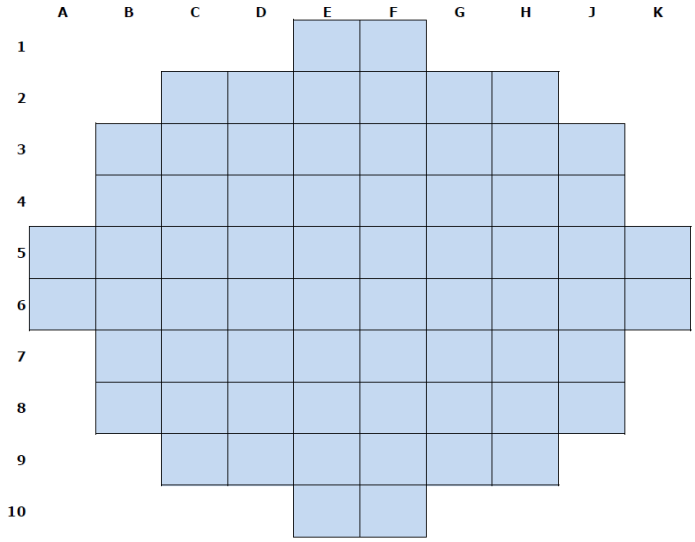

Figure 2-6. Diagram Illustrating Basket Cell Location Convention

The axial decay heat profile assumed for the GE 8x8 fuel within the canisters was modeled with a generic profile for BWR fuel, since axial burnup distributions for the fuel were not included in the fuel data package from Hope Creek. This profile, shown in Figure 2-7, is based on representative burnup distributions for BWR fuel (Turner 1989). More accurate information on the axial decay heat profile would result in more accurate predictions of peak component temperatures within the canister. Because the profile for spent fuel is expected to be relatively flat, the uncertainty in peak temperature predictions due to this approximation is generally assumed to be relatively small. Near the ends of the fuel region, however, the profile drops to near zero over a relatively short distance. This gradient strongly influences the temperature profile near the ends of the canister. The generic profile, rather than profiles representative of the fuel stored in these modules, is a source of uncertainty in the predictions of axial temperature distribution in the thermal modeling.

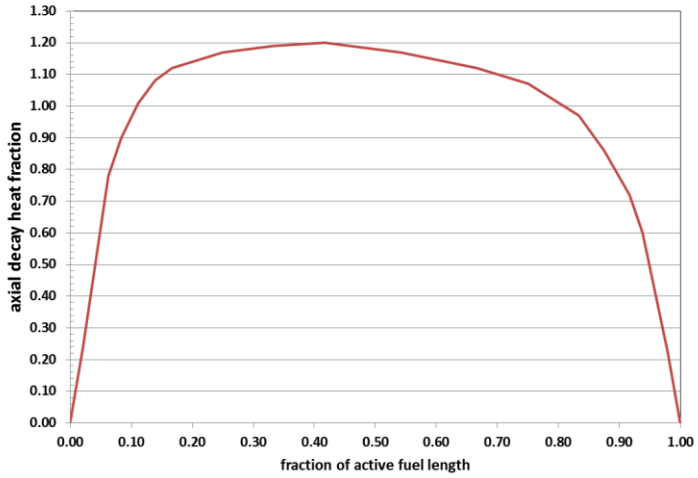

Figure 2-7. Generic Axial Decay Heat Profile for BWR Spent Fuel

2.2 Alternative Assembly Decay Heat Values from Oak Ridge National Laboratory

As part of the post-inspection evaluations, additional calculations were performed at Oak Ridge National Laboratory (ORNL), using the SCALE code[9], to verify the assembly decay heat values for the fuel in the inspected modules. It is expected that the values provided by Hope Creek are purposely conservative, as an operational safety feature, and are therefore probably slightly higher than the actual decay heat of the assemblies in these canisters. The calculations at ORNL were performed in an attempt to quantify the magnitude of this conservatism. However, sufficient detail on the fuel cycle history for the particular assemblies in these canisters was not provided, and the modeling could not be further refined. The simplifying assumptions required for this modeling, due to lack of specific assembly data, yielded slightly more conservative results than the decay heat values that had been provided by PSEG, from their ORIGEN modeling. This is illustrated by the comparison in Table 2-3.

Table 2-3. Decay heat values as of 8/1/2013 for modules inspected at the Hope Creek ISFSI

module	**from Hope Creek –**		**from ORNL –**
	ORIGEN modeling	**RG 3.57 modeling**	
MPC-144	9.286	11.402	10.10
MPC-145	9.237	11.130	10.15

Evaluations were performed with the COBRA-SFS model utilizing the revised assembly decay heat values and total decay heat values from the ORNL calculations. As expected, the slightly higher total decay heat load resulted in slightly higher peak cladding temperature prediction for these two canisters. However, lacking additional information on the fuel cycle history for the

[9] **S**tandardized **C**omputer **A**nalyses for **L**icensing **E**valuations system.

fuel assemblies in these particular modules, there is no reason to suppose that the new results from ORNL are in this case in any sense a "better estimate" of the decay heat load in the canister than is provided by the ORIGEN modeling at Hope Creek. Therefore, these estimates of decay heat were not used in the post-inspection analysis. All comparisons with measured data obtained during the inspection are based on pre-inspection predictions using the decay heat values from the ORIGEN modeling originally provided by PSEG, as listed in Table 2-2.

2.3 Ambient Conditions

Ambient conditions at the time of the inspection are expected to have a significant effect on the temperatures measured in the storage module. The inspection procedures obtained canister side surface temperature measurements by inserting a specially designed instrument down into the annulus, and bringing it into contact with the outer shell surface at selected locations along the axial length of the canister. Because the primary mode of heat removal from the canister at the outer shell is convection to the air flowing up the annulus, the shell surface temperature is directly dependent on the inlet air temperature.

For the pre-inspection evaluations, since it was not known what the air temperature would be at the time of the inspection (originally scheduled for August 2013) an average ambient temperature of 80°F (27°C) was assumed. This is a reasonable estimate of typical average daytime ambient temperatures at the Hope Creek ISFSI site in high summer, based on data[10] obtained from the National Oceanic and Atmospheric Administration (NOAA 2013). This is illustrated by the plot in Figure 2-8, showing monthly maximum, minimum, and average temperatures over the past year, from August 2012 to July 2013. Figure 2-9 shows the average maximum and average minimum temperatures on a monthly basis over this time period.

[10] This data will be archived after final quality control review (after the end of 2013), by the National Climatic Data Center and will be publicly available at http://www.ncdc.noaa.gov.

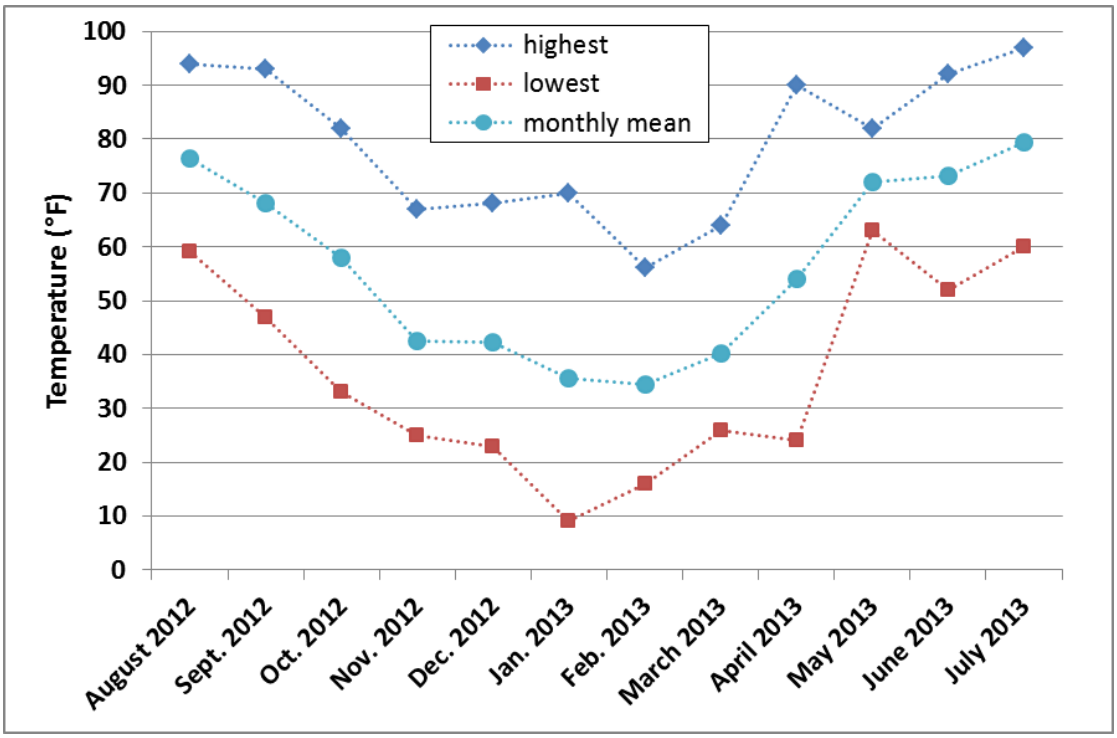

Figure 2-8. Monthly Maximum, Minimum, and Average Temperatures Reported at the New Castle County Airport, Wilmington, Delaware (NOAA 2013)

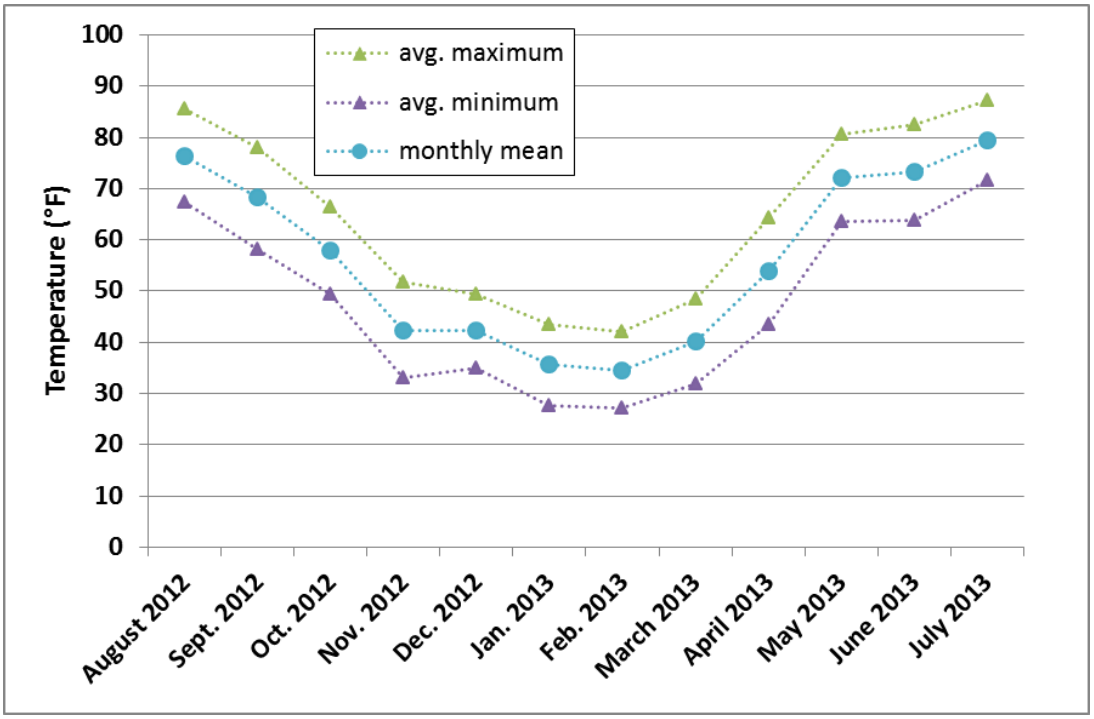

Figure 2-9. Monthly Average Maximum and Minimum Temperatures Reported at the New Castle County Airport, Wilmington, Delaware (NOAA 2013)

The ambient air temperature data shown in Figures 2-8 and 2-9 are archived data from the reporting station at the New Castle County Airport in Wilmington, Delaware, approximately 18 miles northeast of the Hope Creek plant. This station is the NOAA weather reporting station for the surrounding area, including Hancocks Bridge, New Jersey, where the plant is located. Ambient temperature data from a monitoring station located at the ISFSI would yield a more accurate estimate of local ambient conditions, but such data is not available. Ambient air temperature data from an on-site meteorological tower on the Hope Creek site was provided, after to the actual inspection, but no site-specific data was available for the pre-inspection predictions.

Because of the uncertainty in local ambient conditions and the shifting time-frame of the inspection, additional calculations were performed over a range of assumed ambient conditions. These calculations were performed only for Modules 144 and 145, which were identified[11] as the specific modules that would be inspected. The range of ambient conditions evaluated are for an extraordinarily hot day at 90°F (32.2°C) and a more moderate day at 70°F (21.1°C). In addition, because of the possibility that the inspection might not be performed until late autumn, a third case assumed a chilly ambient of 50°F (10°C). This was a fortuitous choice, as the inspection was actually carried out in November of 2013. The measured ambient temperatures at the time that thermocouple measurements were made on the MPC sides and top lids are recorded as being in the range 45 to 55°F (7 to 13°C).

In all cases, the analysis assumes that these ambient conditions are with still air. Consideration of wind effects in the current modeling effort would require detailed information on wind speed, direction, and variation over time at the ISFSI location, to estimate the effect on flow velocities at the inlet vents of the specific modules to be inspected. By definition, this information is not available for pre-inspection calculations. The study of wind effects on storage system performance is a topic of some interest in general for a number of reasons, but it is beyond the scope of the current work. The specific weather conditions for the site during the actual inspection are discussed in Section 4.0, with the presentation of the measured temperature data.

The external solar heat load on the modules assumed for these calculations is based on the solar radiation assumptions specified in 10 CFR 71.71 (10 CFR 71 2003). This regulation is defined for transport conditions, but the specified values are generally used for stationary storage systems, as well. Solar radiation over a 12-hour period is defined in 10 CFR 71.71 as

- 800 cal/cm^2 (2950 Btu/ft^2) for horizontal surfaces
- 400 cal/cm^2 (1475 Btu/ft^2) for curved surfaces.

Adjusting for the surface emissivity, which in these evaluations is assumed to be 0.9 for the painted exterior surfaces of the overpack, the above specified values are averaged over a 24-hour period, to obtain the following solar heat flux values for this system:

[11] Marschman S. 2013. Email message from Steve Marschman (Idaho National Laboratory to Harold E. Adkins [of PNNL] "More", sent Monday, August 12, 2013 10:20AM [PDT]).

- 349 W/m^2 (110.6 Btu/hr-ft^2) on the overpack lid
- 175 W/m^2 (55.3 Btu/hr-ft^2) on the outer shell.

These values may be conservative for the solar heat load on the modules at the time of the actual inspection, but in the absence of site-specific information, they will have to do.

3.0 PRE-INSPECTION PREDICTIONS OF COMPONENT TEMPERATURES

This section is an exact duplicate of Section 3.0 in the "pre-inspection" report (Cuta and Adkins 2013). It is repeated here simply for convenience. As noted in the discussion of the COBRA-SFS model in Section 2.0, no new thermal analyses were performed after the actual inspection, since there was no additional site-specific information available on the inspected modules, and the pre-inspection predictions encompassed the boundary conditions (specifically, ambient temperature) at the site during the actual inspection.

The COBRA-SFS model described in Section 2.0 was used to obtain predictions of component temperatures within the four modules being considered for inspection at the Hope Creek ISFSI. (As of mid-August 2013, Modules 144 and 145 have been selected as the modules to be inspected.) Calculations were performed for the total decay heat values and assembly decay heat distributions provided based on the ORIGEN methodology and the RG 3.54 methodology. These calculations assume an average ambient temperature of 80°F (27°C), in still air, with external solar heat load as specified in 10 CFR 71. Table 3-1 summarizes peak temperatures predicted for components of the canister for each case. Table 3-2 summarizes peak temperatures predicted for components of the overpack.

Table 3-1. Peak Component Temperatures, °F (°C), in MPCs (ambient 80°F [27°C])

	Fuel cladding	**Fuel channel**	**Basket plate**	**Basket periphery**	**Basket support**	**Canister inner surface**	**Canister outer surface**
ORIGEN							
Module 143	264 (128.7)	262 (127.5)	262 (127.5)	214 (101.0)	200 (93.4)	170 (76.9)	169 (76.1)
Module 144	254 (123.2)	252 (122.2)	252 (122.2)	209 (98.2)	194 (90.0)	165 (74.1)	164 (73.4)
Module 145	244 (117.5)	242 (116.7)	242 (116.7)	200 (93.4)	188 (86.7)	162 (72.3)	161 (71.6)
Module 146	245 (118.2)	243 (117.3)	243 (117.3)	201 (93.8)	189 (87.2)	163 (72.6)	161 (71.9)
RG 3.54							
Module 143	296 (146.6)	294 (145.3)	294 (145.3)	238 (114.2)	221 (105.2)	185 (85.2)	184 (84.2)
Module 144	285 (140.7)	283 (139.6)	283 (139.6)	232 (111.3)	215 (101.5)	180 (82.1)	178 (81.2)
Module 145	270 (132.1)	268 (131.2)	268 (131.2)	220 (104.2)	206 (96.4)	174 (79.1)	173 (78.3)
Module 146	271 (133.0)	269 (131.9)	269 (131.9)	221 (104.8)	207 (97.0)	175 (79.5)	174 (78.6)

Table 3-2. Peak Component Temperatures, °F (°C), in Overpack (ambient 80°F [27°C])

	Annulus shims	**Overpack inner shell**	**Overpack concrete**	**Overpack outer shell**	**Overpack lid inner surface**	**Overpack lid outer surface**
ORIGEN						
Module 143	169 (76.1)	169 (75.9)	165 (73.6)	94 (34.3)	110 (43.3)	96 (35.3)
Module 144	164 (73.4)	163 (73.2)	164 (73.2)	94 (34.2)	109 (42.7)	95 (35.2)
Module 145	161 (71.4)	160 (71.4)	157 (69.4)	93 (34.1)	108 (42.2)	95 (35.2)
Module 146	161 (71.7)	161 (71.7)	157 (69.6)	93 (34.1)	108 (42.3)	95 (35.2)
RG 3.54						
Module 143	183 (84.0)	183 (84.0)	178 (81.3)	95 (34.8)	113 (45.3)	96 (35.5)
Module 144	178 (81.0)	178 (80.9)	173 (78.4)	94 (34.6)	112 (44.6)	96 (35.5)
Module 145	173 (78.1)	172 (78.0)	168 (75.6)	94 (34.4)	111 (43.8)	96 35.4
Module 146	173 (78.4)	173 (78.4)	169 (76.0)	94 (34.4)	111 (43.9)	96 35.4

Axial temperature distributions on the canister shell are presented in Figures 3-1 through 3-4 for the four modules. These plots show temperatures determined for the decay heat values from the ORIGEN methodology and from the RG 3.54 methodology. The RG 3.54 methodology yields somewhat higher temperatures, due to the higher decay heat values predicted for the fuel within the modules. For a given methodology, however, the axial temperature profiles on the canister shell are very similar.

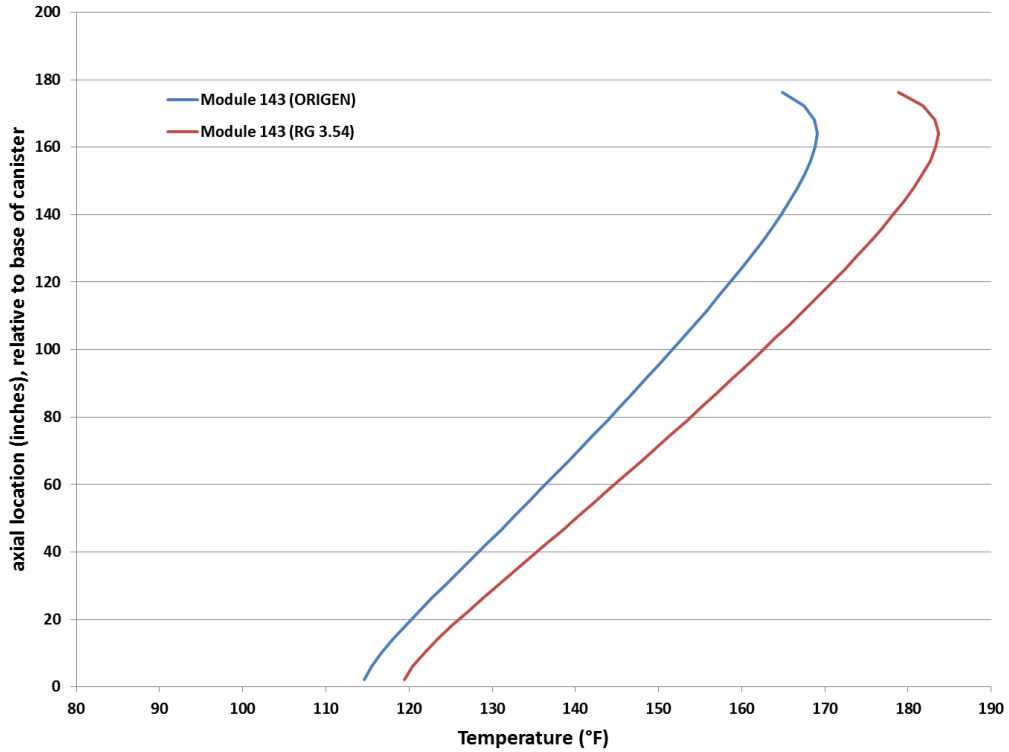

Figure 3-1. Axial Temperature Profile on MPC Outer Shell: Module 143 80°F (27°C) Ambient

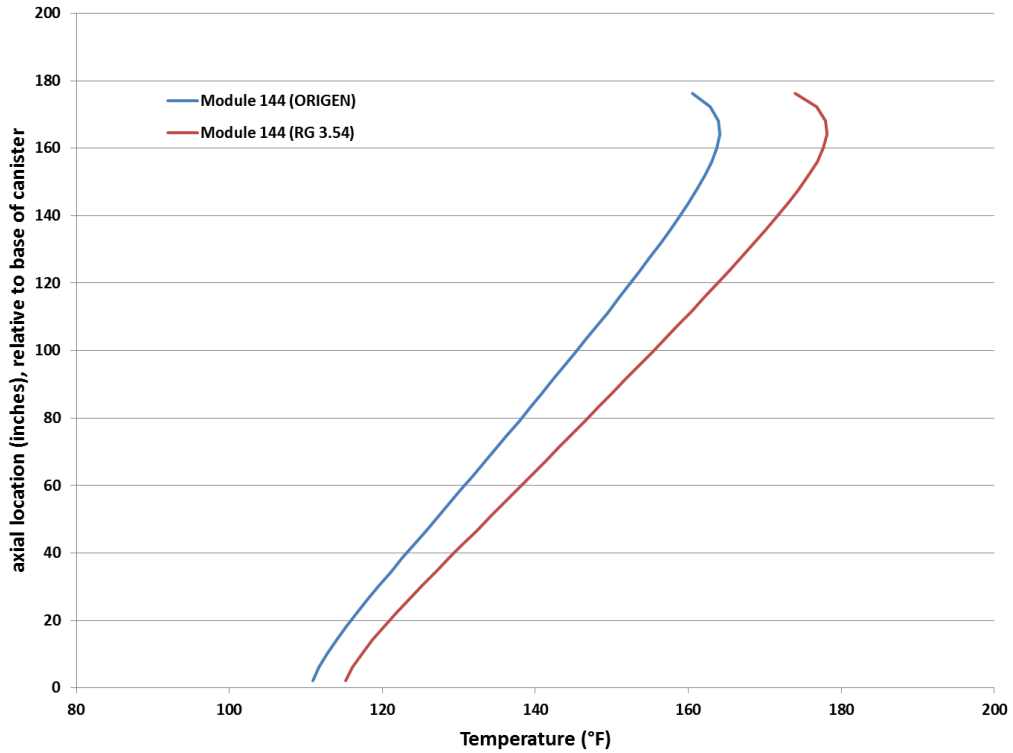

Figure 3-2. Axial Temperature Profile on MPC Outer Shell: Module 144 80°F (27°C) Ambient

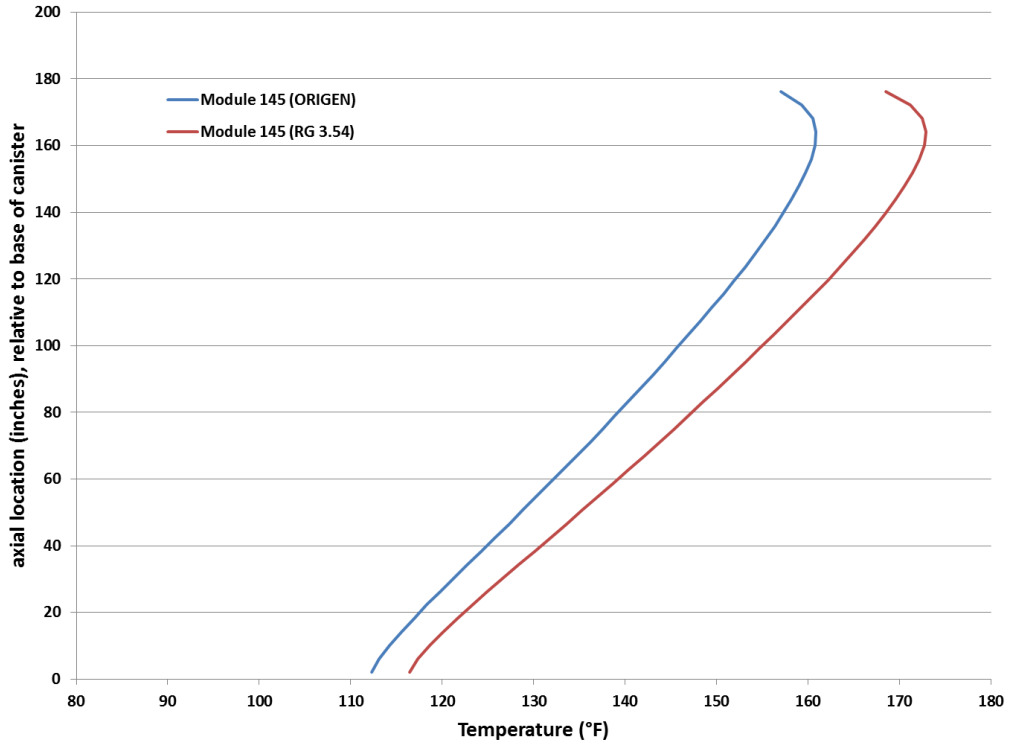

Figure 3-3. Axial Temperature Profile on MPC Outer Shell: Module 145 80°F (27°C) Ambient

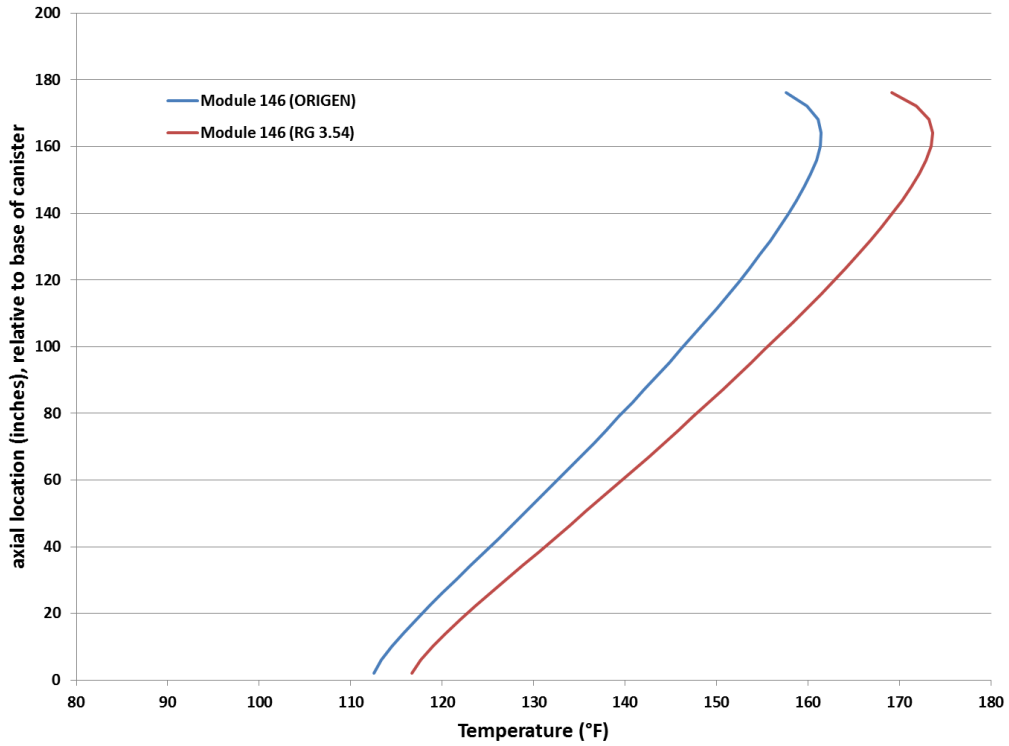

Figure 3-4. Axial Temperature Profile on MPC Outer Shell: Module 146 80°F (27°C) Ambient

The axial temperature profiles shown in Figures 3-1 through 3-4 are on a vertical line through the peak canister shell temperature location. However, the circumferential variation in predicted temperature at any given axial location on the canister shell is quite small. The symmetrical geometry of the air flow path through the module (i.e., inlet vents, annulus, and outlet vents), is designed to assure uniform distribution of air around the annulus between the canister shell and the overpack inner wall. In the 100S Version B design specifically, the air inlet flow path through the upper base plate provides an extremely effective flow distributor to ensure uniform distribution of air flow into the annulus.

Given the geometric design of the system and the assumption of still air external to the module, the only significant source of circumferential variation in predicted temperatures is in asymmetries in the fuel loading pattern within the canister basket. However, close examination of the loading patterns within the baskets of these four canisters (refer to Table 2-2) shows that the distribution of the decay heat load in each individual canister is remarkably symmetrical. This is illustrated in Figure 3-5, with plots of the decay heat values (from ORIGEN) in the peripheral assemblies of the basket (refer to Figure 2-6 for basket cell numbering convention.) Table 3-3 summarizes the maximum, minimum, and average assembly decay heat values for these peripheral assemblies.

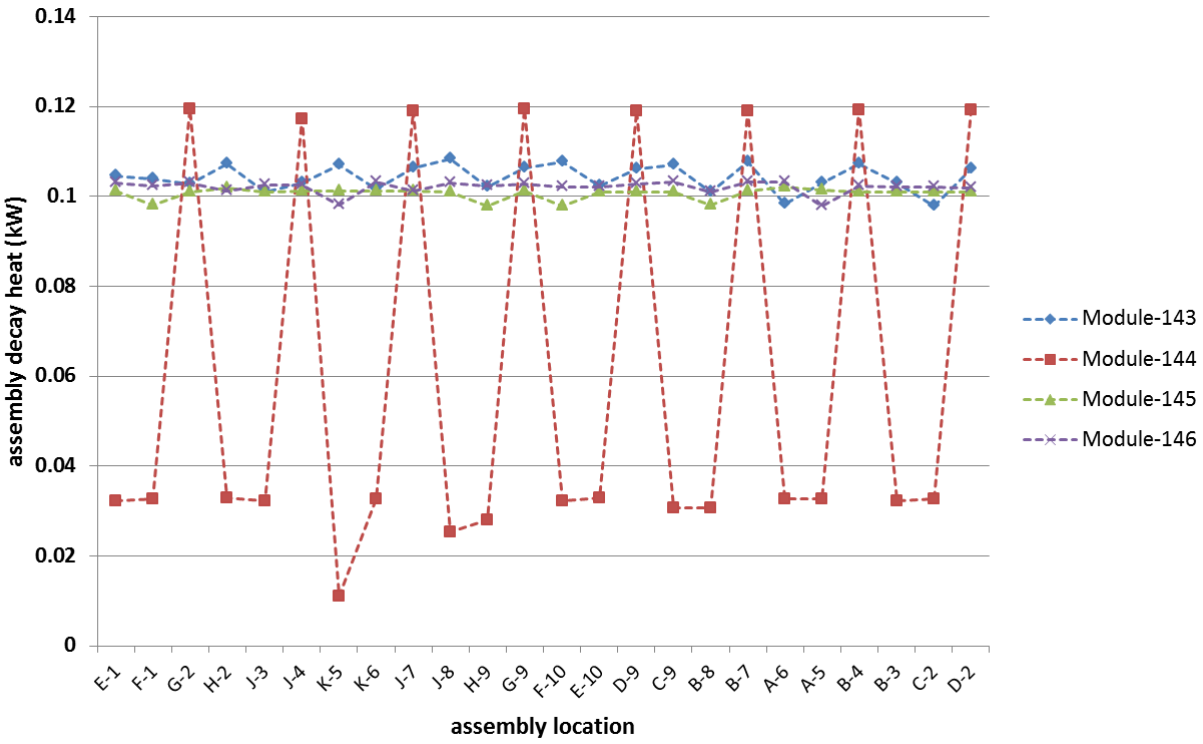

Figure 3-5. Decay Heat Values for Assemblies on Basket Periphery

Table 3-3. Summary of Decay Heat Variation Around Basket Periphery

	Maximum	**Minimum**	**Average**	**Maximum deviation from average**
Module 143	0.10834	0.0978	0.1042	6.1%
Module 144				
"hot" assemblies	0.1194	0.1172	0.1189	1.5%
"cold" assemblies	0.0330	0.0111	0.0297	63%
Module 145	0.1021	0.0978	0.1006	2.8%
Module 146	0.1032	0.0978	0.1020	4.1%

With the exception of Module 144, which has extremely "cold" assemblies in the paired basket end locations (e.g., E-1, F-1), the peripheral assemblies in a given basket all have nearly the same decay heat load. Even in Module 144, the variation is uniformly distributed around the circumference of the basket, and the "hot" assemblies all have nearly the same decay heat load (within 1.5% of the average). In addition to the relative uniformity of the heat load distribution, the downflow of helium gas in the spaces between the basket and the canister shell, due to natural circulation within the canister, tends to smooth out circumferential temperature gradients in the basket periphery and the canister shell.

Predicted temperature distributions around the circumference of the canister are shown in Figures 3-6 through 3-9 for the four modules, at selected axial locations along the canister height. These plots show the circumferential temperature distributions at the canister base, the canister midplane, and at the axial location of the peak outer shell temperature. As expected for the geometry and boundary conditions for this model, the circumferential variation in temperature on the canister shell is quite small. The plots in Figures 3-6 through 3-9 are for results with decay heat values from the ORIGEN modeling. Slightly higher temperatures are obtained with the decay heat values from the RG 3.54 modeling (as illustrated by the axial plots in Figures 3-1 through 3-4), but the circumferential gradients on the canister shell show essentially the same pattern.

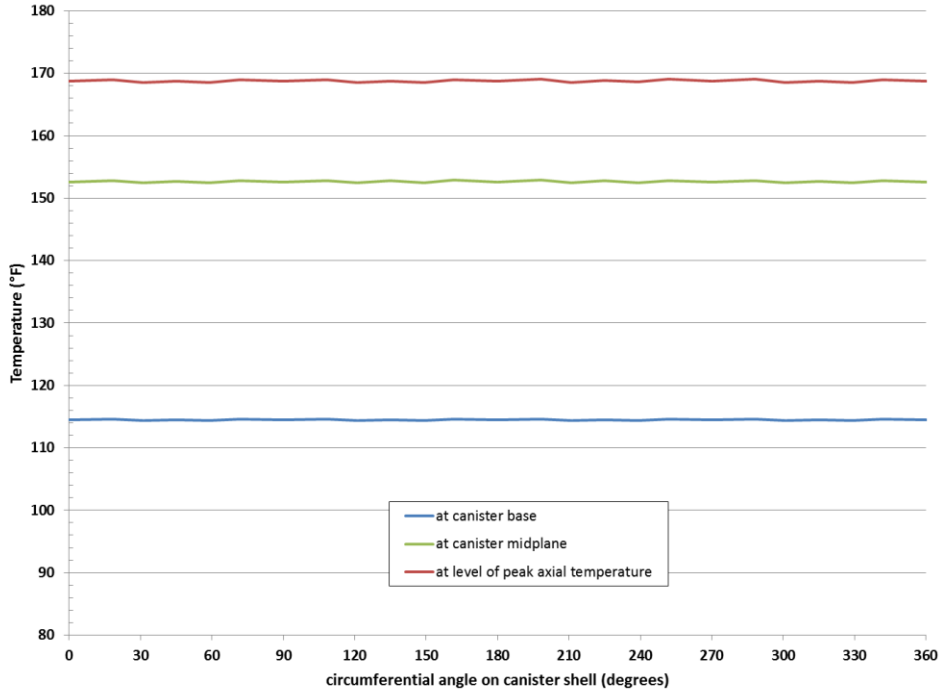

Figure 3-6. Circumferential Temperature Distribution on MPC Outer Shell for Module 143 (80°F [27°C] ambient, with decay heat values from ORIGEN modeling)

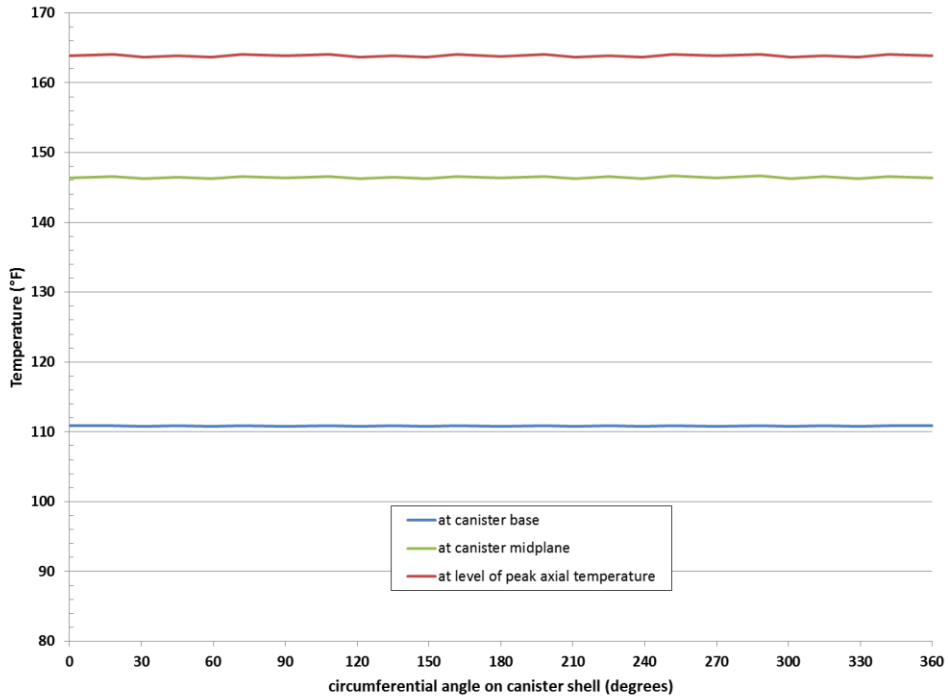

Figure 3-7. Circumferential Temperature Distribution on MPC Outer Shell for Module 144 (80°F [27°C] ambient, with decay heat values from ORIGEN modeling)

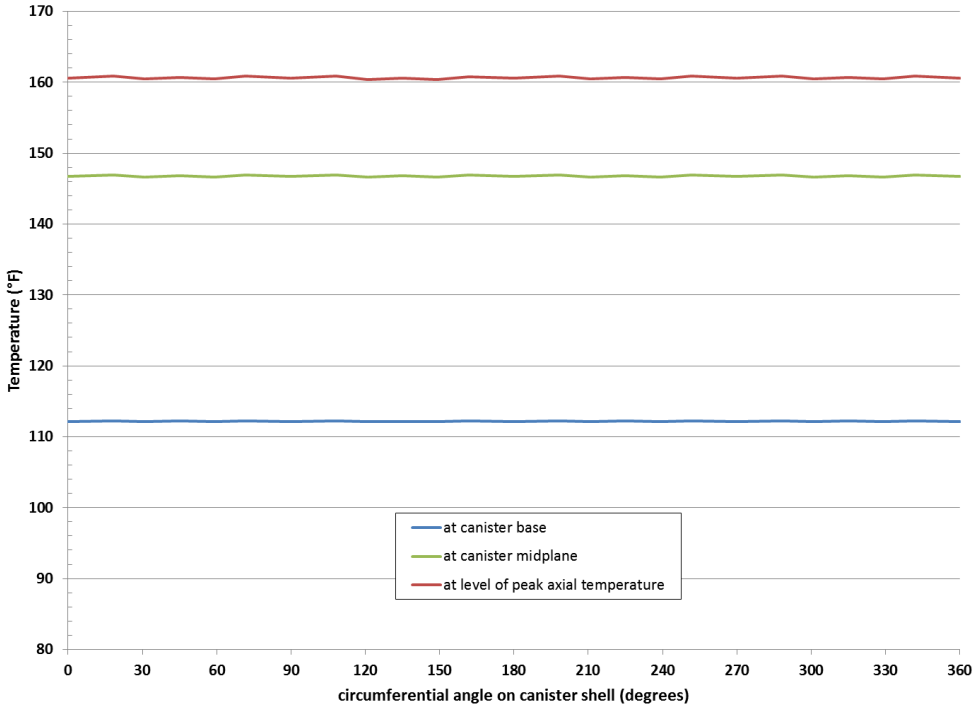

Figure 3-8. Circumferential Temperature Distribution on MPC Outer Shell for Module 145 (80°F [27°C] ambient, with decay heat values from ORIGEN modeling)

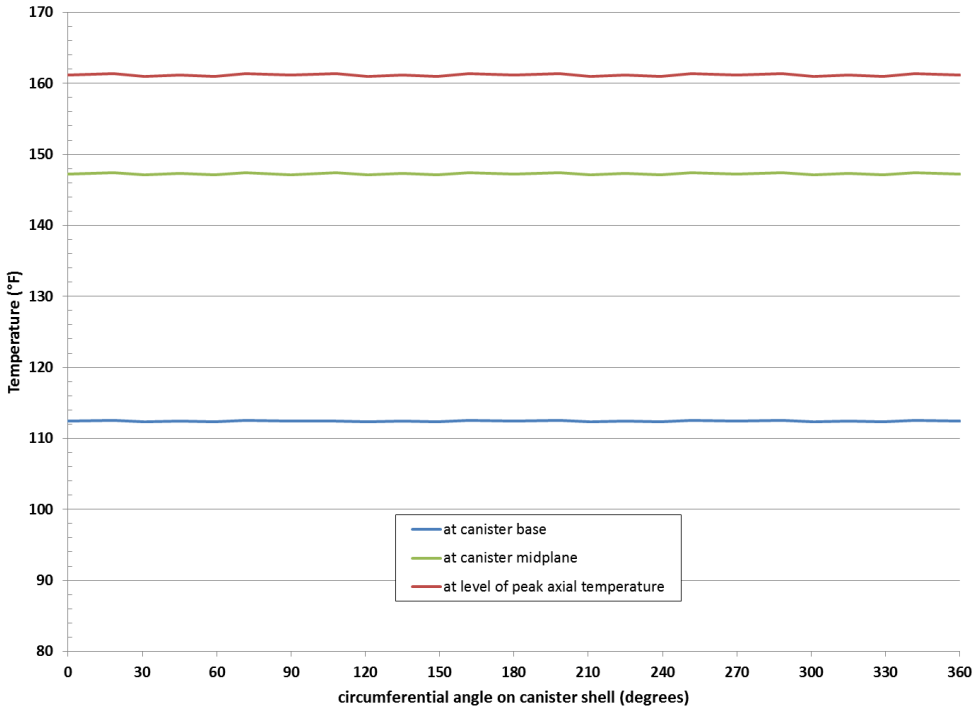

Figure 3-9. Circumferential Temperature Distribution on MPC Outer Shell for Module 146 (80°F [27°C] ambient, with decay heat values from ORIGEN modeling)

The predicted temperatures for the storage modules are sensitive to the ambient temperature, and there is some uncertainty in what the ambient temperature will be at the time of inspection. Therefore, an additional set of cases were run for Modules 144 and 145, which have been identified as the modules to be inspected. These cases provide temperature predictions for assumed daytime ambient temperatures of 90°F (32.2°C), 70°F (21.1°C), and 50°F (10°C). These calculations were performed only for the decay heat loadings based on the ORIGEN modeling, on the assumption that these are likely to be the more accurate of the two sets of projected decay heat loads for these fuel assemblies. Tables 3-4 and 3-5 show the effect of the variation in this boundary condition on the peak temperatures predicted for the two modules. Figure 3-10 shows the effect on the canister shell temperature profile in Module 144. Figure 3-11 shows the effect in Module 145.

Table 3-4. Summary of Effect of Ambient Temperature on Peak Component Temperatures °F (°C), in the MPC

Ambient temperature	Fuel cladding	Fuel channel	Basket plate	Basket periphery	Basket support	Canister inner surface	Canister outer surface
Module 144							
50°F (10°C)	219 (103.7)	217 (102.8)	217 (102.8)	178 (81.1)	163 (72.8)	134 (56.5)	132 (55.7)
70°F (21°C)	242 (116.6)	240 (115.6)	240 (115.6)	198 (92.4)	183 (84.2)	155 (68.1)	153 (67.4)
80°F (27°C)	254 (123.2)	252 (122.2)	252 (122.2)	209 (98.2)	194 (90.0)	165 (74.1)	164 (73.4)
90°F (32°C)	266 (129.9)	264 (128.9)	264 (128.9)	219 (104.0)	205 (95.9)	176 (80.2)	175 (79.5)
Module 145							
50°F (10°C)	215 (101.5)	213 (100.7)	213 (100.7)	174 (78.8)	161 (71.8)	134 (56.6)	133 (55.9)
70°F (21°C)	233 (111.6)	231 (110.8)	231 (110.8)	191 (88.1)	178 (81.3)	152 (66.6)	151 (65.9)
80°F (27°C)	244 (117.5)	242 (116.7)	242 (116.7)	200 (93.4)	188 (86.7)	162 (72.3)	161 (71.6)
90°F (32°C)	255 (124.1)	254 (123.2)	254 (123.2)	211 (99.3)	199 (92.7)	173 (78.5)	172 (77.8)

It is important to note that the temperatures reported here are based on steady-state calculations. This analysis does not capture the effect of diurnal temperature variation throughout the system. Thermal inertia will tend to slow the rate of change of temperatures on canister internal components in response to ambient conditions (specifically, the peak fuel cladding temperature, peak fuel channel temperature, and hottest basket plate). However, the canister shell temperature, which is directly cooled by ambient air flowing in the annulus, is expected to track local ambient temperature fairly closely, and therefore the ambient temperature will have an effect on the measured temperatures at the time of the inspection.

Table 3-5. Summary of Effect of Ambient Temperature on Peak Component Temperatures, °F (°C), in the Overpack

Ambient temperature	Annulus shims	Overpack inner shell	Overpack concrete	Overpack outer shell	Overpack lid inner surface	Overpack lid outer surface
Module 144						
50°F (10°C)	132 (55.5)	132 (55.5)	128 (53.4)	64 (17.5)	109 (42.7)	95 (35.2)
70°F (21°C)	153 (67.2)	153 (67.2)	149 (65.0)	84 (28.6)	109 (42.7)	95 (35.2)
80°F (27°C)	164 (73.4)	163 (73.2)	164 (73.2)	94 (34.2)	109 (42.7)	95 (35.2)
90°F (32°C)	175 (79.3)	175 (79.3)	175 (79.3)	104 (39.7)	109 (42.7)	95 (35.2)
Module 145						
50°F (10°C)	132 (55.7)	132 (55.7)	129 (53.6)	65 (18.5)	108 (42.2)	95 (35.2)
70°F (21°C)	150 (65.7)	150 (65.7)	147 (63.6)	84 (28.6)	108 (42.2)	95 (35.2)
80°F (27°C)	161 (71.4)	160 (71.4)	157 (69.4)	93 (34.1)	108 (42.2)	95 (35.2)
90°F (32°C)	172 (77.7)	172 (77.6)	168 (75.6)	103 (39.6)	108 (42.2)	95 (35.2)

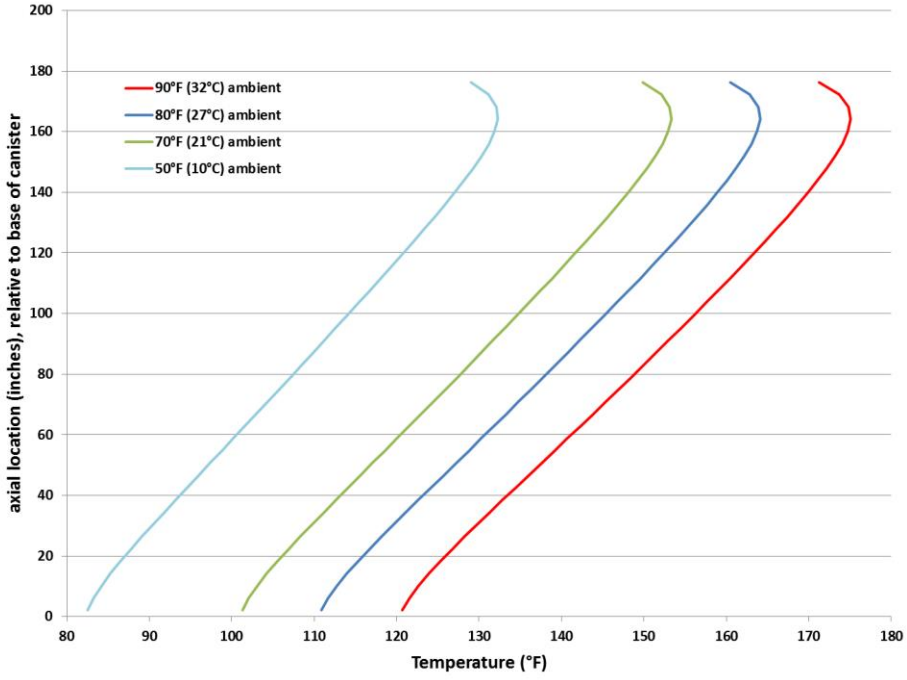

Figure 3-10. Axial Temperature Profile on MPC Outer Shell for Module 144 for a Range of Ambient Temperatures (with decay heat values from ORIGEN modeling)

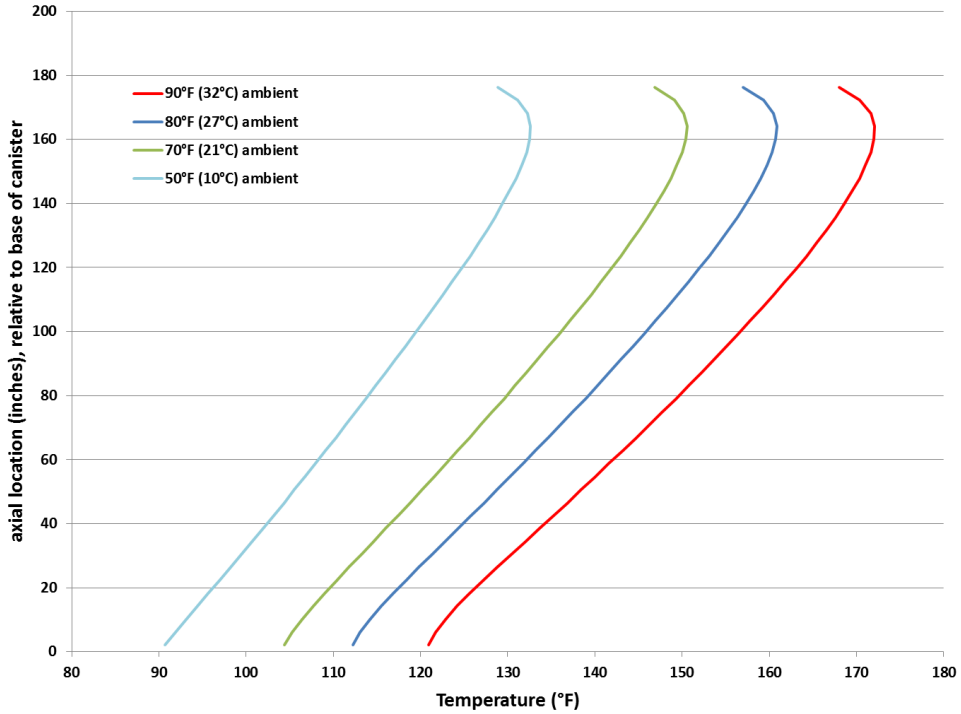

Figure 3-11. Axial Temperature Profile on MPC Outer Shell for Module 145 for Range of Ambient Temperatures (with decay heat values from ORIGEN modeling)

4.0 MEASURED TEMPERATURES FROM HOPE CREEK SITE INSPECTION

The site inspection of MPC-144 and MPC-145 at the Hope Creek ISFSI was carried out over a 4-day period, November 19-22, 2013. The data obtained in the inspection is documented by Holtec (Holtec 2014). Measurements obtained in the inspection consist of surface sampling on the side and top lid of the MPC, with an inspection tool designed by Holtec, and surface temperature measurements. Some of the reported temperature measurements were taken in conjunction with a surface sample, and some were reported as "temperature only" measurements. The data reported by Holtec does not report a timestamp for any of the measurements. In the case of the top lid surface measurements, some temperature measurements are reported twice, giving the erroneous impression that they are replicate points, when in fact they simply echo an earlier measurement at the same location.

No information is given in the Holtec report on the instrumentation used to measure the temperatures (for either the MPC surfaces or ambient air) during the inspection, other than to note that the instrument is "a thermocouple". Nor is the procedure used to make the measurements described in sufficient detail to determine how or when the measurements were obtained, in relationship to the surface sampling. The limited information on the construction of the measurement probe, as described in the Holtec report and observations from team members on-site at the time of the inspection, indicate that the local canister surface temperature measurements were obtained using a thermocouple taped to the back of a contact probe that appeared to have a substantial thermal mass. This design invited potential issues with secure contact of the thermocouple with the probe, and also suggests that a significant length of time in secure contact would be required for the instrument to reach equilibrium temperature with the surface being measured. Because of lack of details describing the test procedures (as planned or as actually carried out), there is insufficient information available for a quantitative assessment of measurement uncertainty, or to determine reasonable estimates of sensitivity of surface temperatures to wind conditions.

Additional information to supplement some of the gaps in the Holtec report has been supplied by anecdotal reports from UFDC team members present on-site at the time of the inspection. The physical structure of the HI-STORM 100 storage module presented considerable difficulties in inserting the instrumentation probe to the desired measurement point and holding it in place for sufficient time and with adequate pressure to obtain reliable local measurements. The magnitude of the difficulty can be appreciated by examining the required pathway (shown by the dashed arrows) in the generic module section view in Figure 4-1. The wind speed was high and fluctuated significantly during the initial day of the test period, and in subsequent days, wind was at all times significantly variable, although at generally lower speeds than on the first day. In addition, the ambient temperature had unusual and greater than normal variation during the entire inspection period. As would be expected for such ambient conditions, the thermal plume from the cask outlet vent could be clearly seen to fluctuate significantly with varying wind speed and changing wind direction, while measurements were being taken. Uncalibrated local wind meter readings in the range of 35 mph at the site were witnessed by observer team members during periods of data collection. These conditions were approaching the wind speed limit mandated

for operation of the Genie lift being used to support equipment and personnel carrying out the test measurements.

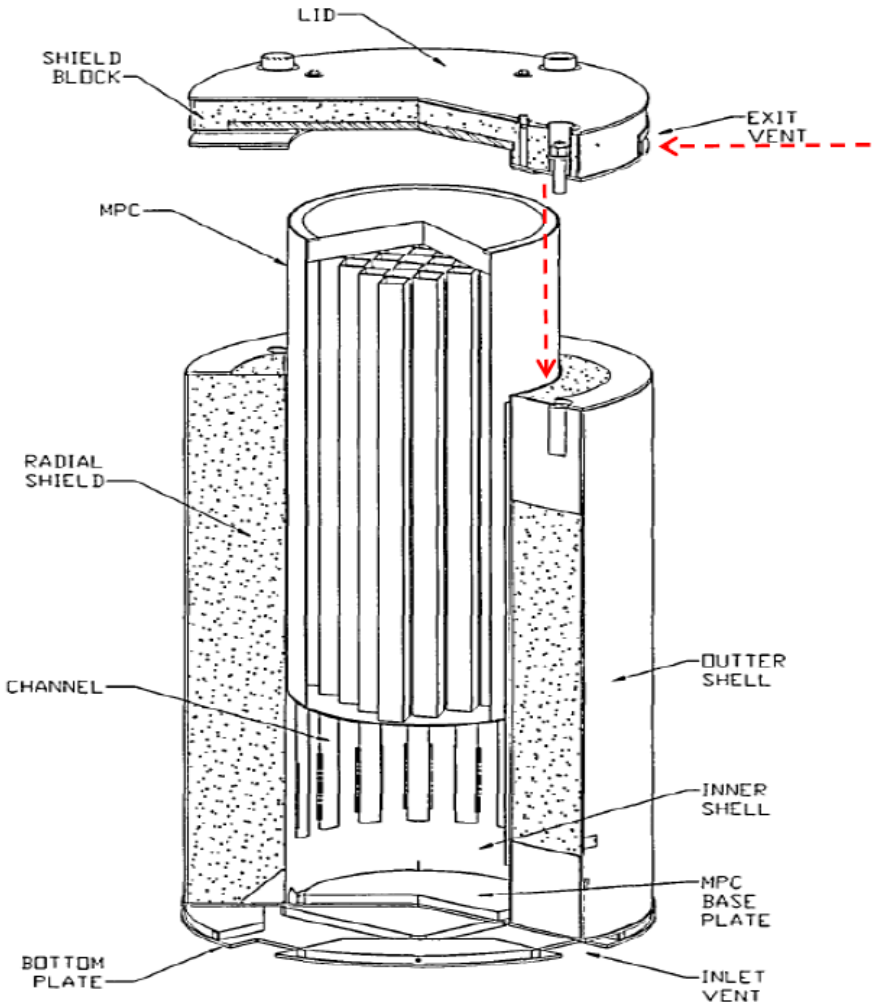

Figure 4-1. Illustration of Instrument Access Path for Canister Surface Measurements (Image courtesy of Holtec International; reprinted with permission)

Information on site weather at the time of the inspection has been supplied by PSEG[12], from an on-site meteorological tower recording wind speed, direction, and local ambient temperature. This tower is located approximately one mile south-east of the ISFSI, and the reported data is from instrumentation at an elevation of 33 ft above local ground level. Since the Hope Creek site is very flat and low-lying, it is a reasonable assumption that this would correspond to

[12] Email from Glenn Schwartz of PSEG, sent Wednesday 1/15/2014, 6:18AM PST; subject line "Site atmospheric data during PSEG inspection week."

approximately 33 ft above ground level at the ISFSI, as well. The height of the storage modules is approximately 18 ft, so the meteorological data is from a height approximately twice as far above the ground, and a mile away.

Based on the limited information in the Holtec report, and anecdotal evidence supplied by on-site observers, Table 4-1 summarizes the general data gathering activities of the inspection. The specific surface temperature measurements and ambient air temperature measurements obtained in the course of the inspection are presented in Sections 4.1 through 4.4, for each day of the 4-day site visit, along with the meteorological data for the corresponding day, obtained from the on-site tower. According to on-site observers, the time-frame of activities on any given day occurred over the span of a typical "day shift" from about 9:00AM to 4:00PM. This is consistent with the stated time limit of 7 hours per day for measurement activities, as documented by Holtec (Holtec 2014), defining the maximum length of time the inspection tool and associated hardware would be allowed to continuously block the outlet vent. The tower data noted in the "weather summary" column of Table 4-1 summarizes conditions over this 9:00AM to 4:00PM time span each day.

Table 4-1. Summary of Measurement Activities in the Site Inspection at the Hope Creek ISFSI, November 19-22, 2013

Date	Module inspected	Inferred sequence of measurements	Weather summary
11/19/2013	MPC-145	THREE surface sampling measurements taken on side of MPC (sample ID numbers 145-002 through -005); side surface temperatures and ambient air temperature also recorded insertion depths of 13.5 ft, 8.5 ft, and 1.5 ft down the annulus	site ambient temperature recorded as 50-52°F; tower data range was 44-47°F ambient; wind speed range 10 to 17 mph
11/20/2013	MPC-145	THREE surface sampling measurements taken on side of MPC (sample ID numbers 145-006, -007, and -014; one "temperature only", no ID assigned); surface temperature and ambient air temperature also recorded insertion depths of 13 ft, 7.5 ft, and 1 ft down the annulus	site ambient air temperature recorded as 38°F, 49°F, and 46°F; tower data range was 33-43°F ambient, and wind speed range 3 to 8 mph
		THREE "temperature-only" measurements taken on the top lid of the MPC (sample ID numbers 145-008 to -010); ambient air temperature also recorded insertion depths of 64.5 inches, 58.5 inches, and 41.75 inches across top lid	site ambient air temperature recorded as 48°F to 53°F

		THREE sampling measurements taken on top lid surface of MPC (sample ID numbers 145-011 through 145-013) no new surface or ambient temperature measurements taken in conjunction with these samples	

Table 4-1. (continued)

Date	Module inspected	Inferred sequence of measurements	Weather summary
11/21/2013	MPC-144	ELEVEN sampling measurements taken on side surface of MPC (sample ID numbers 144-005 through -010; ID numbers not assigned for temperature-only measurements); surface temperature and ambient air temperature also recorded insertion depths from 13.5 to 1.0 ft down the annulus	site ambient air temperature ranged from 46°F to 54°F; tower data range was 36-50°F ambient , wind speed range was 2.4 to 8.7 mph
11/22/2013	MPC-144	THREE temperature-only measurements taken on top lid of MPC; ambient air temperature also recorded insertion depths of 40.5 inches, 58.5 inches, and 64.5 inches	site ambient air temperature recorded as 52°F to 53°F; tower data range was 51-56°F ambient, wind speed range 2.9 to 8.5 mph
		FOUR sampling measurements taken on top lid of the MPC (sample ID numbers 144-011 through -014) NOTE: NO NEW SURFACE TEMPERATURES RECORDED IN CONJUNCTION WITH THESE SAMPLES	

Based on the meteorological data from the tower approximately 1 mile southeast of the ISFSI, the ambient temperature followed an unusual diurnal cycle over the week of the inspection, and the wind speed varied over a large range. Figure 4-2 shows a plot of the ambient temperature recorded at the tower, presented as measurements at half-hour intervals over the time period of interest. The plot in this figure notes the number and type of inspection measurements taken on each day. This plot shows that the day prior to the inspection was unusually warm, then temperatures cooled significantly over the next two days (Day 1 and Day 2 of the inspection). At about mid-morning of Day 3, the ambient air temperature climbed rapidly from nearly 30°F to about 50°F, and remained at this value without significant change through the night and most of the following morning (Day 4 of the inspection). Shortly before noon on Day 4, the ambient temperature began to climb again, at a slower rate than the day before.

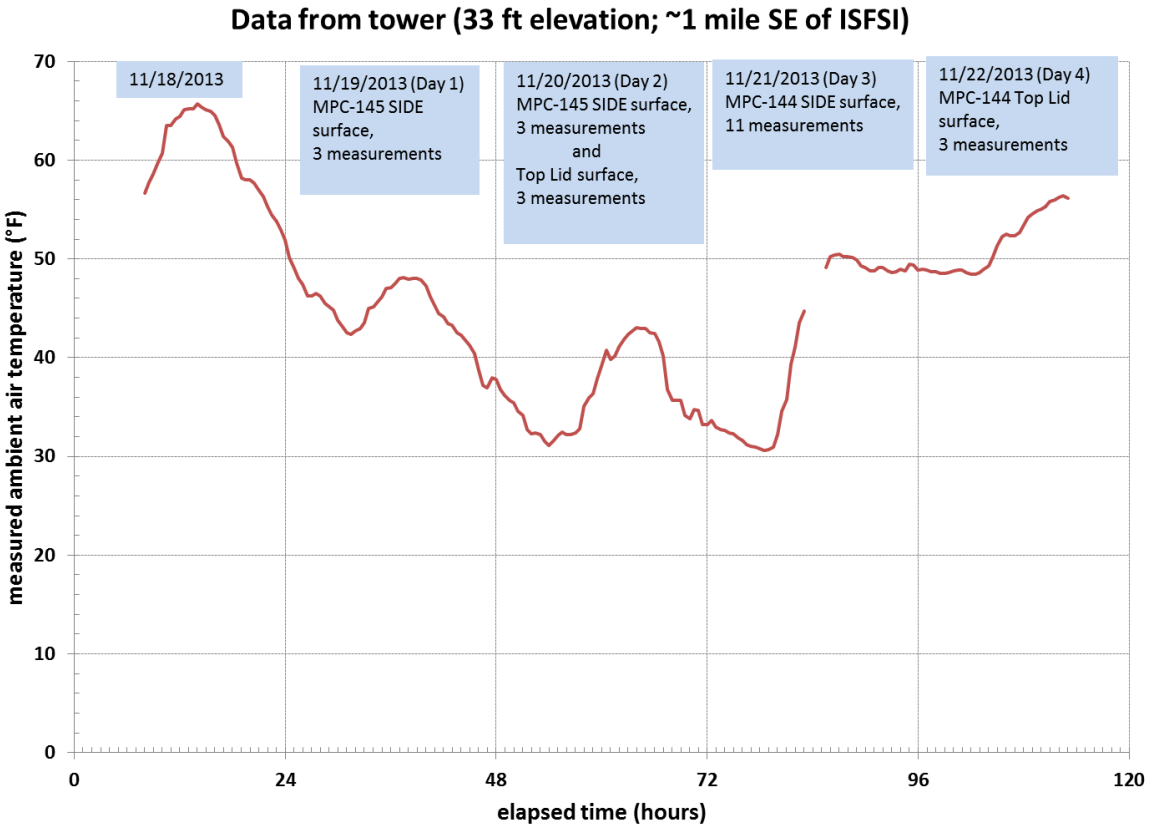

Figure 4-2. Ambient Air Temperature Recorded by Instrumentation on Meteorological Tower during Inspection Week

Wind conditions that accompanied the temperature trace in Figure 4-2 are plotted in Figure 4-3. This plot shows high and gusty winds on the day before the inspection, and throughout the daytime hours of Day 1 of the inspection. There was significantly less wind on Days 2, 3, and 4 of the inspection, but wind was at all times present, and showed significant variation over time. Compared to the wind conditions on Day 1, the conditions on the other three days might be described as "light and variable", but the significant observation on this data is that at no time during the inspection did the condition of "still air" prevail. The effect of forced convection within the modules due to wind "chimneying" through the annulus at varying speed throughout the inspection period, and the non-uniform diurnal variation of ambient air temperature, make it highly unlikely that the surface temperatures on the canisters within the modules would have been at steady-state when measurements were taken.

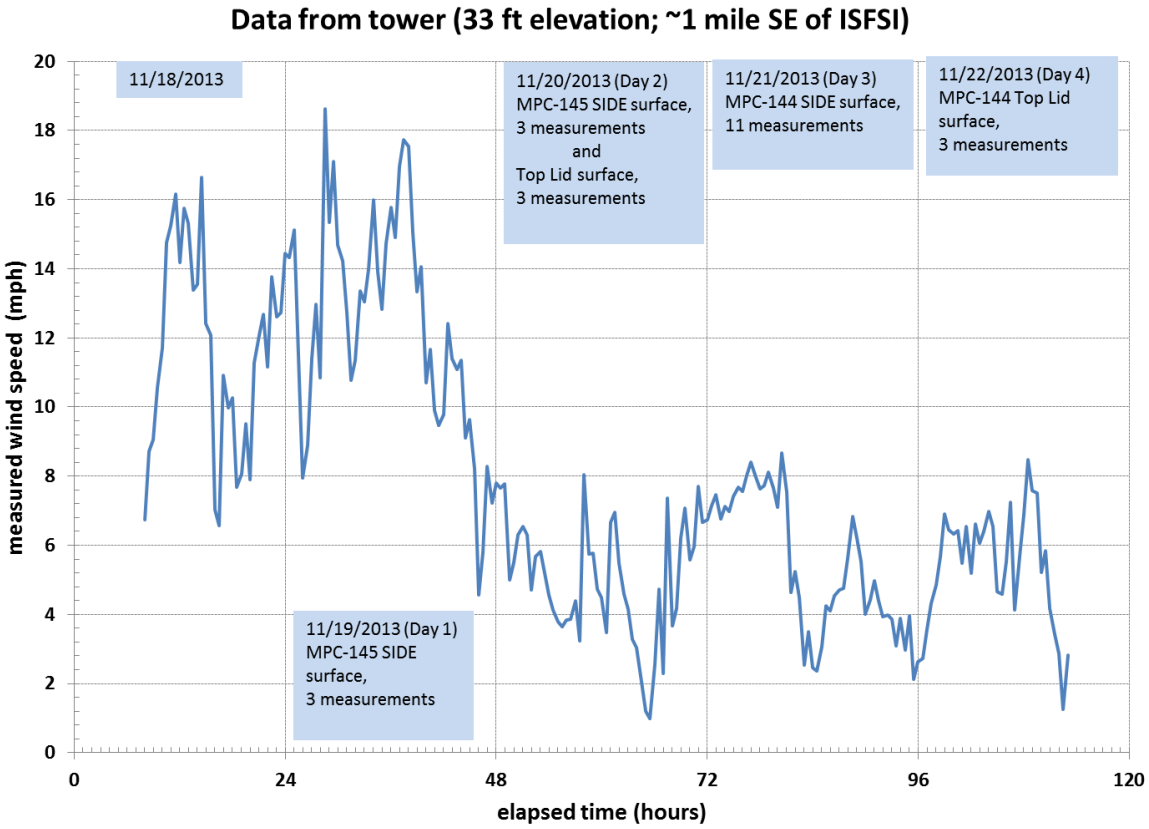

Figure 4-3. Wind Speed Recorded by Instrumentation on Meteorological Tower during Inspection Week

Wind effects and the unusual diurnal swings over the inspection week introduce some unquantifiable uncertainty in the measurements obtained during the inspection, particularly when evaluated in comparison to steady-state temperature predictions. Evaluation of ambient conditions on-site are further complicated by the distance between the ISFSI, where the canister surface temperature measurements and local ambient air temperatures were obtained, and the location of the tower, as shown in Figure 4-4. In this image, the larger yellow box marks the location of the ISFSI; the smaller box, enclosing the triangular pad, marks the location of the tower. Ambient conditions for each day of the inspection, including the on-site ambient temperature measurements, are presented in detail in the following subsections, showing specific ambient conditions from the meteorological tower during the time interval (9:00AM to 4:00PM) of inspection activities.

Figure 4-4. Location of the Meteorological Tower Relative to the ISFSI

4.1 Site Inspection Day 1: November 19, 2013

Conditions for the first day of the inspection, 11/19/2013, were not ideal at the ISFSI site, with high wind and unusual ambient temperature conditions. Figure 4-5 shows the wind speeds recorded at an on-site meteorological tower approximately 1 mile south-east of the ISFSI, at an altitude of 33 ft above ground level. For Day 1 of the inspection, the wind speed recorded at the tower ranged from a minimum of about 10 mph to a maximum of nearly 18 mph, over the estimated timeframe of inspection activities.

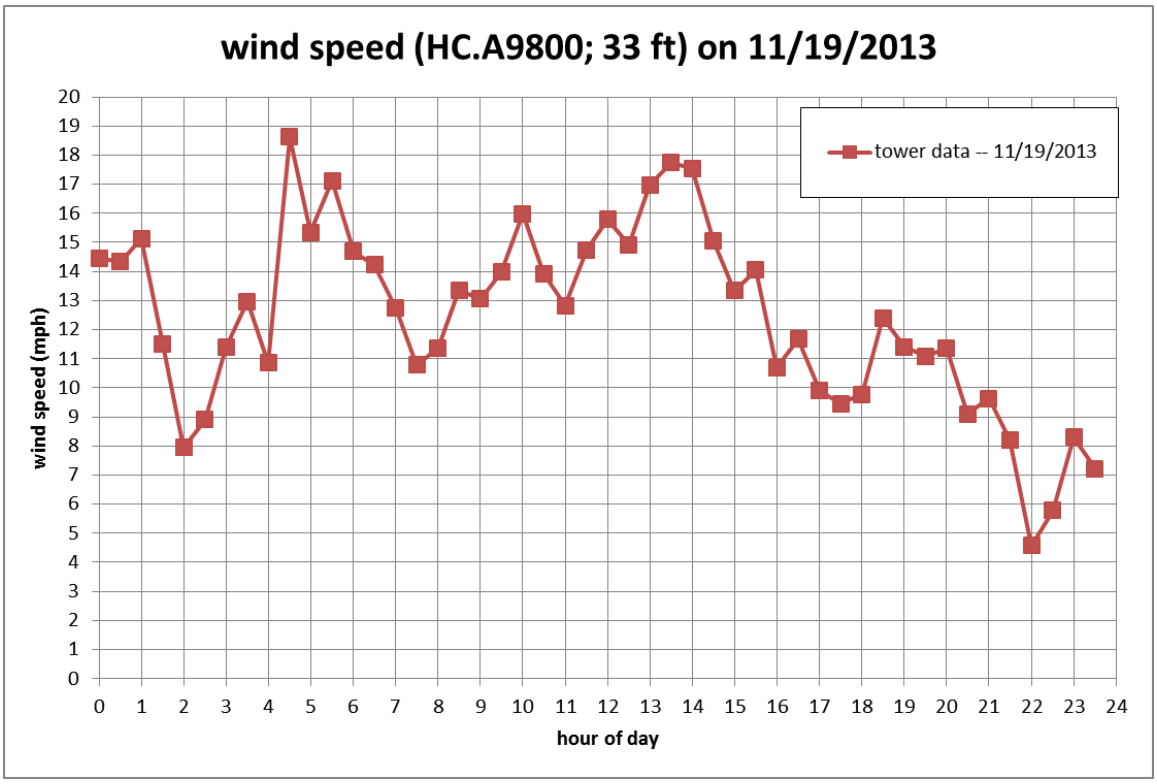

Figure 4-5. Wind Speed Recorded on Meteorological Tower (33-ft elevation) on 11/19/2013

The ambient temperature recorded at the tower is shown in Figure 4-6, over the 24-hour period from midnight on 11/18/2013 to midnight on 11/19/2013. This plot also includes the ambient temperature recorded at the tower during the afternoon and evening of 11/18/2013. This shows that the previous day was a much hotter day than Day 1 of the inspection, such that the ambient temperature at 11:30PM on 11/18/2013 was 53°F. The temperature at midnight is 52°F, and is the highest temperature recorded for the 24-hour period of Day 1 (11/19/2013).

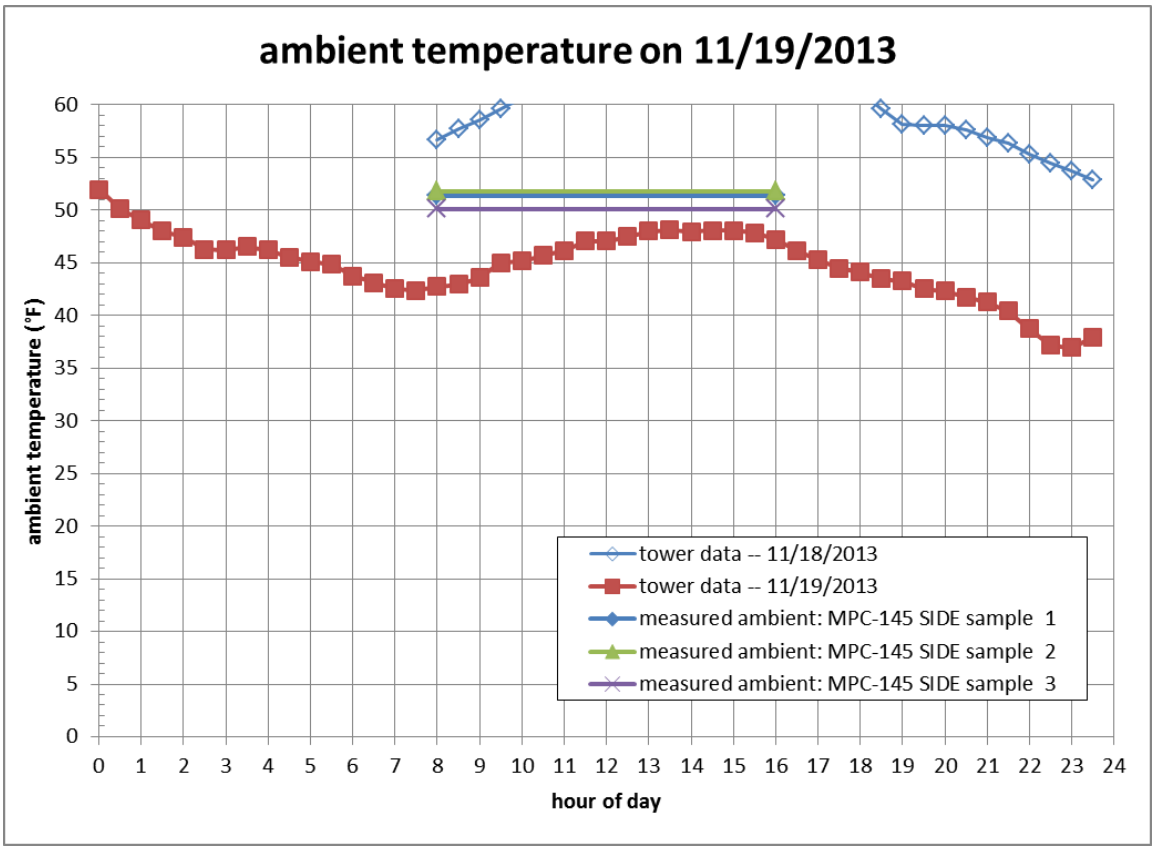

Figure 4-6. Ambient Air Temperature Recorded on Meteorological Tower (33-ft elevation) on 11/19/2013, with Ambient Temperatures Measured during Inspection of MPC-145

Three surface temperature measurements were taken on the side of MPC-145, obtained in conjunction with dry and wet sampling with the Holtec-designed sampling tool. Table 4-2 summarizes the measured temperatures reported by Holtec (Holtec 2014) for the side surface of MPC-145 on the first day of the inspection. The weather data plotted in Figure 4-6 also includes the local measured ambient air temperatures reported in conjunction with the three side surface measurements on MPC-145. The method of determining the ambient air temperature is not documented in the Holtec report, nor is any mention made of where this temperature was measured, in relationship to the storage module being inspected. The measurements appear to indicate that the ambient temperature in the vicinity of the module is somewhat higher than at the tower, approximately 1 mile away, and at a location on the tower about 2 times higher off the ground than the top of the storage module.

Table 4-2. Site Inspection Results: Temperature Measurements on MPC-145 Side (11/19/2013)

Date	Insertion depth (ft)	Measured side surface temperature (°F)	Measured ambient air temperature (°F)
11/19/2013	13.5	70.9	51.4
	8.5	93.3	51.8
	1.5	122.5	50.1

4.2 Site Inspection Day 2: November 20, 2013

Conditions for the second day of the inspection, 11/20/2013, were somewhat improved at the ISFSI site, with less wind and more typical ambient temperature conditions, although the cooling trend continued. Figure 4-7 shows the wind speeds recorded at the same on-site meteorological tower (approximately 1 mile south-east of the ISFSI, at an altitude of 33 ft above ground level). During the 7-hour time interval allowed for the inspection, the wind speed ranged from around 4-5 mph in the morning, with variable peaks up to 7 and 8 mph around noon, then steadily decreasing to a minimum of about 1 mph in the late afternoon.

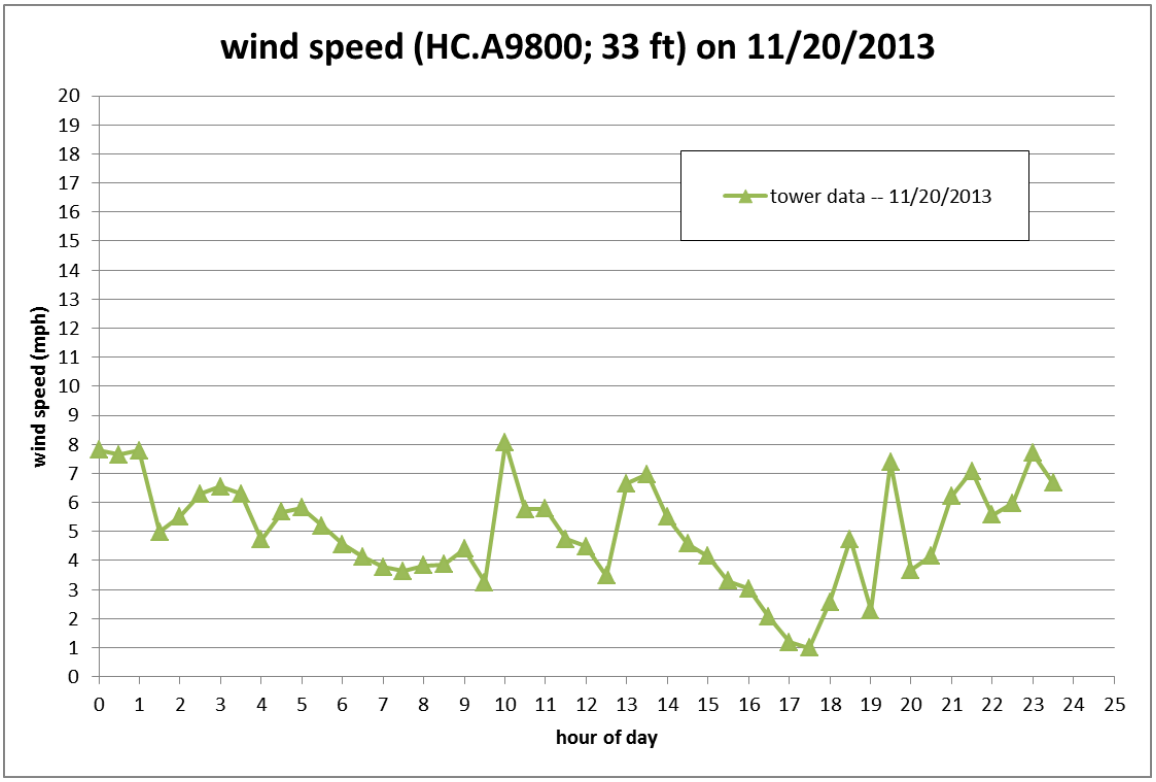

Figure 4-7. Wind Speed Recorded on Meteorological Tower (33-ft elevation) on 11/20/2013

The ambient temperature recorded at the tower is shown in Figure 4-8, over the 24-hour period from midnight on 11/19/2013 to midnight on 11/20/2013. This plot also includes the ambient temperature recorded on 11/19/2013 (Day 1), showing that the cooling trend is continuing, with lower overall temperatures on the 20th, compared to the 19th, but with a somewhat more typical diurnal swing on Day 2.

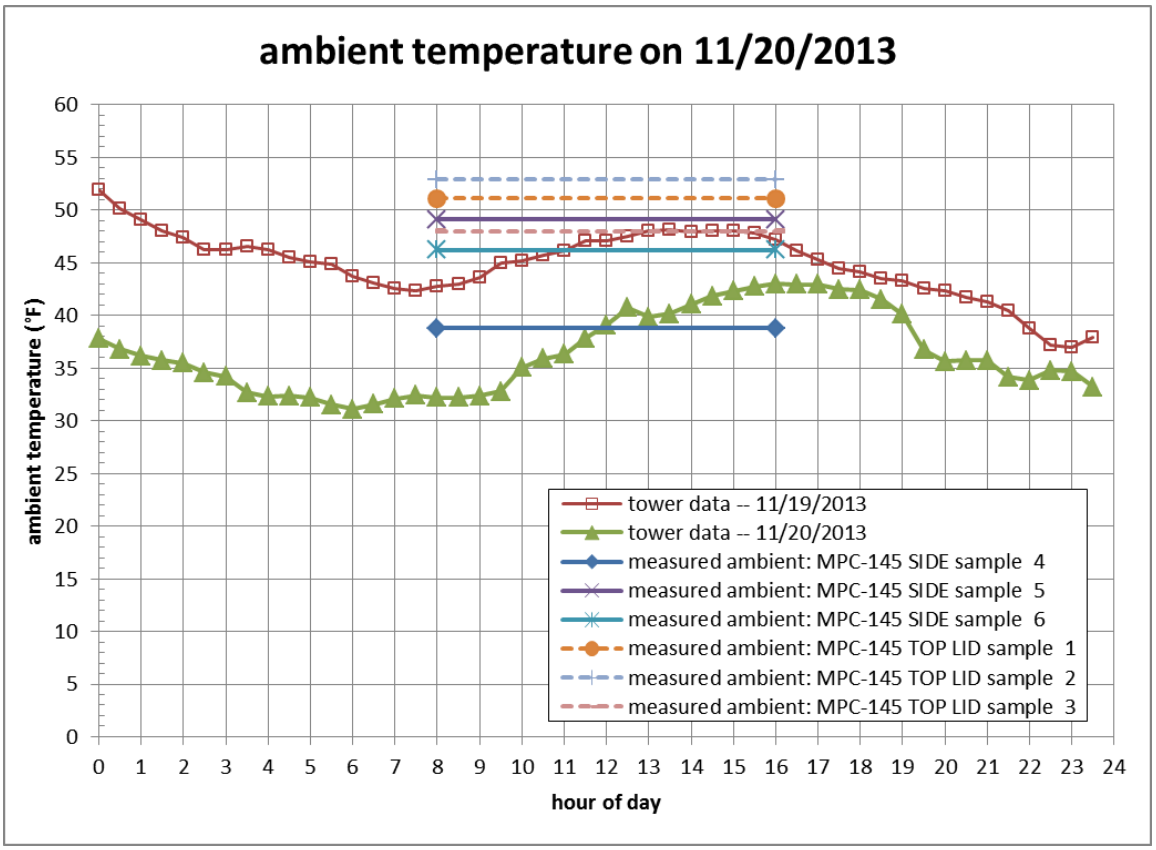

Figure 4-8. Ambient Air Temperature Recorded on Meteorological Tower (33-ft elevation) on 11/20/2013, with Ambient Temperatures Measured during Inspection of MPC-145

The three side surface temperature measurements on MPC-145 were obtained at approximately the same insertion depths as the measurements on the previous day. An additional three surface temperature measurements were also obtained on the top lid surface of MPC-145. Table 4-3 summarizes the measured temperatures for the MPC-145 side surface reported by Holtec. Table 4-4 summarizes these measured temperatures for the MPC-145 top lid surface. The plot in Figure 4-8 also includes the measured ambient air temperatures reported with these six measurements. The side measurement at 13-ft insertion depth (labeled "MPC-145 SIDE sample 4" in Figure 4-8) appears to indicate that the ambient temperature in the vicinity of the module may have been measured sometime around noon on the 20th. However, all other ambient temperature measurements in the vicinity of MPC-145 shown in Figure 4-8, associated with side and top lid surface measurements obtained on 11/20/2013, suggest that the ambient temperature at the site of the storage module was somewhat higher than the values measured at the tower.

The overlay of site ambient measurements, compared to the tower ambient temperature data makes it appear that these measurements could have been obtained on 11/19/2013, instead of 11/20/2013. However, that is not consistent with other information on the site inspection. So it is simpler to assume that the relationship between the tower ambient and the site ambient might be a little skewed, possibly due to the thermal load of the storage modules at the site, or perhaps

due only to different local conditions. Lacking sufficient information on the measurement procedure and timeframe, this is the simplest explanation for the observed relationships.

Table 4-3. Site Inspection Results: Temperature Measurements on MPC-145 Side (11/20/2013)

Date	Insertion depth (ft)	Measured side surface temperature (°F)	Measured ambient air temperature (°F)
11/20/2013	13	70.6	38.8
	7.5	100.8	49.1
	1	130.3	46.2

Table 4-4. Site Inspection Results: Temperature Measurements on MPC-145 Top Lid (11/20/2013)

Date	Insertion depth (inches)	Measured top lid surface temperature (°F)	Measured ambient air temperature (°F)
11/20/2013	64.5	172.1	51.1
	58.5	174.1	52.9
	41.75	129	48

4.3 Site Inspection Day 3: November 21, 2013

Conditions for the third day of the inspection, 11/21/2013, were similar to the previous day, until about 9:00AM, at which point the ambient temperature recorded at the on-site meteorological tower (approximately 1 mile south-east of the ISFSI) showed a steady rise to afternoon temperatures significantly above the high of the day before. Wind conditions recorded at the tower were similar, fairly steady at 7-8 mph in the morning, dropping to ~2 mph by noon, then somewhat variable around 3-4 mph through the afternoon, as shown in Figure 4-9. During the estimated 7-hour time interval allowed for the inspection, the wind speed ranged from a minimum of about 2 mph to a maximum of nearly 8 mph, with some variability.

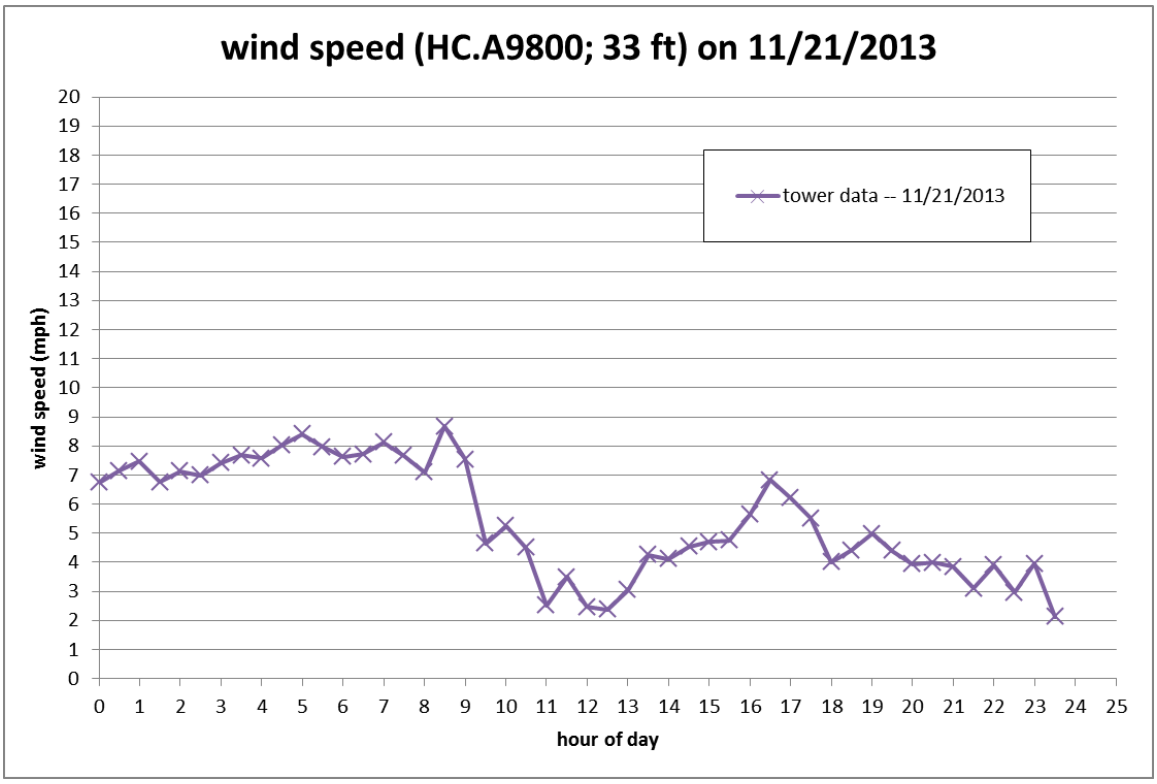

Figure 4-9. Wind Speed Recorded on Meteorological Tower (33-ft elevation) on 11/21/2013

The ambient temperature recorded at the tower is shown in Figure 4-10, over the 24-hour period from midnight on 11/20/2013 to midnight on 11/21/2013. There is a gap of approximately 2 hours in the data, presumably due to instrumentation problems at the tower, around noon on 11/21/2013, but it is reasonable to infer that the ambient temperature continued to increase gradually in this time interval, based on the generally consistent trend of this data. This plot also includes the ambient temperature recorded on 11/20/2013, which shows higher afternoon temperatures on the 21st, compared to the 20th. The diurnal swing also reflects this reversal, in that the ambient temperature does not cool down appreciably in the evening (after about 5:00PM), and at midnight is still near the day's high (i.e., 49°F, compared to the peak of 50°F at about 2:00PM).

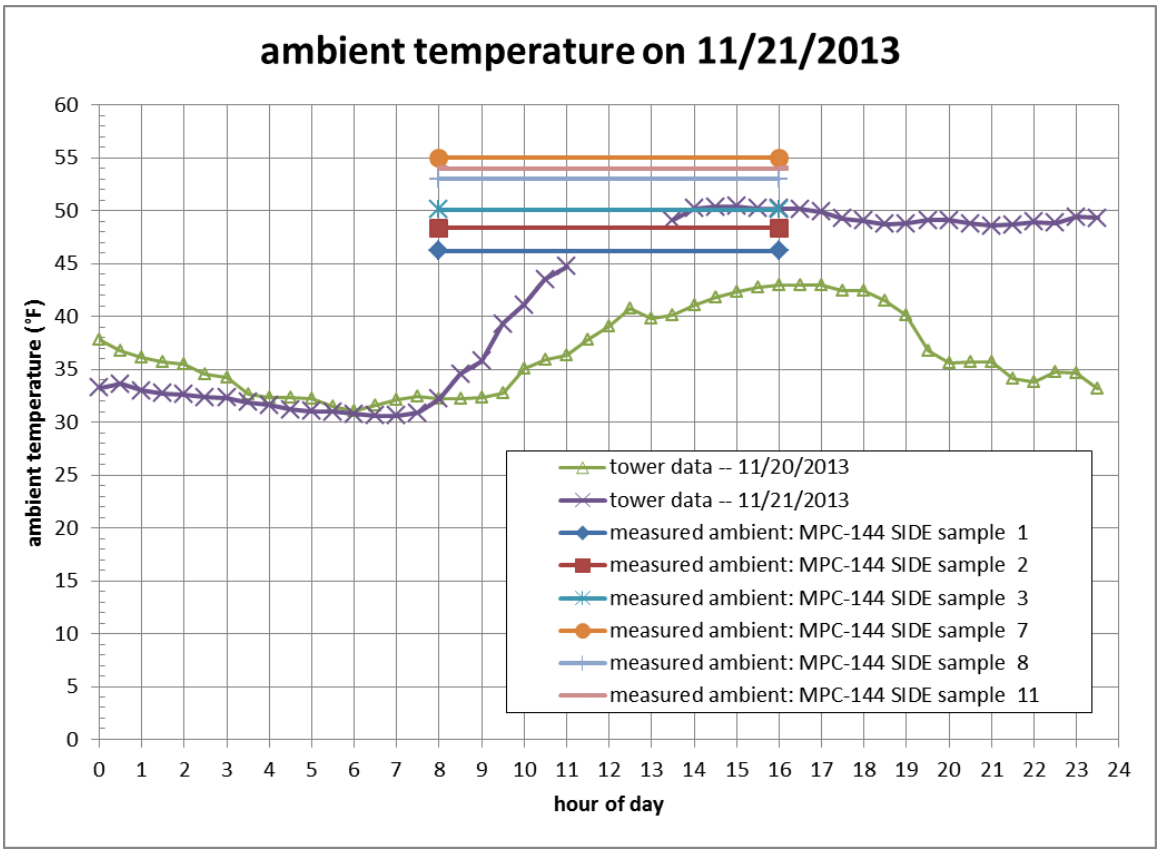

Figure 4-10. Ambient Air Temperature Recorded on Meteorological Tower (33-ft elevation) on 11/21/2013, with Ambient Temperatures Measured during Inspection of MPC-144

The plot in Figure 4-10 also includes representative ambient air temperatures obtained in conjunction with the surface measurements obtained on the side of MPC-144 in the course of the inspection on this day. The side surface temperature measurements were obtained at a larger number of insertion depths on this canister, attempting to capture a more complete resolution of the axial temperature profile, compared to the measurements obtained on the MPC-145 side surface on the previous day. For clarity of presentation, only six of the eleven ambient temperature measurements are shown on the plot. The measurements included on the plot span the range observed for the site data, and show the variation in these measurements over the time-span of inspection activities on this day. Table 4-5 summarizes the measured temperatures for the MPC-144 side surface, as reported by Holtec. As the largest single data set in the series, the measured temperatures in this table give the best illustration of the variability of the surface temperatures with changing ambient conditions, including wind speed.

Table 4-5. Site Inspection Results: Temperature Measurements on MPC-144 Side (11/21/2013)

Date	Insertion depth (ft)	Measured side surface temperature (°F)	Measured ambient air temperature (°F)
11/21/2013	13.5	84.1	46.2
	10	85.6	48.4
	8.5	89.6	50.1
	5	104.4	49.3
	12	110.7	49.3
	5	105	50.5
	2.5	118	55
	1	126.4	53
	13	93.2	53
	7.5	116.5	52.7
	1	133.9	54

4.4 Site Inspection Day 4: November 22, 2013

Conditions for the fourth day of the inspection, 11/22/2013, continued the warming trend from the day before. Wind conditions were fairly steady at 5-8 mph in the morning, then decreasing through the afternoon, as shown in Figure 4-11, with data from the on-site meteorological tower (approximately 1 mile south-east of the ISFSI). The ambient temperature recorded at the tower is shown in Figure 4-12, over the period from midnight on 11/21/2013 to 5:00PM on 11/22/2013. This plot shows an essentially constant temperature of 50°F through the night and early morning hours on this final day of the inspection. After about 9:00AM, the ambient temperature showed a steady rise to slightly higher afternoon temperatures of 55-56°F.

Reports from on-site observers indicate that the three temperature measurements taken on the top lid surface of MPC-144 on this day were obtained over the time span from about 9:00AM to noon. This is consistent with the way the measured ambient temperatures at the site lie on the tower data in Figure 4-12. Of all the measurements of ambient air temperature at the inspection site obtained in the 4-day period, this data shows the most consistent match-up with the tower data. Given that the ambient temperature had not varied by more than about 5 degrees-F in the previous 20 hours, this harmonious agreement suggests that the ambient air temperature was probably quite stable over this time period throughout the Hope Creek site. The final three surface temperature measurements obtained in the site inspection are summarized in Table 4-6, as reported by Holtec.

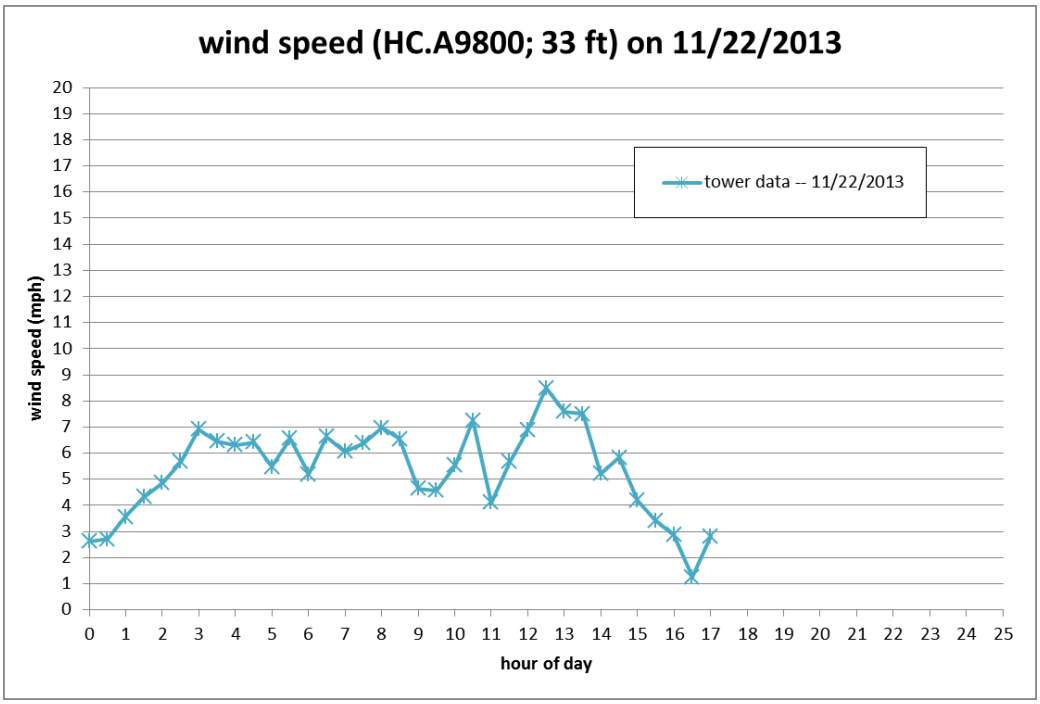

Figure 4-11. Wind Speed Recorded on Meteorological Tower (33-ft elevation) on 11/22/2013

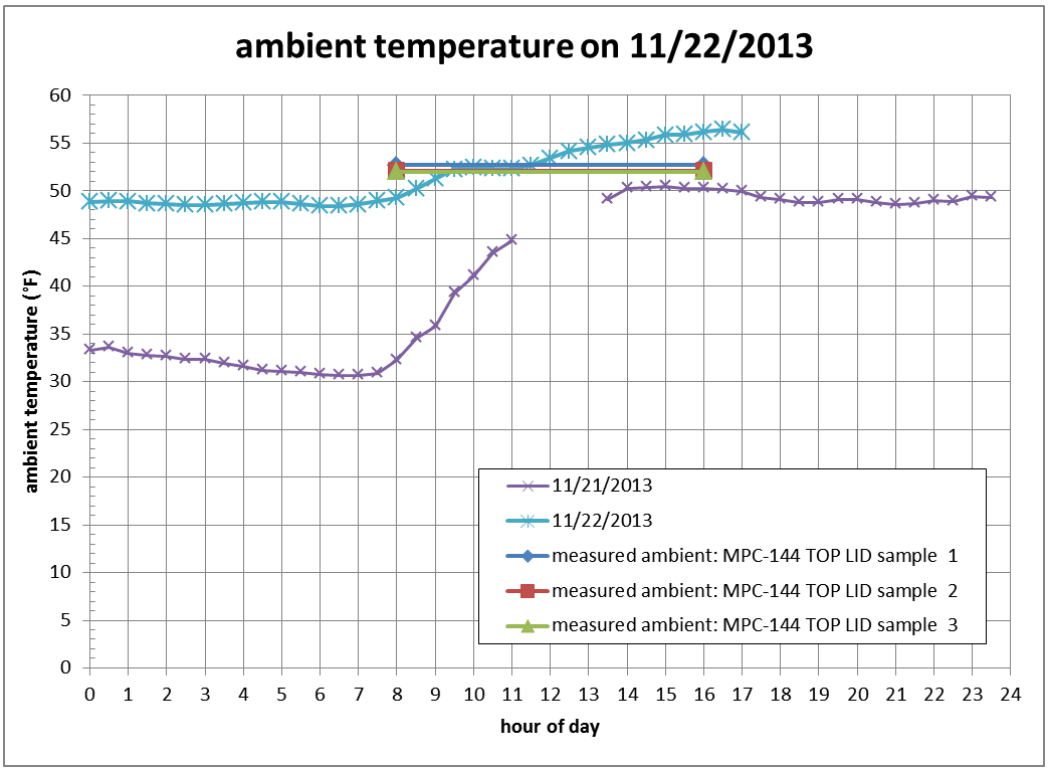

Figure 4-12. Ambient Air Temperature Recorded on Meteorological Tower (33-ft elevation) on 11/22/2013, with Ambient Temperatures Measured during Inspection of MPC-144

Table 4-6. Site Inspection Results: Temperature Measurements on MPC-144 Top Lid (11/22/2013)

Date	Insertion depth (inches)	Measured top lid surface temperature (°F)	Measured ambient air temperature (°F)
11/22/2013	40.5	141.2	52.7
	58.5	138	52.1
	64.5	132.6	52

5.0 PRE-INSPECTION THERMAL MODELING RESULTS COMPARED TO INSPECTION DATA

This section presents a direct comparison of the results of the pre-inspection thermal modeling with the measured data obtained during the inspection of MPC-144 and MPC-145, within their respective HI-STORM100 storage modules in the Hope Creek ISFSI. The site measurements are compared to the pre-inspection results obtained with the COBRA-SFS model for an assumed ambient temperature of 50°F. As described in Section 2.0 and Section 3.0, these calculations assume steady-state conditions, at the specified ambient air temperature, assuming still air. Evaluation of the effect of wind conditions on the thermal performance of the systems would require long-term transient calculations, taking into account actual variations in wind and ambient temperature. Data on local wind conditions over time at the ISFSI site near the modules inspected is not available, nor is there sufficient data on the local ambient temperature over the time of interest.

Evaluation of these local transient effects is beyond the scope of this analysis. The local ambient air temperatures measured during the inspection were recorded in the range of 45-55°F, as shown by the plot in Figure 5-1. This plot shows all 23 local ambient air temperature measurements obtained in the course of the 4-day inspection. The mean value is 49.8°F, and the median is 50.1°F, with a maximum of 55°F and a minimum of 38.8°F. Neglecting the lowest value of 38.8°F, which the plot in Figure 5-1 and the weather data presented in Section 4.0 shows is not typical of conditions during the inspection, the minimum measured ambient air temperature is 46.2°F.

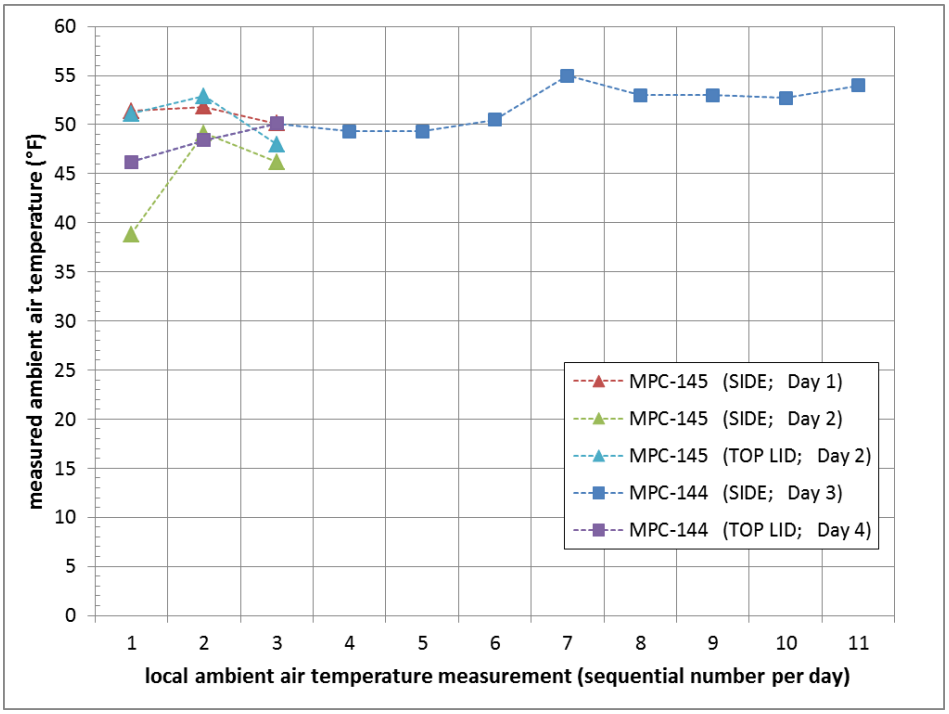

Figure 5-1. Local Ambient Air Temperatures Measured during Inspection at Hope Creek ISFSI

The variation in measured ambient air temperature is small enough to be within the overall uncertainty in the data and in the modeling assumptions. Therefore, modeling results based on an assumed ambient air temperature of 50°F should produce analytical results that can be expected to be in reasonable agreement with the measured temperatures on the MPC surfaces, for still air conditions. For ambient conditions with wind, the results obtained with evaluations assuming still air should at least be reasonably bounding on the measured data. These blithe convictions are tested by comparison of the inspection data to pre-inspection predictions from the COBRA-SFS thermal modeling evaluations for assumed ambient still air temperature of 50°F. Section 5.1 presents the comparison for MPC-145, and Section 5.2 presents the comparison for MPC-144.

5.1 Thermal Evaluation Results Compared to Measured Temperatures on MPC-145

The temperatures measured on the side surface of MPC-145 were obtained on the first two days of the inspection; three measurements on 11/19/2013, and three measurements on 11/20/2013, as shown in Figure 5-2. The insertion depths of the measurement tool down the annulus in each of the two sets of measurements were approximately the same; 13.5 ft, 8.5 ft, and 1.5 ft on 11/19/2013 (Day 1); 13 ft, 7.5 ft, and 1 ft on 11/20/2013 (Day 2). Measured ambient air temperatures were approximately the same, with the exception of the one measurement (at 13 ft) on Day 2, which has the lowest (38.8°F) air temperature measured during the entire inspection time span. Wind conditions were quite different on these two days, however, with the measurements on Day 1 taken with wind speed in the range 10-17 mph (see Figure 4-1). On Day 2, the wind speed was in the range 3 to 8 mph, depending on the actual time of the measurement.

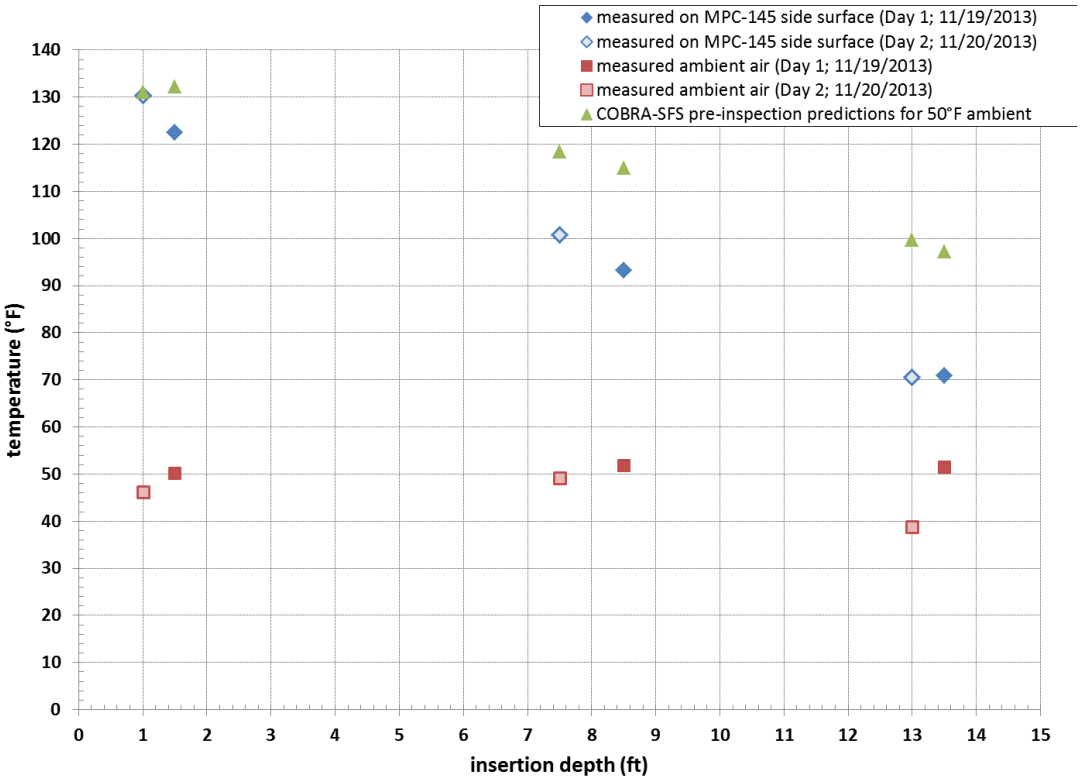

Figure 5-2. Point-by-Point Comparison of COBRA-SFS Pre-Inspection Temperature Predictions to Measured Temperatures on MPC-145 Side Surface

The comparison in Figure 5-2 shows that the thermal modeling predictions assuming still air, in general give reasonable bounding temperatures for the MPC side surface. Figure 5-3 shows the same measured data compared to the axial temperature profile predicted with the COBRA-SFS model, assuming still air. Both plots show the expected result when comparing predictions obtained assuming still air temperatures to surface temperatures that would be achieved with additional forced convection cooling due to wind. The predicted temperatures are in general higher than the measured temperatures. The temperatures predicted with the thermal model at 1 ft and 1.5 ft insertion depth show very good agreement with the measured temperatures. This is because these locations are only a few inches below the bottom of the lid of the MPC. The lid of the MPC is a 9.5-inch thick plug of solid steel, and as such, provides considerable thermal inertia that would tend to damp out the effect of temperature variations due to variation in boundary conditions.

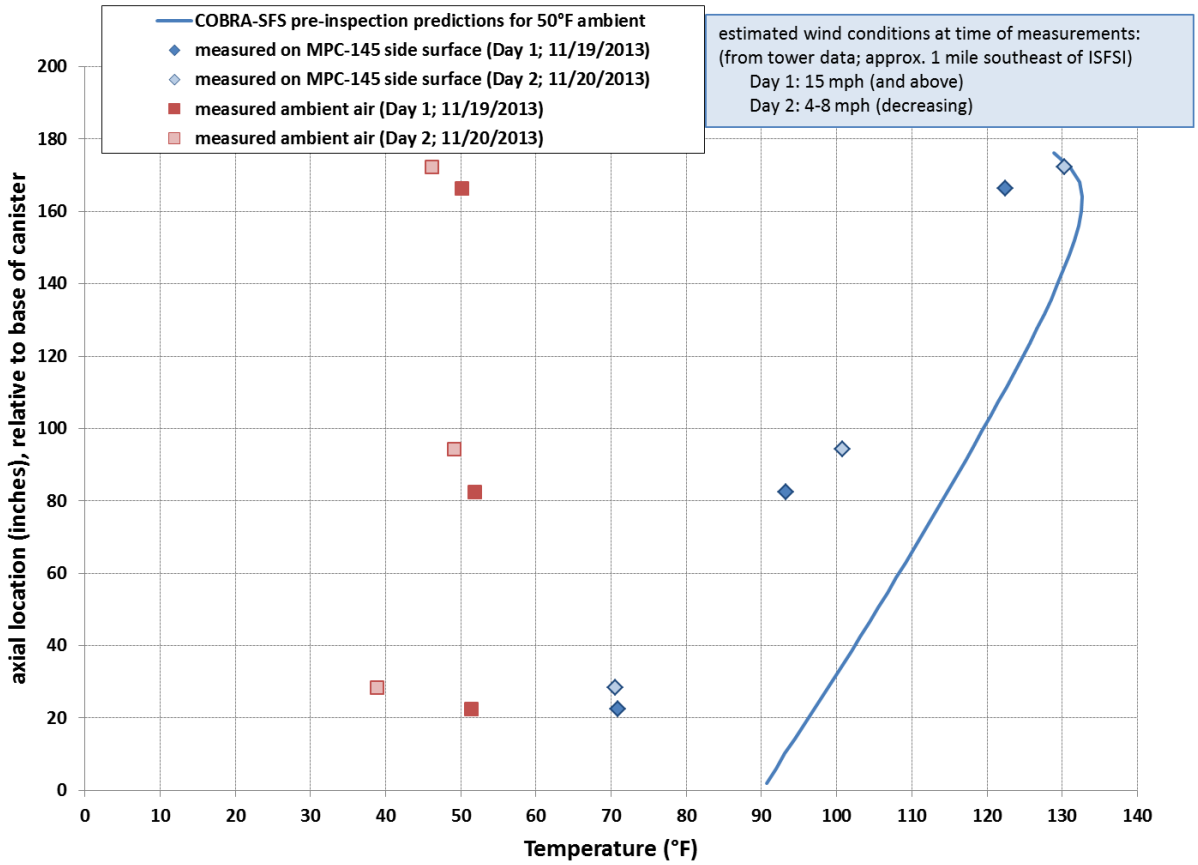

Figure 5-3. Axial Profile Comparison of COBRA-SFS Pre-Inspection Temperature Predictions to Measured Temperatures on MPC-145 Side Surface

With only three measurements on each of the two days, at slightly different locations and for differing ambient air temperatures, it is difficult to make generalizations on the effect of wind conditions alone on canister surface temperatures. The trend shown by the data on a given day is what one might expect due to wind; that is, the temperatures are generally lower than those predicted with the assumption of still air. The wind speed measurements at the tower (a mile away) indicate fairly large differences in wind speed on Day 1 and Day 2. However, the measured temperatures do not show very much difference between the two days. This might simply mean that the local wind conditions at the ISFSI site were not significantly different on the two days. Or it could be that uncertainties in the temperature measurements are great enough (due to location uncertainty and instrumentation performance, for example) to obscure differences due to wind velocity alone. The only thing that can be stated with confidence in this particular comparison of measured data to pre-inspection predictions is that the COBRA-SFS model is giving reasonable bounding values for canister surface temperatures. The assumption of still air in the calculations is conservative, as would be expected for a ventilated storage module of this design.

The temperatures measured on the top lid of MPC-145 were all obtained on Day 2 of the inspection (11/20/2013). Three locations were measured; one approximately 1 ft in from the

edge of the MPC, and the other two at about 2.5 to 3 ft from the edge. (The diameter of the MPC is about 6.5 ft.) The COBRA-SFS model of the lid is essentially 1-D, with resolution of the axial temperature gradient through the lid structures, from the canister inner cavity to the top lid surface. Radial gradients are not captured in this modeling approach, as described in Section 2.0. Therefore, the temperature predicted with the model is in effect an average surface temperature for the top lid surface. Figure 5-3 compares this average lid temperature with the local point measurements obtained with the inspection tool in contact with the top lid surface of MPC-145.

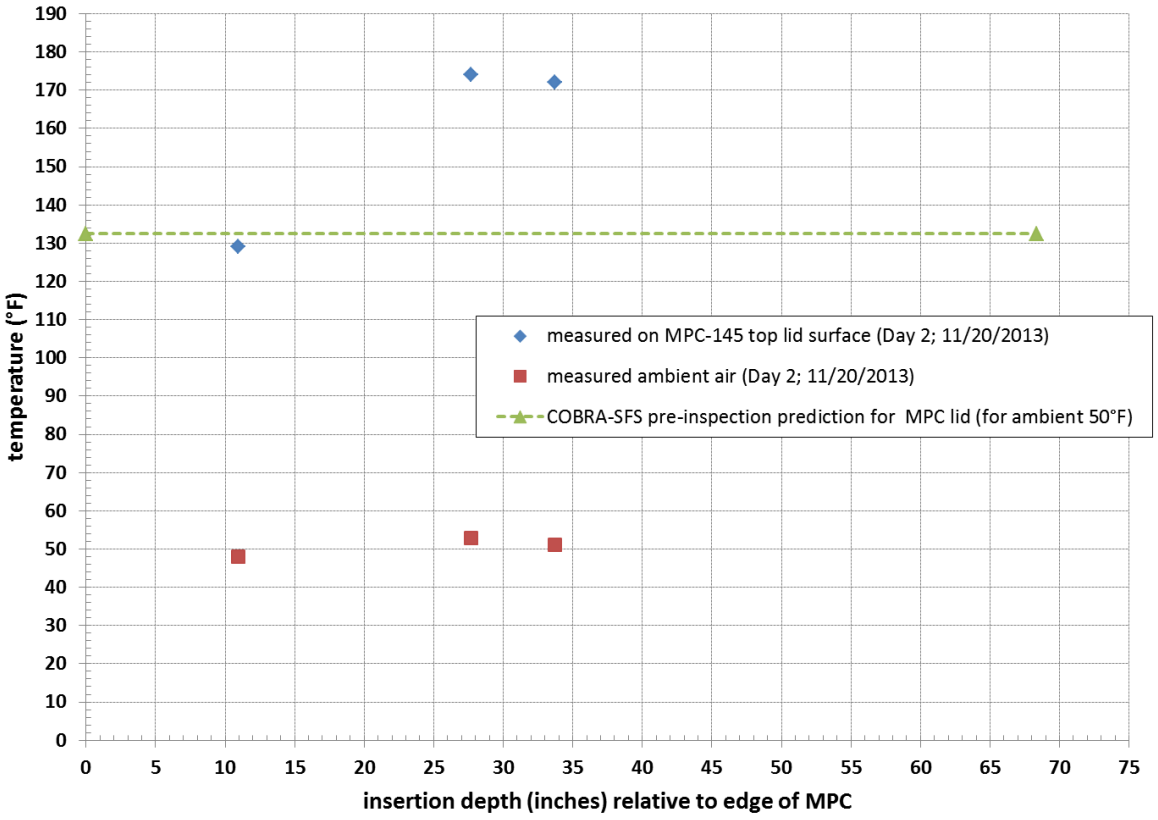

Figure 5-4. Comparison of COBRA-SFS Pre-Inspection Temperature Predictions to Measured Temperatures on MPC-145 Top Lid Surface

These results suggest that the average lid temperature of 132°F predicted with the COBRA-SFS model is perhaps a little low. Based on the three measured temperatures, the lid average temperature would be expected to be somewhat higher, possibly on the order of 150-160°F, assuming a moderately parabolic distribution across the lid surface. However, it should be noted that with all three measurement points on the same side of the lid, it is not possible to infer the actual lid temperature distribution. For this particular day, it seems quite unlikely that the distribution would be symmetrical for the reported wind conditions.

The high measured temperatures, relative to the computed average, also seem a little odd, given that the measured side temperatures (see Figure 5-1) on Day 2 are somewhat lower than the

values predicted with the model (which were calculated assuming still air). If wind effects are providing a bit of extra cooling to the MPC side, it seems likely that the top lid would also see a similar effect. But it is also likely that the actual temperature distribution across the lid would be quite different from that obtained in still air conditions.

On-site observers reported that air flow out the exit vents was noticeably non-symmetrical (visible in shifting patterns of "heat shimmer" due to hot air exiting some vents and not others), in response to wind effects. It is therefore unlikely that the lid temperatures measured on Day 2 can be used to infer an average lid temperature that could be usefully compared to the COBRA-SFS model predictions. The only meaningful observation that can be derived from this comparison is that differences between measured and predicted temperatures can be reasonably attributed to wind effects.

5.2 Thermal Evaluation Results Compared to Measured Temperatures on MPC-144

The eleven temperatures measured on the side surface of MPC-144 were all obtained on 11/21/2013, Day 3 of the inspection. Measurements were obtained at approximately 3-ft intervals down the annulus, from 13.5 ft to 1 ft, with some attempt to obtain two separate measurements at or near the same axial locations. (See Table 4-5 for a listing of the reported locations of these measurements.) Measured ambient air temperatures increased steadily throughout the day, but over a fairly narrow range, from a low of 46.2°F to a high of 54°F. Wind conditions could be termed "light and variable", in the range 2.4 to 8.7 mph. The comparison with COBRA-SFS predictions presented in Figure 5-5 and Figure 5-6 show that the model predictions are in reasonable agreement with the measured data, within the limitations of the boundary conditions and modeling assumptions.

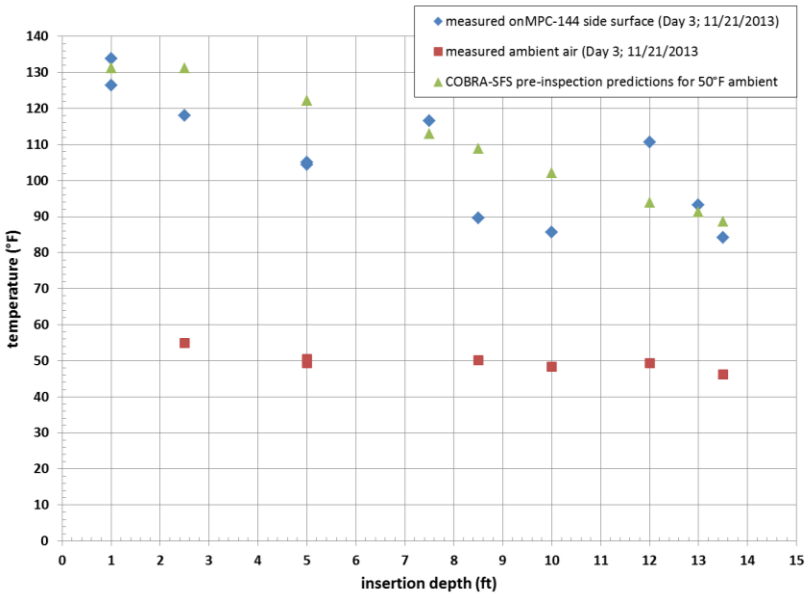

Figure 5-5. Point-by-Point Comparison of COBRA-SFS Pre-Inspection Temperature Predictions to Measured Temperatures on MPC-144 Side Surface

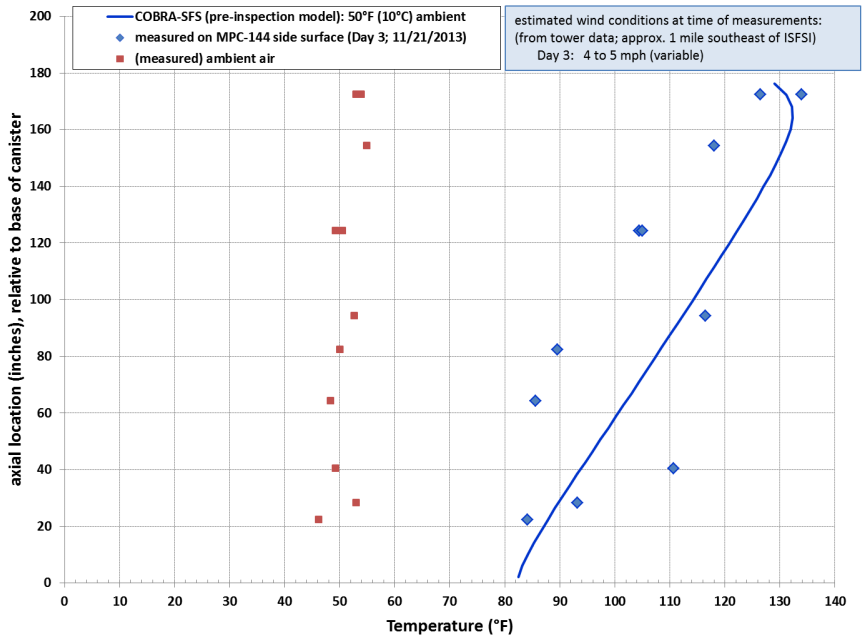

Figure 5-6. Axial Profile Comparison of COBRA-SFS Pre-Inspection Temperature Predictions to Measured Temperatures on MPC-144 Side Surface

The comparisons in Figure 5-5 and Figure 5-6 show that there are some interesting variations in the measured temperatures that are not reflected in the COBRA-SFS model predictions, and are a little difficult to interpret, in terms of what is known about the configuration of the storage system and the design of the MPC internals. The simplest explanation is that the somewhat erratic axial variation in the continuity of the measured temperatures may simply be the effect of the "light and variable" winds experienced on site during the estimated 7-hours over which the measurements were obtained. In addition to wind effects, there may also be contributions due to measurement uncertainty and thermal non-equilibrium due to the unusual diurnal variation in ambient air temperatures over the week of the inspection.

Without appropriate means to quantify measurement uncertainty and repeatability, no firm conclusions can be drawn as to the specific reason(s) for the observed difference between measurements and predictions for these side surface temperatures. Given the differences between actual conditions at the time of the inspection, and the assumed conditions for the pre-inspection thermal evaluations, the agreement between predictions and measurements is better than might be expected, and the differences are reasonable.

The three temperatures measured on the top lid of MPC-144 were obtained on the fourth day of the inspection (11/22/2013). This was the last day of the inspection, and these three measurements were the only temperature measurements obtained on MPC-144 on this day. Three locations were measured, at the same insertion depths as for the top lid measurements on MPC-145. Figure 5-7 compares the measured temperatures to the top lid average surface temperature predicted in the thermal modeling with COBRA-SFS. This average temperature is a reasonable, although slightly low, estimate of the measured values, and is well within the uncertainty of the measurements.

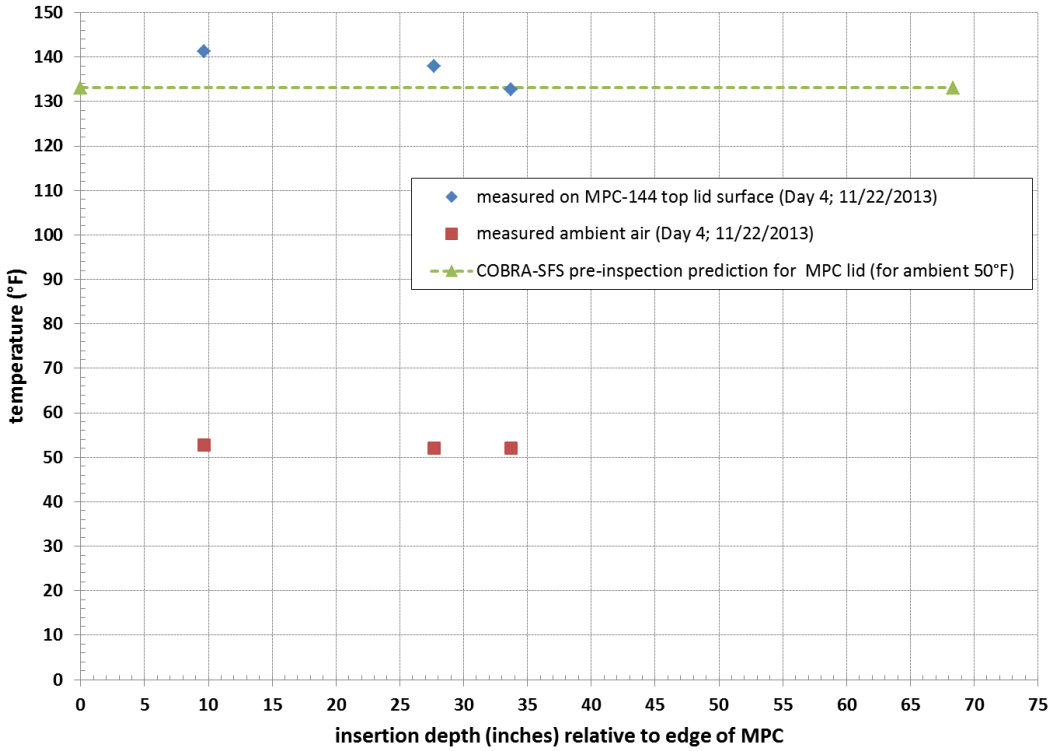

Figure 5-7. Comparison of COBRA-SFS Pre-Inspection Temperature Predictions to Measured Temperatures on MPC-144 Top Lid Surface

The most significant thing about the comparison in Figure 5-7 is that it shows the expected relatively flat temperature distribution across the MPC lid for conditions of the least wind during the inspection days. This as close as actual conditions came to the COBRA-SFS modeling assumption of still air, and gives the best agreement between measured and predicted temperatures obtained for the MPC lid temperatures. This could be merely a coincidence, but it tends to confirm the appropriateness of the usual COBRA-SFS modeling assumption that axial gradients are more significant than radial gradients in the lid structures of the MPC and overpack in ventilated vertical storage modules such as the HI-STORM100.

The edge-to-center gradient shown by the measured temperatures for the MPC-144 top lid, with the lowest temperature near the center of the lid and highest temperature measured closer to the edge, is probably due to measurement uncertainty. It is unlikely to be an accurate reflection of the actual temperature gradient across the MPC lid, as it is not physically reasonable for the MPC-144 in low wind conditions (that is, approaching still air conditions). The decay heat loading of MPC-144 has hotter fuel in the center of the basket, compared to the periphery (see Table 2-2). This would tend to result in higher rather than lower temperatures near the center of the lid, reflecting the higher temperatures near the center of the canister cross-section. This radial gradient would be expected to be rather small for the nominally uniform loading of this canister, however, since the radial variation in decay heat generation is relatively small, and the thermal mass of the 9.5-inch thick steel lid of the MPC would tend to smooth out any gradients due to the radial distribution of decay heat loading within the basket.

6.0 CONCLUSIONS

The post-inspection comparison of modeling results to measured surface temperature data from the Hope Creek site inspection shows that thermal modeling with the COBRA-SFS code can yield reasonable estimates of temperatures and temperature distributions in an actual vertical storage module within an operating ISFSI. The assumption of steady-state conditions with still air provides reasonable bounding results as a function of canister decay heat load and loading pattern. The demonstrably non-equilibrium conditions that prevailed at the Hope Creek ISFSI during the site inspection limit the usefulness of the temperature measurements obtained in this inspection. This suggests certain recommendations relative to inspection procedures for obtaining thermal modeling data in future inspections. Specifically, if a major goal of a site inspection is to obtain temperatures for evaluation of thermal conditions and thermal modeling, the following should be considered.

- If possible, inspection dates should be chosen based on expected typical conditions for the time of year, and alternative dates planned, on a contingency basis, so that the inspection can be postponed if conditions are likely to compromise the intended measurements. The effects of wind on storage module thermal performance may be a topic of some interest, but in practical terms, its effect on one-time data gathering efforts is to introduce an unquantifiable and non-uniform uncertainty in the measured temperatures obtained. In this instance of data gathering in highly variable ambient conditions, there is insufficient information to quantify the uncertainty in the measured temperatures.
  - For an actual study of wind effects at an operating ISFSI, measurements would have to be obtained over a large range of conditions, with and without wind, with consistent and repeatable measurement methodologies. (This may be a useful thing to do, but is beyond the current scope of the site inspections, which are aimed primarily at investigations of the potential for conditions that could result in accelerated stress corrosion cracking of the storage canister.)
- On-site data gathering procedures should include time-and-date stamps for every measurement recorded. Ambient conditions should be continuously monitored, using calibrated on-site instrumentation. If such is not available, the Test Plan should include setting up a portable monitoring station at the location of the module being inspected, to create a continuous record of ambient temperature and wind conditions throughout the inspection. This data can then later be reconciled with the date-and-time stamps of measured data, to obtain accurate boundary conditions for thermal modeling of the system at the time the measurements were taken.
- Documentation of on-site inspection measurements and procedures should be complete and specifically circumstantial, and should include an uncertainty analysis relative to the instrumentation uncertainty and the experimental uncertainty.

For the modeling effort, the usefulness of the thermal evaluations for a specific site depends on the accuracy of the model that can be constructed for the site being inspected. This means having timely access to information on the storage module configuration, the configuration and condition of the fuel stored within the canisters to be inspected, and some reasonable estimate of the expected ambient boundary conditions for the time of the inspection.

- Accurate information on assembly axial decay heat profiles (in general corresponding to axial burnup profiles) is needed to fully characterize the axial distribution of temperature on the storage canister outer shell.
  - This information seems generally unavailable at operating ISFSIs, so an alternative approach might be to perform modeling studies to quantify the uncertainty in surface temperatures (and internal component temperatures) due to variation in axial decay heat profile, including realistic profiles and bounding assumptions, for a range of fuel types.
- Accurate information on site-specific variations from the nominal design basis of the storage module or canister is needed to be able to predict accurate detailed temperature distributions, particularly on surfaces that might potentially be accessible for on-site inspection and measurement.

7.0 REFERENCES

10 CFR 71. 2003. "Packaging and Transportation of Radioactive Material." *Code of Federal Regulations*, U.S. Nuclear Regulatory Commission, Washington D.C.

Creer JM, TE Michener, MA McKinnon, JE Tanner, ER Gilbert, and RL Goodman. 1987. *The TN-24P PWR Spent-Fuel Storage Cask: Testing and Analysis*. EPRI-NP-5128/PNL-6054, Electric Power Research Institute, Palo Alto, California.

Cuta JM and HE Adkins. 2013. *Preliminary Thermal Modeling of HI-STORM 100S-218 Version B Storage Modules at Hope Creek Nuclear Power Station ISFSI*. U.S. Department of Energy, Used Fuel Disposition Campaign. FCRD-UFD-2013-000297. PNNL-22552.

Google Earth. 2011. Imagery Date: 7/3/2010. Available at: http://maps.google.com/maps?t=h&hl=en&ie=UTF8&ll=39.470317,-75.536537&spn=0.007669,0.013078&z=17.

Holtec International, February 13, 2010. *Final Safety Analysis Report for the HI-STORM 100 Cask System*, Revision 9. Holtec Report No. HI-2002444, USNRC Docket No. 72-1014. Holtec International, Marlton, NJ. NOTE: this document is copyrighted intellectual property of Holtec International. All rights reserved.

Holtec International (Company Private document). 2014. *MPC Surface Inspection at Hope Creek Nuclear Generating Station*, Revision 0 for EPRI. Holtec Report No. HI-2146300, Holtec Project No. 930. Sponsoring Holtec Division: NPD. Report Class: Safety Related. Approved November 12, 2014.[13]

Lombardo NJ, JM Cuta, TE Michener, DR Rector, and CL Wheeler. 1986. *COBRA-SFS: A Thermal-Hydraulic Analysis Computer Code, Volume III: Validation Assessments*. PNL-6048 Vol. III. Pacific Northwest Laboratory, Richland, Washington.

Michener TE, DR Rector, JM Cuta, RE Dodge, and CW Enderlin. 1995. *COBRA-SFS: A Thermal-Hydraulic Code for Spent Fuel Storage and Transportation Casks*. PNL-10782, Pacific Northwest Laboratory, Richland, Washington.

NOAA – National Oceanic and Atmospheric Administration. 2013. "National Weather Service Forecast Office, Philadelphia/Mount Holly." Data for Wilmington, DE station at the New Castle County Airport accessed 8/21/2013 at http://www.nws.noaa.gov/climate/index.php?wfo=phi.

[13] This report is referenced slightly differently (as "Holtec Report HI-2146300, *MPC Surface Inspection at Salem & Hope Creek NPP*, Latest Revision.") in the report on the site inspection at Diablo Canyon (see Section 4, HI-2146301, Revision 0). The version provided for reference here, in the Hope Creek post-inspection analysis, may not be the final version of HI-2146300.

NRC – U.S. Nuclear Regulatory Commission. 1999. Spent Fuel Heat Generation in an Independent Spent Fuel Storage Installation. Regulatory Guide 3.54, Revision 1. U.S. Nuclear Regulatory Commission, Washington D.C. Available at http://www.nrc.gov/reading-rm/doc-collections/reg-guides/fuels-materials/rg/03-054/.

Rector DR, RA McCann, UP Jenquin, CM Heeb, JM Creer, and CL Wheeler. 1986. *CASTOR-1C Spent Fuel Storage Cask Decay Heat, Heat Transfer and Shielding Analysis*. PNL-5974. Pacific Northwest Laboratory, Richland, Washington.

Sparrow EM, and LFA Azevedo. 1985. "Vertical-channel natural convection spanning between the fully-developed limit and the single-plate boundary-layer limit." *International Journal of Heat and Mass Transfer*, 28(10):1847-1857.

Sparrow EM, AL Loeffler, and HA Hubbard. 1961. "Heat Transfer to Longitudinal Laminar Flow between Cylinders." *Journal of Heat Transfer*, 83:415.

Suffield SR, JM Cuta, JA Fort, BA Collins, HE Adkins, and ER Siciliano. 2012. *Thermal Modeling of NUHOMS HSM-15 and HSM-1 Storage Modules at Calvert Cliffs Nuclear Power Station ISFSI*. PNNL-21788, Pacific Northwest National Laboratory, Richland, Washington.

Turner SE. 1989. "Uncertainty Analysis – Axial Burnup Distribution Effects." Presented in *Proceedings of a Workshop on the Use of Burnup Credit in Spent Fuel Transportation Casks*, SAND-89-0018. Sandia National Laboratories, Albuquerque, New Mexico.

Appendix A

Pre-Inspection Predictions of Axial Temperature Distribution on Canister Shell

Appendix A: Pre-Inspection Predictions of Axial Temperature Distribution on Canister Shell

This appendix presents the axial temperature distributions on the MPC outer shell predicted with the COBRA-SFS models of Modules 143, 144, 145, and 146. These profiles are through the location of the peak temperature on the MPC outer shell for each configuration. The axial location in the tables is relative to the inner surface of the canister base. Results are presented for each of the four canisters in Tables A-1 through A-4. These tables contain results based on the decay heat values determined with the ORIGEN modeling and with the RG 3.54 modeling. Tables A-5 and A-6 present results for a range of ambient conditions, in Modules 144 and 145 only, which have been identified as the modules to be inspected. The results in these tables were obtained with the decay heat values from the ORIGEN modeling.

Table A-1. Canister Shell Axial Temperature Distribution: Module 143 (80°F [27°C Ambient])

Axial location (inches)	ORIGEN model: 80°F (27°C) ambient			RG 3.54 model: 80°F (27°C) ambient	
	(°F)	(°C)		(°F)	(°C)
2.05	114.6	45.9		119.4	48.6
6.10	115.5	46.4		120.5	49.1
10.15	116.7	47.1		121.9	49.9
14.20	118.1	47.8		123.5	50.8
18.25	119.6	48.7		125.2	51.8
22.30	121.2	49.5		127.0	52.8
26.35	122.8	50.4		128.9	53.8
30.40	124.4	51.3		130.8	54.9
34.45	126.1	52.3		132.7	56.0
38.50	127.7	53.2		134.6	57.0
42.55	129.4	54.1		136.5	58.1
46.60	131.0	55.0		138.5	59.1
50.65	132.7	55.9		140.4	60.2
54.70	134.3	56.8		142.3	61.3
58.75	135.9	57.7		144.2	62.3
62.80	137.5	58.6		146.0	63.4
66.85	139.1	59.5		147.9	64.4
70.90	140.7	60.4		149.8	65.4
74.95	142.3	61.3		151.6	66.4
79.00	143.8	62.1		153.4	67.5
83.05	145.4	63.0		155.2	68.5
87.15	146.9	63.8		157.0	69.5
91.20	148.4	64.7		158.8	70.4
95.25	149.9	65.5		160.6	71.4
99.30	151.4	66.3		162.3	72.4
103.35	152.9	67.1		164.0	73.4
107.40	154.3	67.9		165.7	74.3
111.45	155.7	68.7		167.4	75.2
115.50	157.1	69.5		169.1	76.2

Table A-1. (continued)

Axial location (inches)	ORIGEN model: 80°F (27°C) ambient			RG 3.54 model: 80°F (27°C) ambient	
	(°F)	(°C)		(°F)	(°C)
119.55	158.5	70.3		170.7	77.1
123.60	159.8	71.0		172.3	77.9
127.65	161.1	71.7		173.9	78.8
131.70	162.4	72.4		175.4	79.6
135.75	163.5	73.1		176.8	80.4
139.80	164.7	73.7		178.2	81.2
143.85	165.7	74.3		179.4	81.9
147.90	166.7	74.8		180.6	82.6
151.95	167.6	75.3		181.7	83.2
156.00	168.3	75.7		182.7	83.7
160.05	168.8	76.0		183.3	84.1
164.10	169.0	76.1		183.6	84.2
168.15	168.7	75.9		183.3	84.0
172.20	167.4	75.2		181.8	83.2
176.25	164.9	73.8		178.8	81.6

Table A-2. Canister Shell Axial Temperature Distribution: Module 144 (80°F [27°C Ambient])

Axial location (inches)	ORIGEN model: 80°F (27°C) ambient			RG 3.54 model: 80°F (27°C) ambient	
	(°F)	(°C)		(°F)	(°C)
2.05	110.9	43.8		115.2	46.2
6.10	111.7	44.3		116.1	46.7
10.15	112.8	44.9		117.3	47.4
14.20	114.0	45.6		118.7	48.2
18.25	115.3	46.3		120.3	49.0
22.30	116.7	47.1		121.9	49.9
26.35	118.2	47.9		123.5	50.9
30.40	119.6	48.7		125.2	51.8
34.45	121.1	49.5		127.0	52.8
38.50	122.6	50.4		128.7	53.7
42.55	124.2	51.2		130.5	54.7
46.60	125.7	52.1		132.3	55.7
50.65	127.2	52.9		134.1	56.7
54.70	128.7	53.7		135.8	57.7
58.75	130.3	54.6		137.6	58.7
62.80	131.8	55.4		139.4	59.7
66.85	133.3	56.3		141.2	60.6
70.90	134.8	57.1		142.9	61.6
74.95	136.3	58.0		144.7	62.6
79.00	137.8	58.8		146.5	63.6

Table A-2. (continued)

Axial location (inches)	ORIGEN model: 80°F (27°C) ambient			RG 3.54 model: 80°F (27°C) ambient	
	(°F)	(°C)		(°F)	(°C)
83.05	139.3	59.6		148.2	64.6
87.15	140.8	60.4		150.0	65.5
91.20	142.3	61.3		151.7	66.5
95.25	143.7	62.1		153.4	67.5
99.30	145.2	62.9		155.2	68.4
103.35	146.6	63.7		156.9	69.4
107.40	148.1	64.5		158.6	70.3
111.45	149.5	65.3		160.3	71.3
115.50	150.9	66.1		162.0	72.2
119.55	152.3	66.8		163.6	73.1
123.60	153.7	67.6		165.3	74.1
127.65	155.0	68.3		166.9	75.0
131.70	156.3	69.1		168.5	75.8
135.75	157.6	69.8		170.1	76.7
139.80	158.8	70.5		171.6	77.5
143.85	160.0	71.1		173.0	78.4
147.90	161.1	71.7		174.4	79.1
151.95	162.2	72.3		175.7	79.8
156.00	163.1	72.8		176.8	80.5
160.05	163.7	73.2		177.7	80.9
164.10	164.1	73.4		178.2	81.2
168.15	163.9	73.3		178.0	81.1
172.20	162.8	72.7		176.7	80.4
176.25	160.5	71.4		174.0	78.9

Table A-3. Canister Shell Axial Temperature Distribution: Module 145 (80°F [27°C Ambient])

Axial location (inches)	ORIGEN model: 80°F (27°C) ambient			RG 3.54 model: 80°F (27°C) ambient	
	(°F)	(°C)		(°F)	(°C)
2.05	112.26	44.59		116.39	46.88
6.10	113.09	45.05		117.33	47.40
10.15	114.22	45.68		118.61	48.12
14.20	115.50	46.39		120.08	48.93
18.25	116.88	47.16		121.65	49.81
22.30	118.33	47.96		123.30	50.72
26.35	119.80	48.78		124.99	51.66
30.40	121.30	49.61		126.70	52.61
34.45	122.81	50.45		128.42	53.57
38.50	124.31	51.28		130.14	54.52
42.55	125.82	52.12		131.87	55.48
46.60	127.31	52.95		133.58	56.43

Table A-3. (continued)

Axial location (inches)	ORIGEN model: 80°F (27°C) ambient			RG 3.54 model: 80°F (27°C) ambient	
	(°F)	(°C)		(°F)	(°C)
50.65	128.80	53.78		135.29	57.38
54.70	130.28	54.60		136.99	58.33
58.75	131.75	55.42		138.67	59.26
62.80	133.20	56.22		140.35	60.19
66.85	134.64	57.02		142.01	61.11
70.90	136.07	57.82		143.65	62.03
74.95	137.48	58.60		145.28	62.93
79.00	138.88	59.38		146.90	63.83
83.05	140.26	60.15		148.50	64.72
87.15	141.63	60.91		150.08	65.60
91.20	142.98	61.66		151.65	66.47
95.25	144.32	62.40		153.21	67.34
99.30	145.64	63.13		154.74	68.19
103.35	146.94	63.86		156.26	69.03
107.40	148.22	64.57		157.76	69.86
111.45	149.48	65.27		159.23	70.68
115.50	150.71	65.95		160.67	71.49
119.55	151.91	66.62		162.09	72.27
123.60	153.08	67.27		163.47	73.04
127.65	154.21	67.89		164.80	73.78
131.70	155.29	68.49		166.08	74.49
135.75	156.32	69.07		167.31	75.17
139.80	157.28	69.60		168.46	75.81
143.85	158.18	70.10		169.54	76.41
147.90	159.00	70.55		170.53	76.96
151.95	159.72	70.96		171.42	77.45
156.00	160.32	71.29		172.16	77.87
160.05	160.74	71.52		172.69	78.16
164.10	160.85	71.58		172.87	78.26
168.15	160.47	71.37		172.47	78.04
172.20	159.31	70.73		171.14	77.30
176.25	157.03	69.46		168.45	75.81

Table A-4. Canister Shell Axial Temperature Distribution: Module 146 (80°F [27°C Ambient])

Axial location (inches)	ORIGEN model: 80°F (27°C) ambient			RG 3.54 model: 80°F (27°C) ambient	
	(°F)	(°C)		(°F)	(°C)
2.05	112.49	44.72		116.68	47.04
6.10	113.33	45.18		117.62	47.57
10.15	114.46	45.81		118.91	48.28
14.20	115.76	46.53		120.39	49.10

Table A-4. (continued)

Axial location (inches)	ORIGEN model: 80°F (27°C) ambient			RG 3.54 model: 80°F (27°C) ambient	
	(°F)	(°C)		(°F)	(°C)
18.25	117.15	47.31		121.98	49.99
22.30	118.60	48.11		123.64	50.91
26.35	120.09	48.94		125.34	51.86
30.40	121.60	49.78		127.07	52.82
34.45	123.12	50.62		128.80	53.78
38.50	124.64	51.46		130.54	54.75
42.55	126.15	52.31		132.28	55.71
46.60	127.66	53.14		134.01	56.67
50.65	129.16	53.98		135.73	57.63
54.70	130.65	54.81		137.44	58.58
58.75	132.13	55.63		139.14	59.52
62.80	133.59	56.44		140.83	60.46
66.85	135.04	57.25		142.50	61.39
70.90	136.48	58.04		144.16	62.31
74.95	137.90	58.84		145.80	63.22
79.00	139.31	59.62		147.43	64.13
83.05	140.70	60.39		149.04	65.02
87.15	142.08	61.16		150.64	65.91
91.20	143.44	61.91		152.22	66.79
95.25	144.79	62.66		153.78	67.66
99.30	146.12	63.40		155.33	68.52
103.35	147.43	64.13		156.86	69.37
107.40	148.72	64.84		158.37	70.20
111.45	149.99	65.55		159.85	71.03
115.50	151.23	66.24		161.31	71.84
119.55	152.44	66.91		162.73	72.63
123.60	153.61	67.56		164.12	73.40
127.65	154.75	68.19		165.46	74.14
131.70	155.84	68.80		166.75	74.86
135.75	156.87	69.37		167.98	75.55
139.80	157.84	69.91		169.15	76.19
143.85	158.74	70.41		170.23	76.79
147.90	159.56	70.87		171.22	77.35
151.95	160.29	71.27		172.11	77.84
156.00	160.89	71.61		172.86	78.26
160.05	161.31	71.84		173.39	78.55
164.10	161.42	71.90		173.57	78.65
168.15	161.03	71.69		173.16	78.42
172.20	159.86	71.03		171.81	77.67
176.25	157.55	69.75		169.10	76.17

Table A-5. Canister Shell Axial Temperature Distributions for Module 144 for a Range of Ambient Temperatures

Axial location (inches)	ORIGEN model							
	90°F (32°C) ambient		80°F (27°C) ambient		70°F (21°C) ambient		50°F (10°C) ambient	
	(°F)	(°C)	(°F)	(°C)	(°F)	(°C)	(°F)	(°C)
2.05	120.70	49.28	110.9	43.8	101.29	38.49	82.5	28.1
6.10	121.55	49.75	111.7	44.3	102.04	38.91	83.2	28.5
10.15	122.66	50.37	112.8	44.9	103.08	39.49	84.2	29.0
14.20	123.92	51.07	114.0	45.6	104.25	40.14	85.3	29.6
18.25	125.29	51.83	115.3	46.3	105.53	40.85	86.5	30.3
22.30	126.73	52.63	116.7	47.1	106.88	41.60	87.8	31.0
26.35	128.22	53.46	118.2	47.9	108.28	42.38	89.1	31.7
30.40	129.75	54.30	119.6	48.7	109.71	43.17	90.4	32.5
34.45	131.30	55.16	121.1	49.5	111.16	43.98	91.8	33.2
38.50	132.86	56.03	122.6	50.4	112.63	44.80	93.2	34.0
42.55	134.43	56.91	124.2	51.2	114.11	45.62	94.6	34.8
46.60	136.00	57.78	125.7	52.1	115.59	46.44	96.0	35.5
50.65	137.58	58.66	127.2	52.9	117.07	47.26	97.4	36.3
54.70	139.15	59.53	128.7	53.7	118.55	48.09	98.8	37.1
58.75	140.72	60.40	130.3	54.6	120.04	48.91	100.2	37.9
62.80	142.29	61.27	131.8	55.4	121.51	49.73	101.6	38.6
66.85	143.84	62.14	133.3	56.3	122.99	50.55	103.0	39.4
70.90	145.39	63.00	134.8	57.1	124.46	51.36	104.4	40.2
74.95	146.94	63.85	136.3	58.0	125.92	52.18	105.7	41.0
79.00	148.47	64.71	137.8	58.8	127.38	52.99	107.1	41.7
83.05	150.00	65.55	139.3	59.6	128.83	53.79	108.5	42.5
87.15	151.52	66.40	140.8	60.4	130.27	54.60	109.9	43.3
91.20	153.02	67.24	142.3	61.3	131.71	55.40	111.3	44.0
95.25	154.52	68.07	143.7	62.1	133.15	56.19	112.6	44.8
99.30	156.01	68.89	145.2	62.9	134.57	56.98	114.0	45.5
103.35	157.49	69.72	146.6	63.7	135.99	57.77	115.3	46.3
107.40	158.95	70.53	148.1	64.5	137.40	58.55	116.7	47.0
111.45	160.40	71.33	149.5	65.3	138.80	59.33	118.0	47.8
115.50	161.83	72.13	150.9	66.1	140.18	60.10	119.4	48.5
119.55	163.25	72.91	152.3	66.8	141.55	60.86	120.7	49.3
123.60	164.64	73.69	153.7	67.6	142.90	61.61	122.0	50.0
127.65	166.00	74.44	155.0	68.3	144.23	62.35	123.3	50.7
131.70	167.33	75.18	156.3	69.1	145.53	63.07	124.6	51.4
135.75	168.62	75.90	157.6	69.8	146.80	63.78	125.8	52.1
139.80	169.86	76.59	158.8	70.5	148.03	64.46	127.0	52.8
143.85	171.04	77.25	160.0	71.1	149.21	65.12	128.2	53.4
147.90	172.16	77.86	161.1	71.7	150.33	65.74	129.3	54.0
151.95	173.17	78.43	162.2	72.3	151.36	66.31	130.3	54.6
156.00	174.05	78.92	163.1	72.8	152.25	66.81	131.2	55.1
160.05	174.71	79.29	163.7	73.2	152.95	67.19	131.9	55.5

Table A-5. (continued)

Axial location (inches)	ORIGEN model							
	90°F (32°C) ambient		80°F (27°C) ambient		70°F (21°C) ambient		50°F (10°C) ambient	
	(°F)	(°C)	(°F)	(°C)	(°F)	(°C)	(°F)	(°C)
164.10	175.03	79.46	164.1	73.4	153.31	67.39	132.3	55.7
168.15	174.80	79.33	163.9	73.3	153.14	67.30	132.1	55.6
172.20	173.68	78.71	162.8	72.7	152.11	66.73	131.2	55.1
176.25	171.29	77.38	160.5	71.4	149.88	65.49	129.1	53.9

Table A-6. Canister Shell Axial Temperature Distributions for Module 145 for a Range of Ambient Temperatures

Axial location (inches)	ORIGEN model							
	90°F (32°C) ambient		80°F (27°C) ambient		70°F (21°C) ambient		50°F (10°C) ambient	
	(°F)	(°C)	(°F)	(°C)	(°F)	(°C)	(°F)	(°C)
2.05	120.90	49.39	112.26	44.59	104.42	40.23	90.74	32.63
6.10	121.71	49.84	113.09	45.05	105.32	40.73	91.88	33.27
10.15	122.86	50.48	114.22	45.68	106.45	41.36	93.13	33.96
14.20	124.20	51.22	115.50	46.39	107.71	42.06	94.40	34.67
18.25	125.66	52.03	116.88	47.16	109.04	42.80	95.68	35.38
22.30	127.20	52.89	118.33	47.96	110.41	43.56	96.95	36.08
26.35	128.78	53.76	119.80	48.78	111.80	44.33	98.21	36.78
30.40	130.38	54.66	121.30	49.61	113.20	45.11	99.46	37.48
34.45	132.00	55.56	122.81	50.45	114.60	45.89	100.70	38.17
38.50	133.62	56.46	124.31	51.28	116.00	46.67	101.93	38.85
42.55	135.24	57.36	125.82	52.12	117.40	47.45	103.15	39.53
46.60	136.86	58.25	127.31	52.95	118.79	48.22	104.36	40.20
50.65	138.46	59.14	128.80	53.78	120.18	48.99	105.56	40.87
54.70	140.05	60.03	130.28	54.60	121.55	49.75	106.76	41.53
58.75	141.63	60.91	131.75	55.42	122.91	50.51	107.94	42.19
62.80	143.19	61.77	133.20	56.22	124.26	51.26	109.12	42.84
66.85	144.74	62.63	134.64	57.02	125.61	52.00	110.29	43.49
70.90	146.27	63.48	136.07	57.82	126.94	52.74	111.45	44.14
74.95	147.78	64.32	137.48	58.60	128.25	53.47	112.60	44.78
79.00	149.28	65.15	138.88	59.38	129.56	54.20	113.74	45.41
83.05	150.75	65.97	140.26	60.15	130.85	54.92	114.88	46.04
87.15	152.21	66.78	141.63	60.91	132.13	55.63	116.00	46.67
91.20	153.65	67.58	142.98	61.66	133.40	56.33	117.12	47.29
95.25	155.06	68.37	144.32	62.40	134.66	57.03	118.23	47.91
99.30	156.46	69.14	145.64	63.13	135.90	57.72	119.34	48.52
103.35	157.83	69.91	146.94	63.86	137.13	58.41	120.43	49.13
107.40	159.18	70.66	148.22	64.57	138.34	59.08	121.51	49.73
111.45	160.51	71.39	149.48	65.27	139.54	59.74	122.58	50.32
115.50	161.80	72.11	150.71	65.95	140.71	60.39	123.63	50.91
119.55	163.05	72.81	151.91	66.62	141.85	61.03	124.67	51.48
123.60	164.27	73.48	153.08	67.27	142.97	61.65	125.68	52.04

Table A-6. (continued)

Axial location (inches)	ORIGEN model							
	90°F (32°C) ambient		80°F (27°C) ambient		70°F (21°C) ambient		50°F (10°C) ambient	
	(°F)	(°C)	(°F)	(°C)	(°F)	(°C)	(°F)	(°C)
127.65	165.44	74.13	154.21	67.89	144.05	62.25	126.66	52.59
131.70	166.55	74.75	155.29	68.49	145.09	62.83	127.61	53.12
135.75	167.61	75.34	156.32	69.07	146.08	63.38	128.52	53.62
139.80	168.59	75.88	157.28	69.60	147.02	63.90	129.39	54.10
143.85	169.50	76.39	158.18	70.10	147.89	64.39	130.19	54.55
147.90	170.32	76.84	159.00	70.55	148.70	64.83	130.94	54.97
151.95	171.04	77.24	159.72	70.96	149.41	65.23	131.60	55.33
156.00	171.62	77.57	160.32	71.29	150.01	65.56	132.16	55.64
160.05	172.01	77.78	160.74	71.52	150.43	65.79	132.54	55.86
164.10	172.08	77.82	160.85	71.58	150.56	65.87	132.63	55.91
168.15	171.64	77.58	160.47	71.37	150.21	65.67	132.25	55.69
172.20	170.40	76.89	159.31	70.73	149.09	65.05	131.10	55.05
176.25	167.99	75.55	157.03	69.46	146.87	63.82	128.84	53.80